A DIPOLE WITH ACTIVE METASURFACE REFLECTOR FOR POLARIZATION RECONFIGURABILITY

by

Ruan van Aardt

Submitted in partial fulfilment of the requirements for the degree
Master of Engineering (Electronic Engineering)

in the

Department of Electrical, Electronic and Computer Engineering
Faculty of Engineering, Built Environment and Information Technology

UNIVERSITY OF PRETORIA

March 2022

SUMMARY

A DIPOLE WITH ACTIVE METASURFACE REFLECTOR FOR POLARIZATION RECONFIGURABILITY

by

Ruan van Aardt

Supervisor: Prof. J. Joubert

Co-supervisor: Prof. J.W. Odendaal

Department: Electrical, Electronic and Computer Engineering

University: University of Pretoria

Degree: Master of Engineering (Electronic Engineering)

Keywords: Metasurface, polarization diversity, reconfigurable, reconfigurable polarization

In recent years reconfigurable antennas have gained a lot of attention for the advantages they present for diversifying the capabilities of communication systems. Many types of reconfigurable antennas exist that have pattern, frequency, and polarization diversity. These antennas are reconfigured either by mechanical rotating surfaces or by enabling specific sections of a structure with electrical switches. The use of an active reflective metasurface to design an antenna system with reconfigurable polarization was particularly interesting as little research have been done on the topic and presented an interesting concept to expand upon. This study focusses on the concept of a reconfigurable antenna based on an active reflective metasurface with reconfigurable polarization. Subsequently, an antenna system based on an active reflective metasurface combined with a planar dipole is proposed to achieve reconfigurable polarization. The aim of this antenna is achieve reconfigurable polarization through electrical switches positioned on the reflective metasurface. The polarization of the designed antenna can be switched between linear and circular polarization

states through the use of positive-intrinsic-negative (PIN) diodes on the reflective metasurface. The designed antenna was manufactured and tested and functioned as expected. The measured results correlated well with the simulated results. The antenna has a physical size of 308 x 162 x 35 mm^3 with an impedance bandwidth of 4.5% in the linear state, and 7% in the circular state, as well as an axial ratio bandwidth of 8.3%. This gives the antenna an effective bandwidth of 4.5% in the linear state and 7% in the circular state. The final measured results were degraded due to unexpected interference from the biasing network used to control the PIN diodes. However, even with the interference, the concept of a reconfigurable antenna based on an active reflective metasurface was proven. This research contributed to the field of antenna engineering with the focus on expanding the field of reconfigurable antennas.

LIST OF ABBREVIATIONS

AR	Axial ratio
DC	Direct current
DRA	Dielectric resonator antenna
HPBW	Half power beamwidth
LHCP	Left-hand circular polarization
MIMO	Multiple input multiple output
PIN	Positive-intrinsic-negative
RHCP	Right-hand circular polarization
SNR	Signal to noise ratio
XPD	Cross-polar discrimination
4G	Fourth generation cellular radio technologies

TABLE OF CONTENTS

CHAPTER 1 INTRODUCTION

1.1 PROBLEM STATEMENT

1.1.1 Context of the problem

The communication industry has been evolving rapidly over the last decade, with a focus on a more connected world, with the emphasis on wireless technologies. A major stumbling block in this industry has been the demand for networks to have more capacity and throughput while operating in a spectral efficient way. Technologies such as 4G with multiple-input multiple-output (MIMO) antennas with steerable beams have solved some of the challenges. However, the rapidly growing number of connected devices establishes the need for more diverse systems in order to increase the capacity of a network. Reconfigurable antennas have received attention in this regard as they can provide the required diversity [1]. A reconfigurable antenna system would allow increased network capacity by employing a reconfigurable antenna with polarization diversity. This will lead to a more spectral efficient network with higher throughput [1].

As an emerging research field, reconfigurable antennas still allow for significant innovations, which can have major impact on the communication industry. Even though reconfigurable antennas have their challenges, they still provide great advantages in the communication domain compared to traditional antennas. Reconfigurable antennas have shown significant improvements in communication systems, specifically MIMO based systems [2]. By using certain reconfigurable antennas, it is possible to improve the data throughput, signal to noise ratio (SNR), and the bit error rate. Not only does a reconfigurable

antenna improve the performance characteristics, it also makes the antenna multifunctional [3]. There are a few different methods used to design reconfigurable antennas.

Some reconfigurable antenna designs achieve reconfigurability by modifying the structure of the radiating element. This is done by introducing switching elements on the radiating element which enables the user to change the properties of the antenna through a controller. However, by modifying the antenna structure with the addition of switching elements, the antenna performance will be degraded. As shown in [2]–[5], this degradation can be rectified through the addition of inductive chokes to still achieve the desired antennas performance. Reconfigurability can also be accomplished by modifying the feed network by introducing switchable segments that can alter the phase and magnitude of the input signal [6]–[12]. These designs produce antennas with wide bandwidths and high gains. With most of these methods, reconfigurable polarization is the focus of the designs. Another method of altering the polarization of an incident wave is through the use of polarizing surfaces [13]–[15]. These surfaces can be made reconfigurable through the addition of switchable elements. The metasurface can add the element of reconfigurability within an antenna system [16]–[24]. This method produces good results comparable to the other methods used to achieve reconfigurable polarization.

1.1.2 Research gap

In literature most reconfigurable antennas are either designed through modification of the radiating element or the antenna feed structures [2]–[11]. In some of the cases, adding electrical switches on the radiating element degraded the performance of some of the antennas which could however be remedied through the addition of additional structures like radio-frequency (RF) chokes [4], [5], [10]. Another method found in literature to achieve reconfigurability, which presented good results, is the combination of metasurfaces and radiating elements. However, the literature on active metasurfaces combined with radiating elements, which showed promising results, was limited. These antennas are configured in a transmittive configuration where the antenna is placed behind the active metasurface [21].

This prompted an investigation into reflective metasurfaces that are combined with radiating elements to form antenna systems. However, mostly passive and non-reconfigurable systems were discovered in literature. Subsequently, an active reflective metasurface presented and interesting topic to expand upon as it presented potential advantages to that of a transmittive metasurface and other reconfigurable antennas. An advantage of active reflective metasurfaces is that the biasing circuitry can be implemented behind the reflector minimizing any interference on the antenna. Metasurfaces also simplify reconfigurable arrays as the surface can easily be scaled. The unit cell geometry can be designed in such a way to ensure that the switching elements can be implemented in a basic and scalable way. A research gap was identified in open literature namely the implementation of reconfigurable antennas using active reflective metasurfaces to achieve both linear and circular polarization states.

1.2 RESEARCH OBJECTIVES

The primary objective of this study is to prove the concept of an antenna design that achieves reconfigurability through the use of an active reflective metasurface. The focus will be on obtaining reconfigurable polarization with a linear and circular state. The specific objectives of this study include:

1. Proving the concept of a reconfigurable antenna design based on an active reflective metasurface capable of circular and linear polarization.
2. Establishing a design process for reconfigurable antennas based on active and reflective metasurfaces.

1.3 APPROACH

A procedural approach was followed to design an antenna with reconfigurable polarization. First a literature study was conducted to establish what has been done in the field of reconfigurable antennas and to identify an area where new innovations could be made. From literature it was found that there is limited knowledge on reflective metasurfaces combined

with radiating elements. The use of reflective metasurfaces also presented a few potential benefits over the more established methods of creating reconfigurable antennas. The next step was to find the correct unit cell geometry to design a reflective metasurface. The metasurface was then analysed in isolation to fully understand how an antenna could be created by combining it with a radiating element.

After the reflective metasurface was designed and analysed, an initial set of parameters were obtained and a radiating element was introduced above the reflective metasurface. The design was then simulated and optimised using an electromagnetic analyses software tool called CST Studio Suite. Three prototypes were manufactured to establish how the active elements would affect the antenna's performance. The prototypes were measured in the compact range at the University of Pretoria. Finally, the measured and simulated results were compared to verify the performance of the designed antenna and to confirm that all the design goals were met.

1.4 RESEARCH GOALS

The following research goals were identified for the antenna design:

1. The antenna system has to be based on an active reflective metasurface where the switching elements are integrated within the unit cell structure of the metasurface.
2. The antenna's polarization should be reconfigurable through a controller or basic DIP switches attached to the back of the antenna structure. Two polarization states should be available, namely linear or right-hand circular.
3. The antenna should not be complex to manufacture and implement.
4. The measured results have to correlate with the simulated results of the design.

1.5 RESEARCH CONTRIBUTION

This study made the following contribution to the field of antenna engineering:

- **Conceptualised the use of an active reflective metasurface to design an antenna with reconfigurable polarization**: From literature it was evident that the use of active reflective metasurfaces in the design of reconfigurable antenna systems have not been well studied. This work thus focused on studying and conceptualising the use of reflective metasurfaces to design reconfigurable antennas with linear and circular polarization. The concept was proven in this study by successfully designing and implementing a reconfigurable antenna based on a reflective metasurface. The concept can be expanded upon in future work.

1.6 RESEARCH OUTPUTS

A journal article in preparation will be submitted to a special issue journal “Metamaterials and Surfaces: Theoretical and Experimental Research” with the MDPI (Multidisciplinary digital publishing institute). The journal article will share the same title as this dissertation and focus on the use of an active metasurface in the design of a reconfigurable antenna.

1.7 OVERVIEW OF STUDY

In Chapter 2 a comprehensive literature study is conducted on reconfigurable polarization antennas, the methods used to achieve this, their functionality, as well as the use of metasurfaces to achieve this. A research gap is identified in literature where an innovation can be made to produce an antenna system with reconfigurable polarization.

Chapter 3 describes the design of such an antenna. First starting with the design of a new active reflective metasurface capable of switching between polarization states. A new antenna structure is then proposed which combines the reflective metasurface with a dipole element. The combined metasurface and dipole structure is then analysed to better

understand how they interact with each other. Finally a critical parameter set is extracted, the antenna design is optimized, and the design is finalized.

Chapter 4 focuses on the design implementation of the antenna which deals with introducing switching elements on the antenna structure. The challenges posed by biasing the switching elements with a biasing circuit are discussed as well as the solution that was implemented to solve these challenges.

In Chapter 5 the manufacturing and measured results of the antenna are discussed. The measured results are shown and compared to the simulated results of the designed antenna.

In the last chapter, Chapter 6, the study is concluded by summarizing the work that was conducted and the outcomes thereof. A suggestion for future work to further improve the design and performance of the antenna is made.

CHAPTER 2 LITERATURE STUDY

2.1 CHAPTER OVERVIEW

In this section a review of the available literature is provided covering the various aspects related to the design of an antenna with reconfigurable polarization. Section 2.2 gives an overview of reconfigurable antennas in general and the methods by which reconfigurability is achieved. In Section 2.3 the various types of antennas with reconfigurable polarization are discussed where reconfigurability is achieved through the modification of the radiating element and feed network. In Section 2.4 metasurfaces are discussed and how they can be used to implement an antenna with reconfigurable polarization.

2.2 BACKGROUND ON RECONFIGURABLE ANTENNAS

Reconfigurable antennas have long been a topic of interest in antenna theory. These antennas provide the freedom to change the radiation characteristics without having to redesign the antenna structure. This is relevant in today's communication industry, where higher system throughputs are required from wireless communication systems to increase the number of active users and data throughput to each user [1]. Traditional antennas put a limitation on this as they do not provide the diversity that is obtained from reconfigurable antennas. Multiple types of reconfigurable antennas currently exist that provide frequency diversity, pattern diversity, and polarization diversity [3].

These antennas can be implemented through various methods, including the modification of the radiating element [2]–[5], modification of the feed network [6]–[12], and the combination of metasurfaces with traditional antennas [16]–[23]. Reconfigurable antennas

are mostly reconfigured through electrical switches. PIN diodes are the most popular choice for this, since it is simple to bias them. Varactor diodes are also used, although they require more precise control over the biasing voltage as the varied capacitance of the diode controls specific antenna characteristics [5], [23]. Lastly, there are micro electromechanical switches (MEMS) [16]. These switches function very similar to traditional mechanical relays, only miniaturized to a few millimetres or micrometres. All these electrical switches can also be used on active metasurfaces to control certain unit cell elements. An active metasurface is defined as an electrical reconfigurable surface whereas a passive metasurface is defined as a mechanical reconfigurable surface. In the following sections the focus will be on antennas and surfaces with reconfigurable polarization.

2.3 ANTENNAS WITH RECONFIGURABLE POLARIZATION

2.3.1 Antenna reconfigurability through modification of radiating element

As mentioned, a method of realizing a reconfigurable antenna is by altering the physical antenna structure. PIN diodes, MEMS switches, and varactor diodes can be used on the structure of the antenna to give the user the maximum flexibility and control of the antenna characteristics. The simplest form of such an antenna is a patch antenna with truncated corners that can be converted to a square patch through the use of PIN diodes, which then creates a polarization reconfigurable antenna [2].

One method discussed in literature is the addition of microstrip stub lines to an ordinary patch antenna on each of the patch edges [5]. The stubs are connected to the patch structure through varactor diodes. By altering the voltages on each of the varactor diodes, different polarization states can be achieved as the field components can be controlled independently from each other. This stub-based type antenna produces an excellent impedance bandwidth, but only produces an axial ratio bandwidth of 0.96%. This type of antenna can be improved through the introduction of a circular radiator with multiple stubs to give the user even more control over the polarization characteristics of the antenna [4]. With this method the

impedance bandwidth is reduced, while the axial ratio bandwidth is increased to 15.4%. Methods for altering the structure of an antenna always involve either including or excluding certain parts of an antenna structure and then controlling the parts with switches by bridging the structures. This creates the challenge of biasing such switches without altering the radiation characteristics of the antenna and adding necessary direct current (DC) blocking components to the feed network.

2.3.2 Antenna reconfigurability through modification of the feed network

The challenges presented by biasing electrical switches on a radiating element can mostly be mitigated by altering the feed network to get the desired characteristics. This is typically accomplished by delaying the phase of either field components to get a ninety degree (90°) phase difference for circular polarization. All the switching components are implemented and mostly isolated from the radiating element of the antenna, unlike antennas where the structure is altered. With antennas where the feed network is altered, the antenna is already enhanced to achieve excellent characteristics, this forms the basis for an antenna with reconfigurable polarization.

In [6] a reconfigurable dielectric resonator antenna is presented. The antenna uses a reconfigurable crossed coupling feeding slot to excite the dielectric resonator antenna (DRA) elements. Certain segments of the crossed structure are shorted through PIN diodes to alter the modes by which the DRA elements are excited. This produces a circular and linear polarization in certain configurations. The antenna produces an axial ratio bandwidth of 20% and an impedance bandwidth of 30%. The radiating element is complex as very precise manufacturing techniques need to be implemented to manufacture the DRA element. However, the polarization reconfigurability is achieved through the feed network where the implementation is simpler.

Another reconfigurable antenna is discussed in [12] where a square patch antenna is combined with a transmittive metasurface to enhance the bandwidth and gain of the antenna in a linear state. Through the addition of a reconfigurable feed network, the user can alter

the phase of the transmitted field. The feed network is implemented through four paths which can be excited independently using PIN diodes. This design produces an axial ratio bandwidth of 17.8% and an impedance bandwidth of 25%. With an enlarged electrical surface introduced by the metasurface, the gain is also enhanced to 9.85 dBi. Both the designs in [6] and [12] require a DC isolation circuit to ensure the biasing network is isolated from the RF network.

An interesting method of introducing a reconfigurable feed network is through an array where each element can be fed independently and produce unique antenna characteristics. This is similar to implementing a phase shifter on each feed of the array elements. In [8] a two element patch array is enhanced through a partially reflective surface where each patch element can be excited in different feeding modes. This produces an antenna capable of switching between linear vertical and linear horizontal polarization. This design produces an impedance bandwidth of 21%. The array method is improved upon in [9] where a six-element array, in a circular configuration, is used with an unique coupling structure between each element. The antenna is reconfigured using a reconfigurable feed network which uses PIN diodes. The antenna can generate omnidirectional patterns in its linear state and directional patterns in its circular state. The antenna presented produces an impedance bandwidth of 94% and an axial ratio bandwidth of 66%.

In [10] a four arm radiating antenna is proposed with reconfigurable circular polarization. The antenna is constructed from four radiating arms emulating two orthogonally placed dipoles. Each arm has a unique feed network that can be reconfigured using PIN diodes, which changes the feed lengths and alters the phase. Through this mechanism left-hand circular polarization (LHCP) and right-hand circular polarization (RHCP) can be generated. The antenna has an excellent impedance bandwidth of 80% and an axial ratio bandwidth of 23.5%. The bias network for the PIN diodes has a negative impact on the antenna characteristics, which is mitigated using RF chokes on the biasing line on the antenna structure.

A crossed dipole structure with differential ports can also be used to produce an antenna with reconfigurable polarization. A single dipole is linearly polarized where the polarization depends on the orientation of the dipole. In [11] a polarization rotation artificial magnetic conductor surface is added which acts as a circular polarizer. The traditional dipole structure is also changed to a crossed dipole structure with differential ports, which is reconfigurable using a radio frequency integrated circuit (RFIC). Depending on the configuration of the RFIC the antenna can generate RHCP, LHCP, and linear polarization states. The antenna produces an axial ratio bandwidth of 15% and an impedance bandwidth of 20%.

2.4 METASURFACE BASED POLARIZATION CONVERTERS AND POLARIZATION RECONFIGURABLE ANTENNAS

2.4.1 Antenna reconfigurability through parasitic layers

Another method of making an antenna reconfigurable is through the addition of a reconfigurable parasitic layer [16]. A parasitic layer can be defined as a metasurface which is placed in close proximity to a radiating element. In [16] the parasitic layer is placed within the reactive field region of the source antenna. This can then be used to alter the characteristics of the antenna by changing the structure of the parasitic layer through MEMS switches. This configuration allows the antenna to achieve multiple modes of operation, where polarization diversity is one of them. The addition of a parasitic layer allows for a compact and low-profile antenna with multiple configurations, however the performance bandwidth within the different modes is sometimes limited. The design in [16] only achieves an axial ratio and common bandwidth of 1.6%.

The configurations of the parasitic surface are obtained using optimization algorithms. The algorithms are set for specific design goals such as polarization, operating frequency, and main lobe direction. The electrical switching is quite complex, as the MEMS switches require a complex biasing network to function. These parasitic layers can also be implemented in array form for enhanced performance.

2.4.2 Polarization conversion and reconfigurability using metasurface based polarization converters

The previous methods discussed used three methods to reconfigure the transmitted polarization of the antennas, namely radiating element modifications, feed network modifications, and parasitic layers. Another method to change the polarization of an incident field is by using polarizers such as metasurfaces and frequency selective surfaces. When an incident wave interacts with the unit cells of such a surface, it alters the field components to achieve a phase shift which generates a circular polarization state. The axial ratio performance of these surfaces in isolation is excellent, producing very wide bandwidths.

These surfaces can be grouped into two types of surfaces, namely transmittive surfaces and reflective surfaces. Transmittive surfaces are used to change the polarization of an incident wave and let it pass through the surface with a new polarization state. Whereas with reflective surfaces, a surface and a reflector are combined to reflect an incident wave and change the polarization state of the reflected wave.

In [13] a polarizer capable of linear to circular polarization is discussed. The surface is made from a two-layer unit cell with slanted microstrip lines. The polarizer achieves a bandwidth of 60%. This is a transmittive metasurface and it shows how a basic unit cell can alter the polarization of an incident wave with excellent results. These surfaces can also easily be designed to be reconfigurable through mechanical mechanisms or electrical switches such as PIN diodes.

One such surface uses a multi-layered truncated patch unit cell, which can convert an incident wave to RHCP, LHCP, and linear polarization states by rotating the surface by 45° increments [14]. This illustrates the concept of how a reconfigurable surface can be designed. By altering the impedance within the equivalent circuit models, it is possible to create a phase shift between the incident field components. Instead of rotating the surface, the surface can be designed to offer reconfigurability through electrical switches. In [15] a multi-layered

I-shaped unit cell with a grated ground and embedded PIN diodes is designed. The grated ground also serves as a bias network for the PIN diodes. The surface can generate both linear and circular transmitted waves.

2.4.3 Use of metasurfaces to enhance antenna characteristics.

The surfaces discussed in Section 2.4.2 can also be implemented with radiating elements to design non-reconfigurable antennas with enhanced characteristics and different polarization states without altering the structure or feed network. This brings about another challenge as the surface is placed in proximity of the radiating element. The characteristics will start changing as the surface is in the reactive field region of the antenna. Thus, the structure needs to be optimized for optimal operation.

In [25] a circular microstrip line with a slanted strip unit cell is designed to achieve circular polarization. The surface is first designed as a transmittive polarizer with a radiating patch element added in a later stage to form an antenna with circular polarization. The antenna produces an axial ratio bandwidth of 17%. This shows that the concept of a metasurface combined with a radiating element is feasible. In [26] a similar unit cell structure is used. Instead of a circular microstrip line, a square microstrip line with a slanted strip is used. The antenna also uses a transmittive surface. This structure is also chosen so that the impedance perceived by the field components is different to get the phase difference for circular polarization. The surface is used with a patch antenna and produces an axial ratio bandwidth of 7% and an impedance bandwidth of 10%. These two antennas show that metasurfaces in isolation produces a much higher axial ratio when the incident fields have far field characteristics. The radiating element is a limiting factor to the bandwidth of the system. With the radiating element within the reactive region, the bandwidth of the surface is reduced significantly.

With a reflective surface configuration, similar results can be obtained. In [24] a reflective surface is used to alter the main lobe direction of a radiating element illustrating the use of reflective surfaces. In [27] a slanted arrow like unit cell configuration with a reflector is used

for the surface and a dipole is used as the radiating element. The antenna achieves an axial ratio bandwidth of 7% and an impedance bandwidth of 14%. It is shown that the bandwidth of the antenna can be increased by using different types of radiators. One such case is the use of a co-planar waveguide (CPW) fed slot antenna with a transmittive metasurface. This antenna achieves an axial ratio bandwidth of 20% and an impedance bandwidth of 32% [28]. In [29] another CPW fed slot antenna is used with a transmittive surface. In this case, an L-shaped slot is used with the metasurface coupled to the slot layer. This produces an axial ratio bandwidth of 35% and an impedance bandwidth of 48%. Using a L-shape slot enhances the bandwidth significantly.

The literature on metasurfaces with reflective configurations is limited for cases where an omnidirectional radiating element can be transformed into a directional antenna. In [30] a reflective metasurface based on the square patch unit cell with truncated corners is used. In this design the dipole is placed 1.5 mm form the reflective metasurface. The antenna produces an axial ratio bandwidth of 20% and an impedance bandwidth of 27%.

In all previously discussed configurations the metasurfaces are mainly used as polarizers. In [31] the performance of an already circular polarized antenna is enhanced with the use of a metasurface. The antenna produces an axial ratio bandwidth of 23% and an impedance bandwidth of 45%. However, this concept can be extended upon by using a metasurface polarizer to create a linear polarizer through the use of a transmittive surface. Another example is presented in [32] where a circular crossed slot antenna with a transmittive metasurface is used. Here a simple square patch unit cell surface is used to enhance the antenna axial ratio bandwidth from 12.4% to 41.28%.

2.4.4 Use of active and passive metasurfaces with antennas for polarization reconfigurability

As discussed in Section 2.4.3 a metasurface (active or passive) can be used to change the polarization states of incident waves with a form of reconfigurability. Passive metasurfaces combined with radiating elements produce antennas with increased performance in terms of

bandwidth and gain but still lack in reconfigurability. The addition of switches and biasing networks to a reconfigurable surface, can have a significant impact on an antenna's performance. Literature on active metasurfaces combined with antenna elements is limited at this stage.

In [17], a metasurface combined with a radiating element is designed to achieve reconfigurable polarization using mechanical rotation. The unit cell consists of a square patch with tapered edges with a slot antenna placed behind the metasurface in a transmittive configuration. The metasurface is rotated in 45° increments to alter the polarization of the antenna. With the surface at 0° and 180° the antenna is polarized in a RHCP state. When the surface is rotated 90° and 270° the antenna is polarized in LHCP state. Whereas linear polarization is achieved with the surface rotated at 45°, 135°, 225°, and 315°. The antenna produces an axial ratio bandwidth of 14% and an impedance bandwidth of 11%. The drawback of this antenna is that the reconfigurability is achieved through manual mechanical rotation, which will be complex to implement with a motorized approach. In [18] a very similar design approach is followed with a cross slot unit cell used for the metasurface. The antenna is also configured in a transmittive configuration with the slot antenna placed directly beneath the metasurface. The polarization is altered by rotating the metasurface above the source antenna. The antenna produces an axial ratio bandwidth of 2.7% and an impedance bandwidth of 12%.

The second method uses electrical switches to create an active metasurface. In [19] varactor diodes are used on a double layered unit cell metasurface where the capacitance is adjusted by adjusting the biasing voltages of each diode. The antenna uses a CPW fed circular monopole, and can be switched between LHCP and RHCP polarization states. It produces an axial ratio bandwidth of 2.85%. The centre frequency can also be shifted by varying the biasing voltages. The antenna is configured in a reflective configuration. This illustrates an interesting concept which can be expanded on for a specific metasurface. PIN diodes can also be used to design an active metasurface capable of polarization diversity.

In [20], a double layered segmented circular strip with a diagonal strip is designed as the unit cell element for the metasurface. The metasurface is implemented with a slot antenna in a transmittive configuration. The antenna can change between two circular polarization states by either switching the layers on or off. When the top layer is activated, a RHCP wave is transmitted, whereas a LHCP wave is transmitted when the bottom layer is activated. In most cases biasing of PIN diodes is challenging, however the authors in [20] designed a very clever biasing method with the unit cell in mind that compliments the functionality of the metasurface. Each unit cell is biased through a vertical and horizontal microstrip line in order to switch the PIN diodes in parallel in each row. The antenna produces an axial ratio bandwidth of 4.68% and an impedance bandwidth of 17%.

In [21] a double layered meandering elliptical unit cell structure is combined with a horn antenna to form an antenna system. The metasurface has a basic and easy implementable structure, which might be added to another antenna system such as a slot antenna in a transmittive configuration. The system can change polarization from linear to circular by using PIN diodes in the middle of each unit cell. Because of the symmetry of the unit cell structure, the metasurface requires a 45° incident wave on the surface to change the polarization state of the antenna. With either a 0° or 90° incident wave, the field components will perceive the same impedance in both directions, which will not produce a phase shift. The antenna produces an axial ratio bandwidth of 14% with an impedance bandwidth of 14%. The surface provides excellent performance with the way it is implemented.

2.4.5 Proposed polarization reconfigurable antenna based on an active reflective metasurface

A majority of studies found in open literature focuses on antennas with active transmittive metasurfaces and antennas where the structure of the feed network or radiating element is altered. With some of these methods the antenna implementation required complex biasing networks or very precise machining to manufacture the antenna elements. There is still a lot of scope to research the use of metasurfaces in reconfigurable antennas as the current literature is limited. The use of an active reflective metasurface presented an interesting

concept to expand on due to the possible benefits of such a design. Some of the potential benefits derived from the literature study was that the biasing network could be implemented without having an effect on the antenna performance [20]. A reflective metasurface can also be used to implement an array antenna with an element reconfiguration [16], [20].

The proposed antenna will thus be based on an active reflective metasurface that will be combined with a radiating element. The radiating element in this design will be based on a planar dipole as it will serve as a basic element to establish a well-defined design procedure, which can be expanded upon in future work.

CHAPTER 3 DESIGN OF A POLARIZATION RECONFIGURABLE ANTENNA USING AN ACTIVE METASURFACE REFLECTOR

3.1 INTRODUCTION

The focus of this chapter will be on the design of the proposed antenna structure. From the literature study it was clear that the use of an active metasurface, to achieve polarization reconfigurability, provides a lot of flexibility in the design without having to change the structure of the radiating element or feeding structure of the antenna. Theoretically different radiating elements can be implemented with one active metasurface to from a more diverse antenna. The proposed antenna will be based on an active reflective metasurface and will be reconfigurable using electrical switches. The starting point of this design is based on a transmittive metasurface that is based on a meandering elliptical unit cell, which is capable of switching between linear and circular polarization states [21]. The concept is expanded on in this antenna design to only use a single layer unit cell array with a reflector to form an active reflective metasurface.

In Section 3.2 an overview of the proposed antenna structure is given with the envisaged method of operation. In Section 3.3 the design of the reflective metasurface and the design methodology followed is discussed. The requirements of the reflective metasurface, to function as a polarizing surface, as well as the exact mode of operation are provided and explained. The complete antenna design is discussed in Section 3.4. The basic structure and

parameters of the antenna are described in this section. A parametric study is also performed on the critical parameters of the antenna system, which consists of the reflective metasurface combined with a dipole element. The parametric study is conducted to gain a better understanding of the effect of the dipole, as the metasurface design only considers plane wave incidence. After the parametric study, an initial parameter set is extracted and an initial design iteration is performed for an optimal axial ratio. The results from the axial ratio iteration are promising with only the radiation patterns not satisfying the design goals. The antenna design is finalized through a final design iteration which aims to improve the radiation patterns. In Section 3.6 a summary of the design is given.

3.2 PROPOSED RECONFIGURABLE ANTENNA

Multiple reconfigurable antennas were studied, where some were based on modifying the structure of the antenna and others on the modification of the feed network. An alternative method comprised of the introduction of a polarizing metasurfaces in proximity of a radiating element. The literature on polarizers based on metasurfaces were diverse, but limited literature was available on active metasurfaces combined with radiating elements.

The proposed antenna will utilise an active metasurface combined with a radiating element in a reflective configuration. This antenna will operate with a centre frequency of 2.4 GHz with an operational band from 2.35 GHz to 2.45 GHz. The antenna will be designed with two operational modes, the first mode will generate linear-horizontal polarization and the second mode will generate circular polarization. Both polarization states need unidirectional patterns to ensure the usefulness of the antenna. The antenna has to meet the following design goals:

- Right-hand circular polarization state with switches in open state.
- Linear-horizontal polarization state with switches in closed state.
- Unidirectional patterns for both polarization states.

- Cross-polar discrimination of at least 15 dB at the centre frequency of 2.4 GHz and at least 10 dB within the half power beamwidth (HPBW) for both states
- Impedance bandwidth between 2.35 GHz and 2.45 GHz
- Axial ratio bandwidth between 2.35 GHz and 2.45GHz

The proposed antenna design will consist of two components, namely the active reflective metasurface responsible for the element of reconfigurability within the design, and the radiating element. The reflective metasurface will be based on an array of elliptical unit cells with a reflecting ground surface. An array size of 6 x 6 is chosen as a limitation to keep the antenna size to a minimum and to get the optimal antenna performance from the design. Smaller arrays degrade the performance of the antenna, whereas a larger array increases the antenna size drastically. The metasurface is illustrated in the concept design shown in Figure 3.1. The design of the metasurface is discussed in more detail in Section 3.3.

The second component of the proposed antenna is the radiating element. As an active reflective metasurface was proposed the choice of radiating element needs to be compatible with the functionality of the active reflective metasurface as such an omnidirectional element would be required. With it an element with a small footprint would also be ideal. Thus, a planar dipole was chosen for the ease of implementation. The dipole is placed above the reflective metasurface and angled to ensure the antenna achieves the correct polarization states, which are generated through the reflective metasurface. This configuration is also shown Figure 3.1. The combined design is discussed in more detail in Section 3.4.

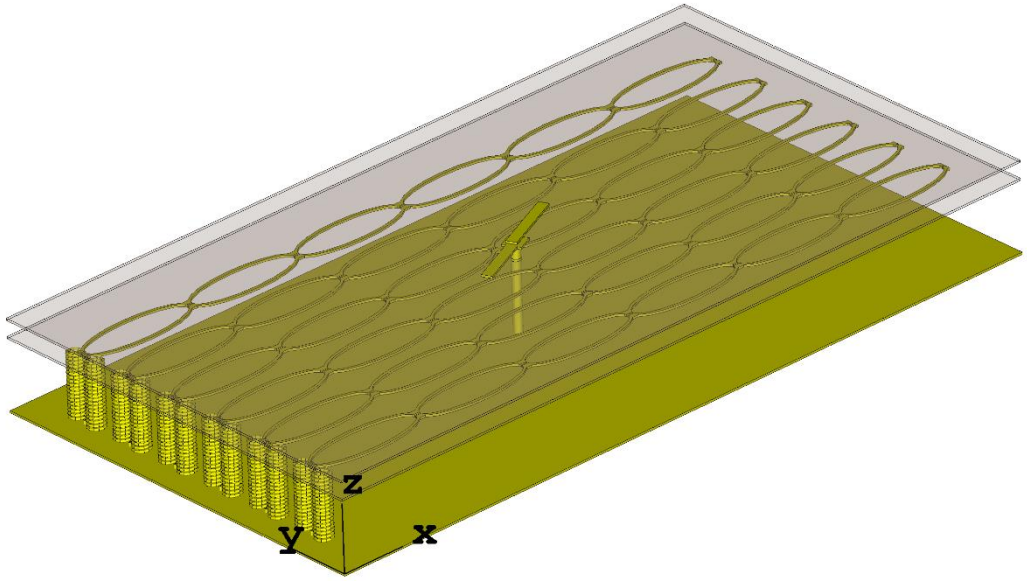

Figure 3.1 Proposed antenna structure

3.3 REFLECTIVE METASURFACE DERIVATION

The unit cell structure used within this design is based on a transmittive metasurface, which is designed with a meandering elliptical unit cells [21]. As the goal is to design an antenna based on an active new reflective metasurface with polarization reconfigurability, it is critical to have a reflective polarization converter. Thus, a new reconfigurable polarization converter is designed, the design expands on the initial concept.

The proposed unit cell structure is shown in Figure 3.2. The unit cell is made from a single layer unit cell element with a reflector added to the back of the unit cell structure. The unit cell can be made reconfigurable by the addition of two electrical switches on the sides of the elliptical unit cell. By shorting the two ends, the unit cell is configured in a linear polarization state and by opening the two ends the unit is configured in a circular/elliptical polarization state. The method of operation is explained through the effect of the metasurface on the field components. In order to get a circular polarized wave, the electric field components, namely E_x and E_y, should have an equal magnitude with a phase difference of 90° between the two

components. For the surface to function it requires an incident polarization angle of 45°. When such an incident wave interacts with the surface, the field components can be broken into two field components, namely E_x and E_y. This also ensures that the E_x and E_y components have equal magnitude. This principle is used with some of the polarizers as discussed in Chapter 2.

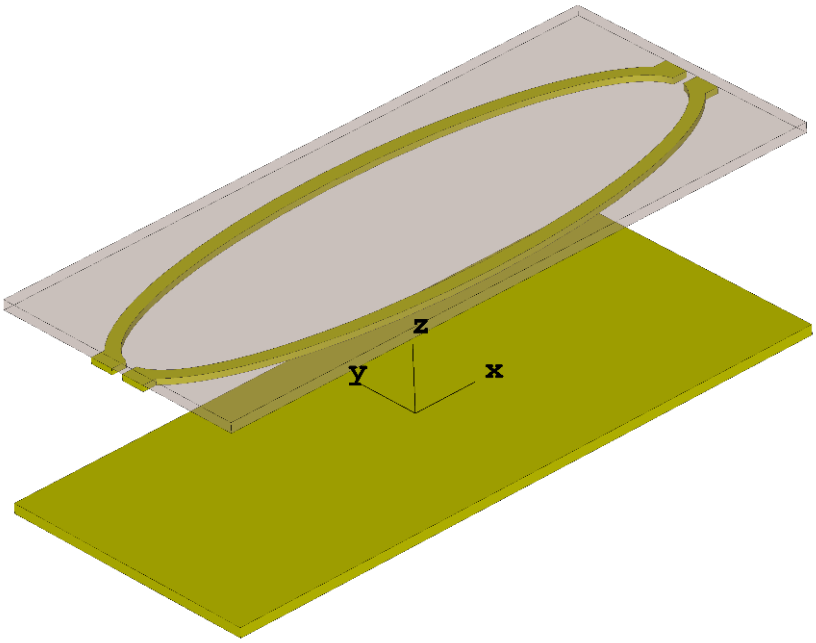

Figure 3.2 Proposed unit cell structure

The impedance seen by the two components differs from each other and is affected by the state of the switches at the ends of the unit cell. When the sides of the unit cell are open, the surface acts as if there is a shunt capacitance applied to the E_y component. This shunt capacitance creates a 90° phase shift for the E_y component and in effect creates a circularly polarized wave. When the sides of the unit cell are shorted it eliminates the shunt capacitance that was applied to the E_y component which then reflects a linearly polarized wave.

With the working principle in mind, the critical parameters of the unit cell can be determined and optimized through simulation. Simulations are performed using CST Studio Suite. The structure is simulated as a complete metasurface with an infinite number of unit cells in both

the *x* and *y* directions. This is accomplished with unit cell boundary conditions which creates two floquet ports. The Z_{max} port is positioned in front of the unit cell and monitors the fields in front of the unit cell and also excites the unit cell through floquet modes. The reflected and transmitted fields are monitored by the port and used to calculate the axial ratio of the unit cell. The Z_{min} port is positioned behind the ground plane and thus not excited. The frequency domain solver is used to solve the problem. Throughout the dissertation all coper surfaces are simulated with a height of zero to simplify the simulation model. Shown in Figure 3.3 and Figure 3.4 is a breakdown of the parameters of the unit cell with the descriptions tabulated in Table 3.1.

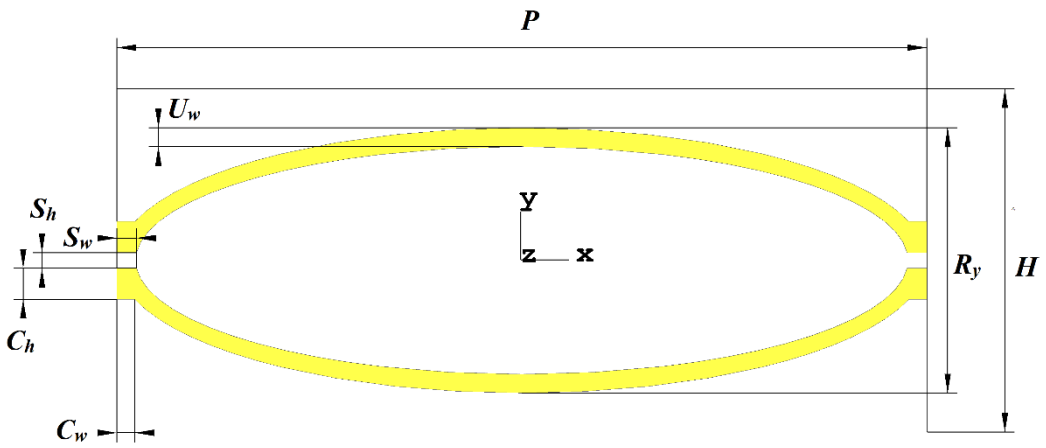

Figure 3.3 Unit cell top view

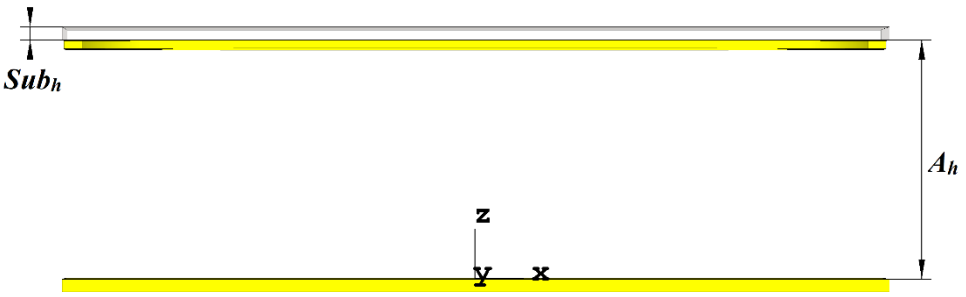

Figure 3.4 Unit cell side view

Table 3.1 Summary of unit cell parameters

Parameter	**Description**
A_h	Air gap between unit cell and reflector
Sub_h	Substrate height
C_h	Connection block height
C_w	Connection block width
S_h	Switch height
S_w	Switch width
P	Unit cell width
H	Unit cell height
R_x	Unit cell ellipse x radius (R_x = P/2)
R_y	Unit cell ellipse y radius
U_w	Unit cell microstrip width
Rot	Incident wave polarization angle

The unit cell is a complex multi-parameter problem. To design the unit cell the critical parameters were determined through a parametric study. The incident polarization angle remains 45° throughout the study. The parameters are varied to better understand the effect of the reflective metasurface on the axial ratio. Multiple configurations are possible with the proposed unit cell with a trade-off that has to be made between the size and the usable axial ratio bandwidth. This design will focus on the useable axial ratio bandwidth. The reflective metasurface was designed to operate at a centre frequency of 2.4 GHz with an axial ratio bandwidth of at least 20%. The reflective metasurface has to have a linear-horizontal and circular polarization state. The critical parameters for adjusting the characteristics of the unit cell include the unit cell width, the unit cell height, the spacing between the reflector and unit cell, and the radii of the elliptical microstrip line. As mentioned, the focus of the parametric study is the axial ratio of the unit cell. The axial ratio is calculated using equations from [22]. The minor and major axes are calculated using (3.1) and (3.2), respectively, where δ is the phase difference between the E_x and E_y field components.

$$Minor\ axis = \sqrt{\frac{1}{2}\left(E_x{}^2 + E_y{}^2 - \sqrt{E_x{}^4 + E_y{}^4 + 2E_x{}^2E_y{}^2 cos2\delta}\right)} \quad \textbf{(3.1)}$$

$$Major\ axis = \sqrt{\frac{1}{2}\left(E_{tx}{}^2 + E_{ty}{}^2 + \sqrt{E_{tx}{}^4 + E_{ty}{}^4 + 2E_{tx}{}^2E_{ty}{}^2 cos2\delta}\right)} \quad \textbf{(3.2)}$$

After both the minor and major axes are calculated it can be used to calculate the axial ratio of the reflected wave from the reflective metasurface using (3.3).

$$AR = \frac{Major\ axis}{Minor\ axis} \quad \textbf{(3.3)}$$

The parameters that are varied in the parametric study are constrained by a few selected physical limits in order to limit the size of the final reflective metasurface. The results of the parametric study is summarized in Table 3.2 where the results are referenced to the centre frequency of 2.4 GHz.

Table 3.2 Summary of parametric study

Parameter	Description	Effect on axial ratio in open state	Effect on axial ratio in closed state
A_h (2-30 mm)	Spacing between unit cell and reflector	Axial ratio minimum shifted right with an increase in A_h and shifted left with a decrease in A_h	Axial ratio decreases with smaller values of A_h and increases with larger values of A_h
P (20-60 mm)	Unit cell width	Axial ratio minimum shifted right until a change of direction is	Axial ratio increases up to P = 48 mm and

		observed at P = 44 mm after which the axial minimum starts shifting left until P = 60 mm	decreases up to P = 60 mm
H (34-50 mm)	Unit cell height	Axial ratio minimum shifted right with an increase in H and shifted left with a decrease in H	Axial ratio remains stable with very small changes (< 0.5 dB)
R_x	Unit cell ellipse x radius (R_x = P/2)	The effect is coupled to that of the unit cell width, P.	The effect is coupled to that of the unit cell width, P.
R_y (3-18 mm)	Unit cell ellipse y radius	Axial ratio minimum shifted right with an increase of R_y and shifted left with a decrease of R_y	Two minima (7 mm and 13 mm) and one maximum (10 mm) observed in axial ratio

After the parametric study is concluded, a rough optimization is done to get a working reflective metasurface. The primary design goal is to achieve the best circular performance in the open state and the best linear performance in the closed state. In ideal conditions, the axial ratio should be 0 dB to obtain circular polarization, and ∞ dB to achieve linear polarization. The optimized parameters of the unit cell are tabulated in Table 3.3.

Table 3.3 Unit cell parameters

Parameter	Description	Value (mm)
A_h	Air gap between unit cell and reflector	15
Sub_h	Substrate height	0.813
C_h	Connection block height	2

C_w	Connection block width	2
S_h	Switch height	1
S_w	Switch width	1.2
P	Unit cell width	52
H	Unit cell height	19
R_x	Unit cell ellipse x radius (R_x = P/2)	26
R_y	Unit cell ellipse y radius	8.5
U_w	Unit cell microstrip width	1.2
Rot	Incident wave polarization angle	45°

The simulated reflected x and y E-field components are shown in Figure 3.5 and Figure 3.6, in the open and closed states, respectively. For the metasurface to operate in a circular configuration, it is critical for the field components to have an equal magnitude and a -3 dB crossing point between the two components at the design frequency. In Figure 3.7 the phase difference between the E-field components is provided. This value is 90° over the entire frequency sweep in the open state as required for circular polarization. This shows that a circular polarized wave will be transmitted by the metasurface in the open state. In the closed state it can be seen that the x component will be transmitted and the y component will not be transmitted, which will generate a linear-horizontal polarized wave.

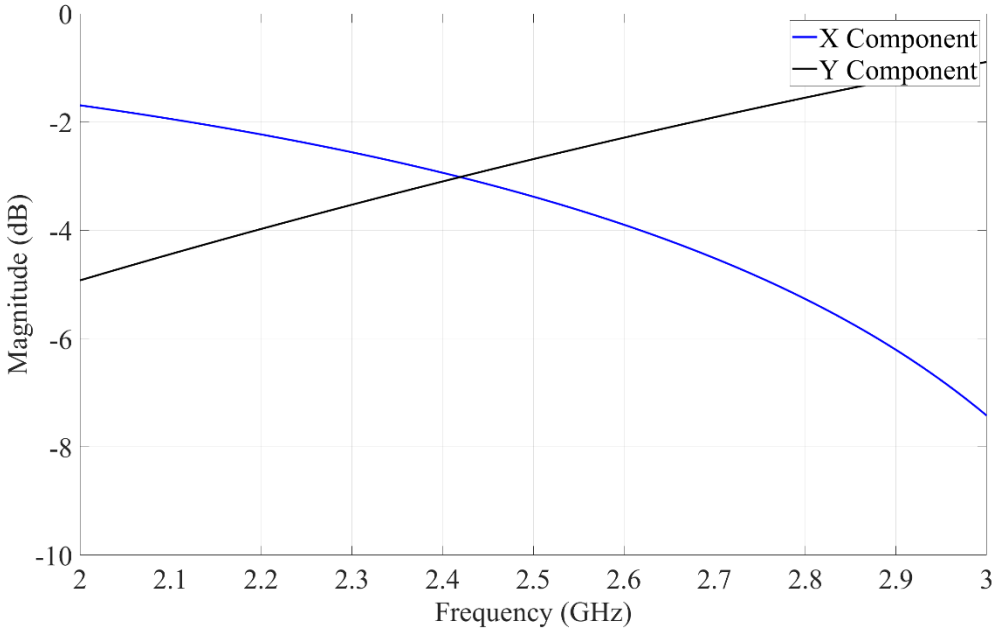

Figure 3.5 Simulated reflected E-field components with the metasurface in open state

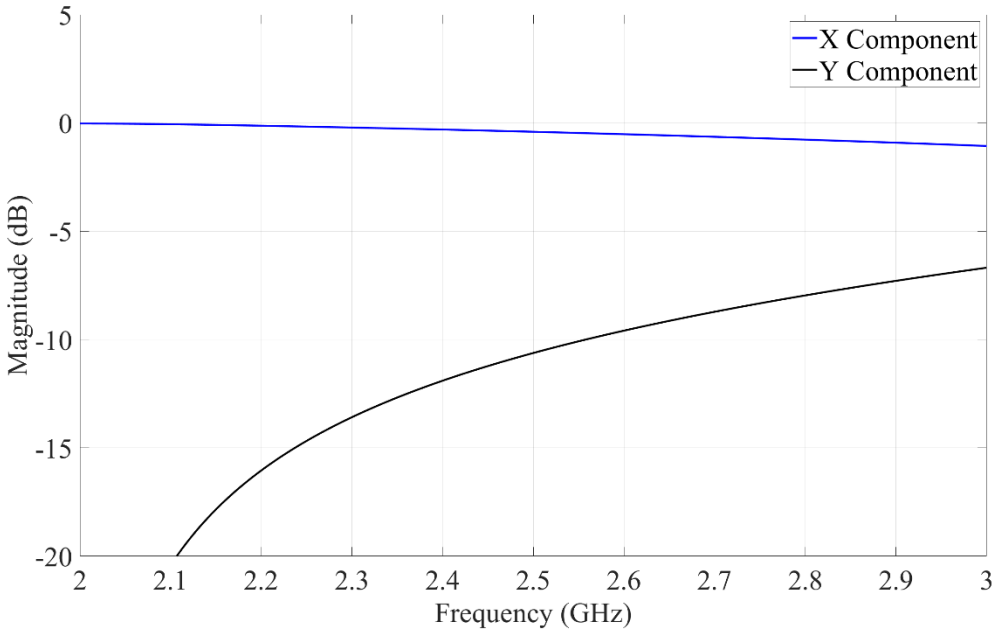

Figure 3.6 Simulated reflected E-field components with the metasurface in closed state

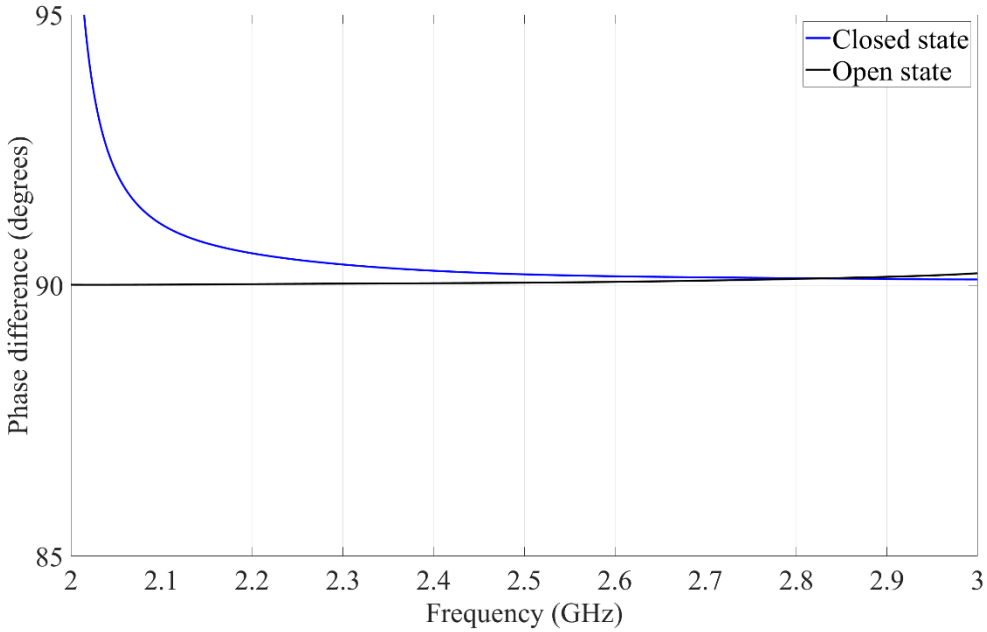

Figure 3.7 Phase difference between the simulated *x* and *y* E-field components with the metasurface in open and closed state

The axial ratio of the metasurface in an open state and closed state is shown in Figure 3.8. The surface in an open state produces an axial ratio bandwidth of 30% from 2.03 GHz to 2.75 GHz. The closed state also produces a high axial ratio, which shows that the reflective metasurface will be linearly polarized within the operating band.

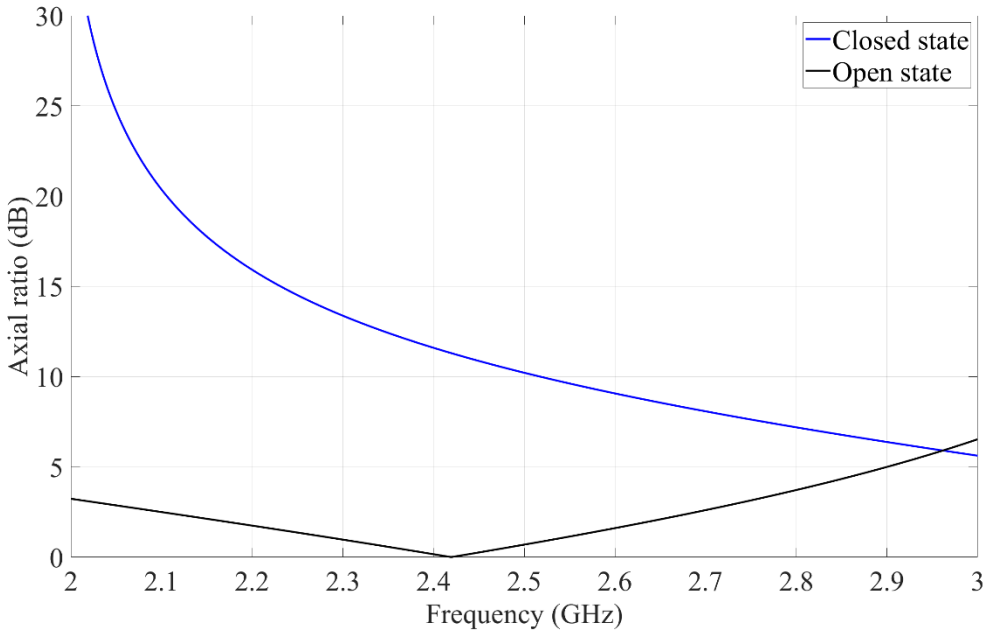

Figure 3.8 Simulated axial ratio of reflective metasurface in a closed and open state

The simulation results of the designed reflective metasurface produced good results. The metasurface can reflect an incident wave with a 45° incident polarization angle into a circular wave when the unit cell switches are open and into a linear horizontal polarized wave when the switches are closed.

3.4 ANTENNA DESIGN

3.4.1 Antenna structure

As mentioned, the antenna is made up of two layers, namely a reflective metasurface and a planar dipole. Using the starting set of parameters, the reflective metasurface can be combined with a dipole element to design the antenna. The structure of the completed antenna design is shown in Figure 3.9.

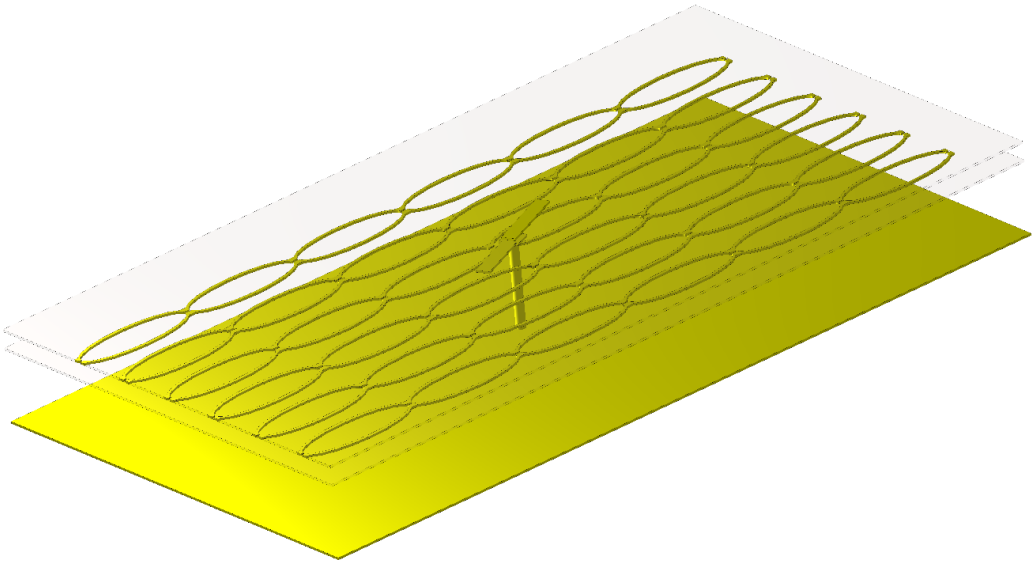

Figure 3.9 3D Antenna structure as modelled in CST Studio Suite

The spacing between the unit cells and the reflector, as well as the spacing between the metasurface and the dipole are critical in the design. For example, if the dipole is placed too far away from the reflective metasurface no sensible reflection is made on the surface. If it is placed too close, the matching and radiation patterns of the antenna are compromised. This requires optimization through simulation. The previous steps in the design process used an infinite number of unit cells in the *x* and *y* directions, however to implement the antenna structure a finite number of unit cells must be used. The optimal number of unit cells was determined to be a 6 x 6 array, as this gave an optimal linear and circular performance. Simulations are performed using CST Studio Suite with open boundary conditions. The radiating element is excited through the use of a coaxial cable with an outer conductor diameter of 3.58 mm, teflon dielectric diameter of 2.58 mm and a conductor diameter of 1 mm. The coaxial cable is excited with a waveguide port with a x and y size double that of the outer conductor diameter. The frequency domain solver is used.

The parameters of the antenna structure are shown in Figure 3.10 and Figure 3.11. Description of these parameters are tabulated in Table 3.9. As part of the design procedure

another parametric study is performed on the critical parameters. Three extra parameters are introduced that are related to the characteristics of the dipole, namely the spacing between the dipole and the surface, the polarization angle of the dipole, and the dipole length. The dipole was designed separately before adding it to the reflective metasurface in order to establish a starting set of parameters. The dipole parameters that were optimized include the matching, axial ratio, and radiation patterns.

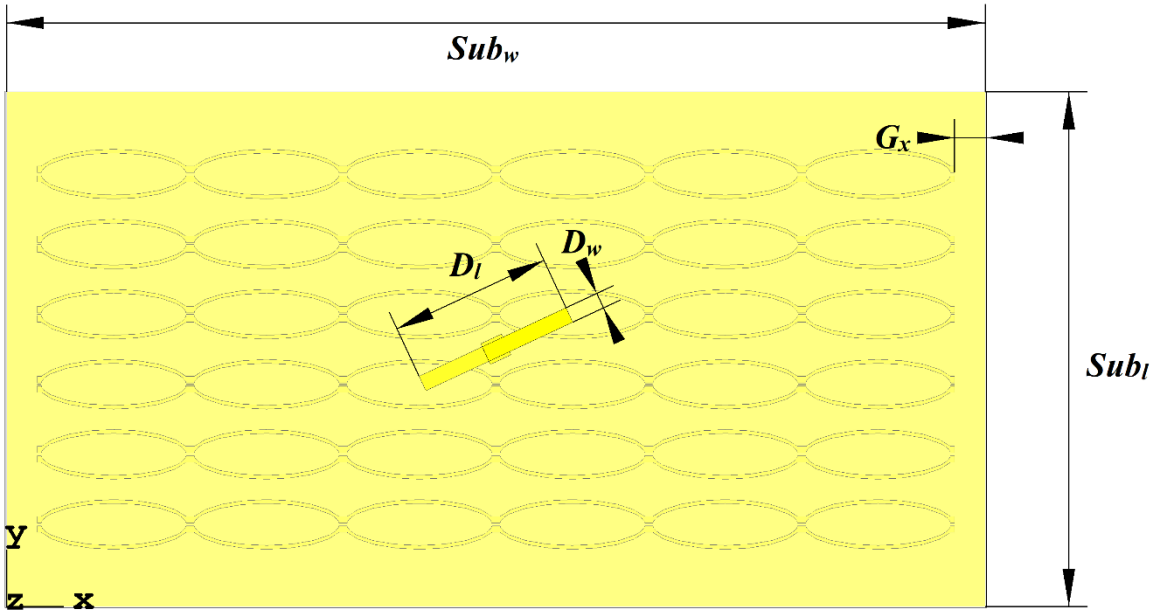

Figure 3.10 Top view of antenna

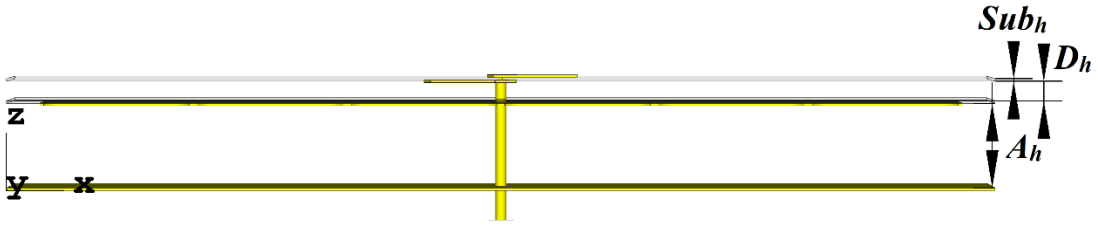

Figure 3.11 Side view of antenna

Table 3.4 Summary of antenna parameters

Parameter	**Description**
A_h	Air gap between unit cell and reflector
H	Unit cell height
R_y	Unit cell ellipse *y* radius
P	Unit cell width
D_h	Air gap between surface and dipole
Sub_h	Substrate height
Sub_w	Substrate width
Sub_l	Substrate length
G_x	Extra substrate
D_l	Dipole length
D_w	Dipole width
Rot	Dipole polarization angle

3.4.2 Parametric study

A detailed parametric study of the proposed antenna structure has to be conducted to better understand the interaction between the dipole and the reflective metasurface. This will assist in designing a functional antenna system. With the initial metasurface design only plane wave incidence was considered. This is however not an accurate representation of the field of a radiating element near a metasurface. Thus, to better understand what effect each parameter has on the system a detailed parametric study is conducted. The final parameters that were obtained with the reflective metasurface design is used with the new parameters that are related to the addition of the dipole element. The dipole parameters are tabulated in Table 3.5

Table 3.5 Dipole parameters

Parameter	Description	Value
Rot	Dipole polarization angle	45°
D_h	Air gap between surface and radiator	10 mm
D_l	Dipole length	56.5 mm
D_w	Dipole width	3 mm

As with the metasurface design, the main design goal of the antenna system is the axial ratio. The main objective is to get an antenna system with a functional axial ratio in both the open and closed states. Subsequently, the focus of the parametric study will be on the axial ratio of the system. The axial ratio is simulated at a zero degree angle of $\theta = 0°$. When the axial ratio is between 0 dB and 3 dB circular polarization is produced, between 3 dB and 10 dB elliptical polarization is produced and anything above 10 dB is considered linear polarization. The critical parameters that are studied are tabulated in Table 3.6. The sweep ranges of the parametric study were chosen to constraint the design to a practical and implementable antenna system. Each parameter was swept independently.

Table 3.6 Parametric study initial value and sweep range

Parameter	Description	Starting value	Sweep range
Rot	Dipole polarization angle	45°	0° to 90°
A_h	Air gap between unit cell and reflector	15 mm	10 to 40 mm
D_h	Air gap between surface and radiator	10 mm	1 to 15 mm
P	Unit cell width	52 mm	30 to 60 mm
H	Unit cell height	19 mm	10 to 40 mm
R_y	Unit cell ellipse y radius	8.5 mm	5 to 9.5 mm

Figure 3.12 shows the simulated axial ratio of the closed and open states for the sweep of the polarization angle of the dipole element. It can be seen that in both the closed and open state a maximum is achieved in the axial ratio at 0° and 90° as expected, since the reflective

metasurface ideally requires an incident wave with a polarization angle of 45° to function properly. In the closed state a minimum axial ratio in the order of 20 dB is achieved at a 35° polarization angle. In the open state a minimum is achieved at 30° of roughly 7 dB. Consequently, a linear polarization state will be achieved in the closed state as expected. However, in the open state circular polarization is not achieved, instead elliptical polarization is achieved. This indicates that a minimum in the axial ratio is achieved at a different polarization angle compared to only the reflective metasurface in isolation.

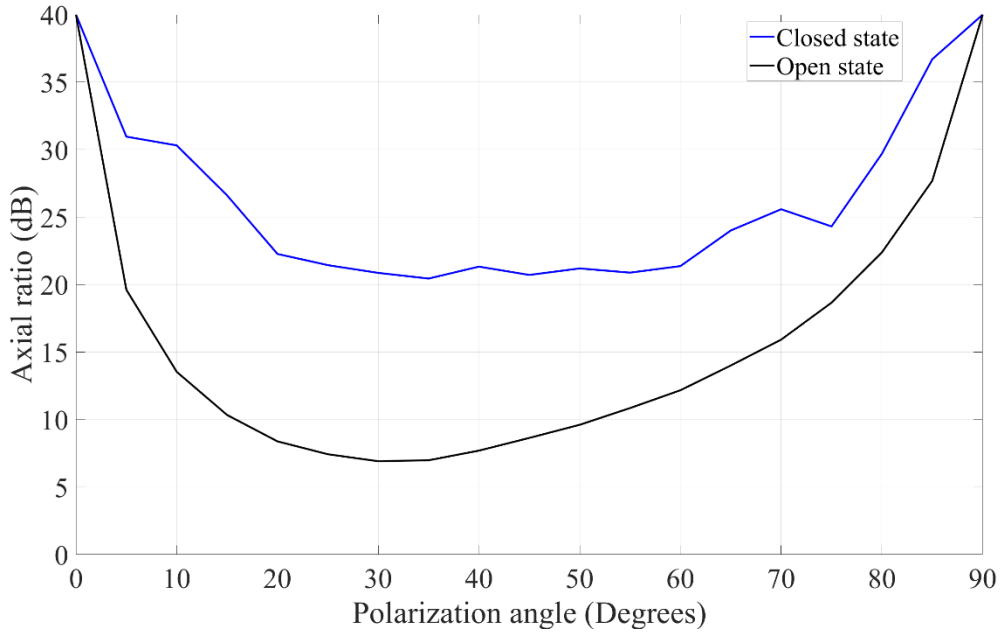

Figure 3.12 Axial ratio as a function of polarization angle

The next parameter that was studied was the air gap between the unit cell and reflector within the reflective metasurface. The results are shown in Figure 3.13. In the closed state the axial ratio has a lot of variance but remains above 10 dB over the sweep range. In the open state a minimum in the axial ratio is achieved at an airgap distance of A_h = 28 mm. This means that in the closed state a linear polarization state will be generated and in the open state a circular polarization state will be generated. It can be seen that both *Rot* and A_h will be critical parameters for minimizing the axial ratio in the open state of the antenna system.

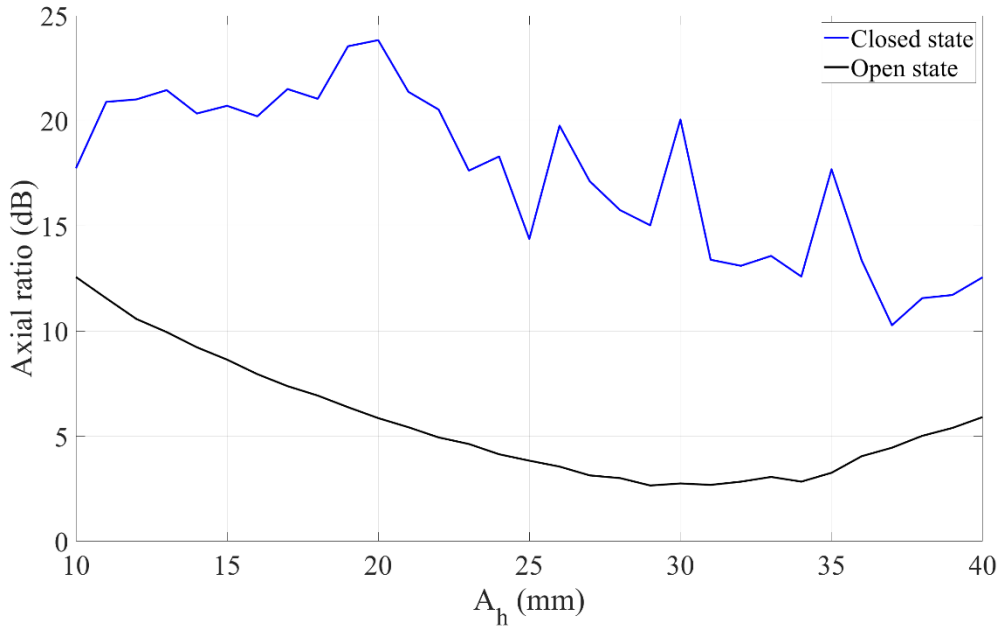

Figure 3.13 Axial ratio as a function of the air gap between the unit cell and reflector

The next parameter that was studied is the air gap between the reflective metasurface and the dipole element. The results are provided in Figure 3.14. Here it can be seen that axial ratio decreases for both the closed and open states as the air gap increases. However, the air gap between the reflective metasurface and the dipole has a minimal effect on the axial ratio.

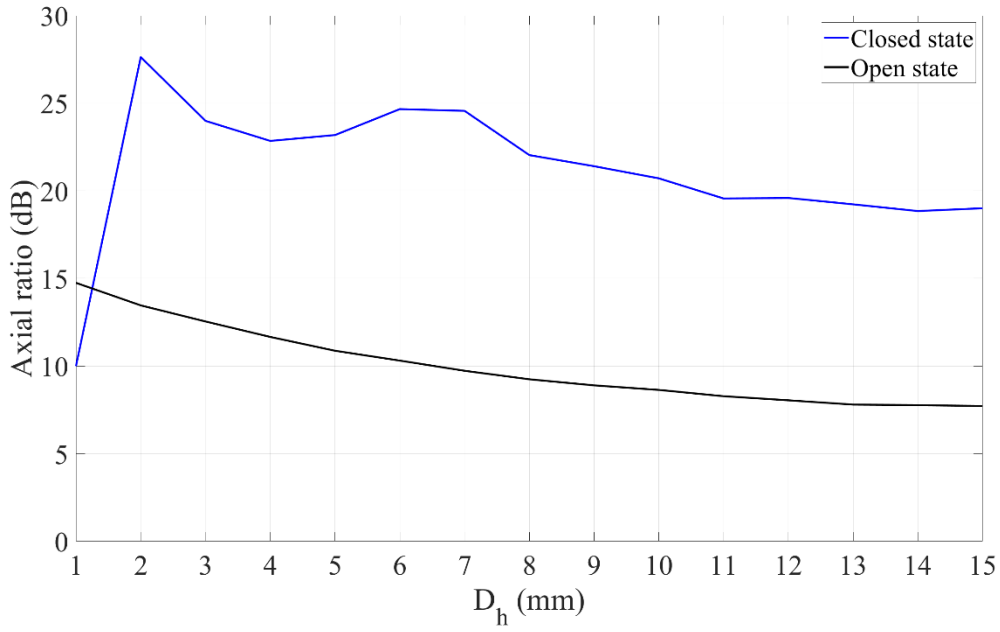

Figure 3.14 Axial ratio as a function of the air gap between the metasurface and dipole radiator

Figure 3.15 shows the simulated relationship between the axial ratio and the unit cell width. In the closed state a lot of variance is observed with some widths producing an axial ratio that would produce an elliptical polarization state. In the open state the axial ratio remains stable between 5 dB and 10 dB. This indicates that the unit cell width will be critical in achieving a functioning linear polarization state for the antenna system but will not affect the circular performance significantly.

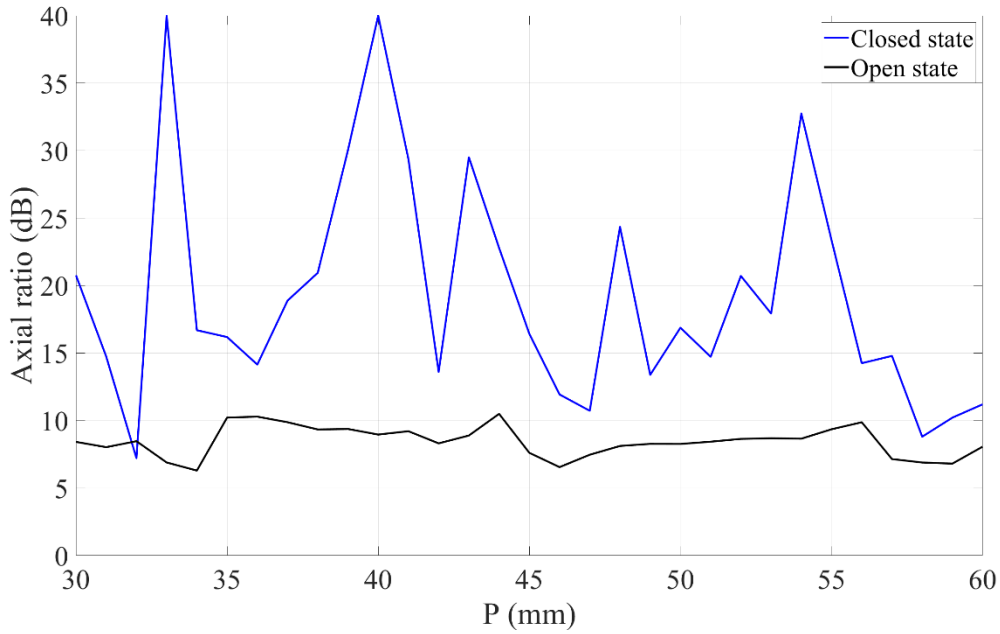

Figure 3.15 Axial ratio vs unit cell width

Figure 3.16 shows the parametric results of the axial ratio as a function of the unit cell height. A similar trend to the unit cell width can be observed with the unit cell height, where in the closed state a lot of variance is observed in the axial ratio. However, since the axial ratio remains larger than 10 dB over the sweep range, this will result in a linear polarization state. In the open state the axial ratio remains stable between 5 dB and 10 dB which indicates the unit cell width will have a minor effect on the open state of the antenna and mostly affects the closed state.

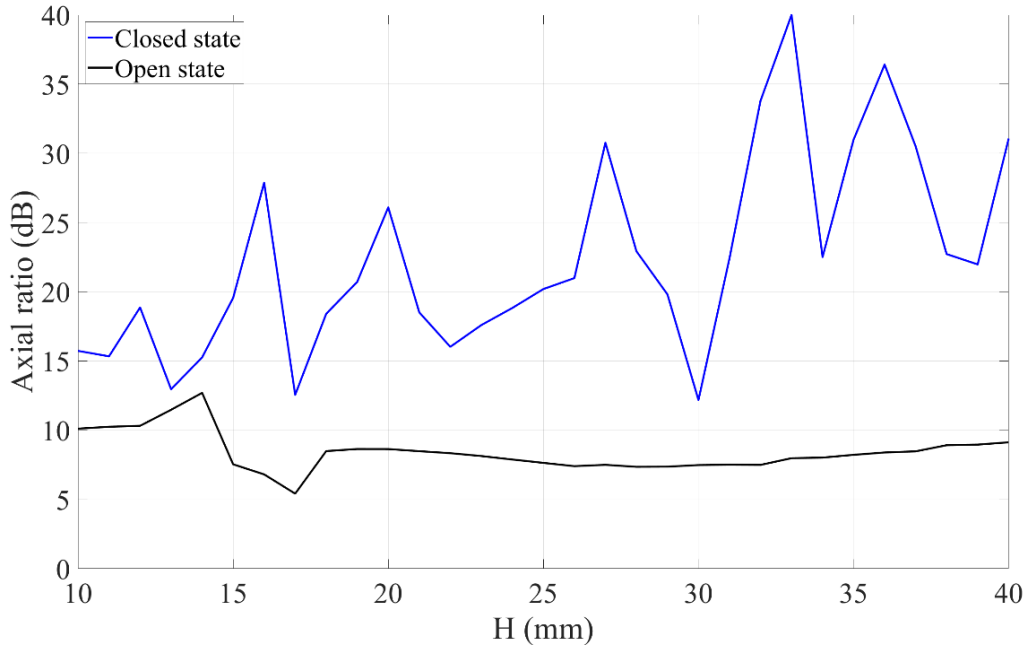

Figure 3.16 Axial ratio vs unit cell height

The final parameter that was studied is the vertical radius of the ellipse of the unit cell. This parameter is constrained by the unit cell height that was initially chosen, as the radius cannot exceed the unit cell height. Figure 3.17 shows the results of the parametric study. In the closed state a maximum is observed in the axial ratio at a vertical radius of $R_y = 6.5mm$.

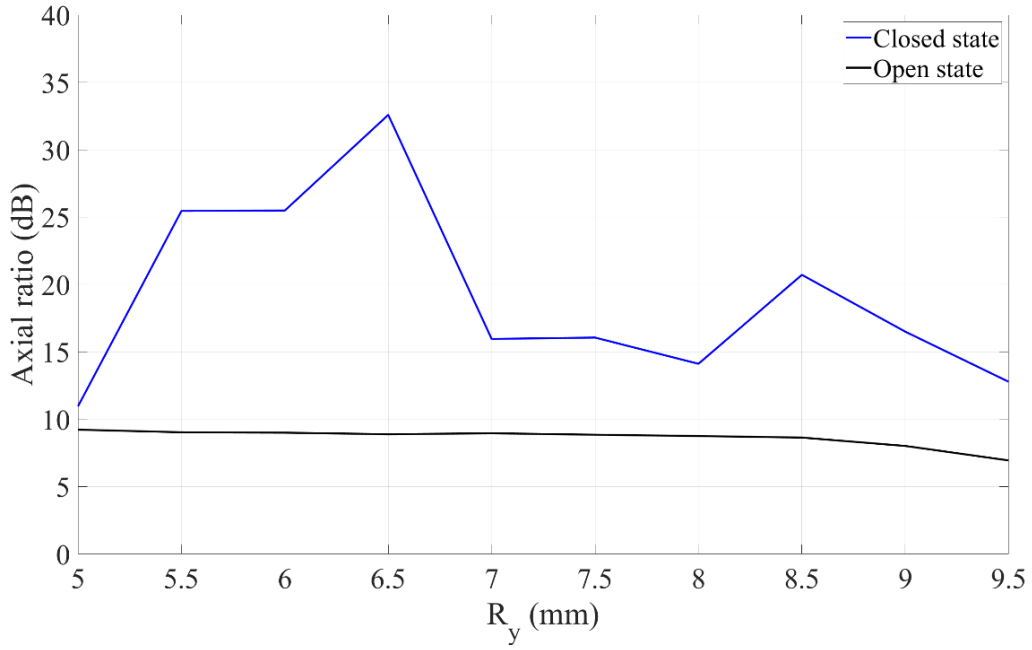

Figure 3.17 Axial ratio vs unit cell *y* ellipse radius

The parametric study resulted in a better understanding of the effect that each parameter has on the axial ratio of the antenna system. From this study it was found that *Rot* and A_h has the greatest effect on the axial ratio in the open state, which can be used to maximize the circular performance of the antenna system. In the closed state the effect on the axial ratio is less. D_h has a minimal effect on both the closed and open states of the antenna system. *P*, *H*, and R_y has the greatest effect on the closed state, which can be used to maximize the linear performance as the circular performance is stable for changes to these parameters.

The next step of the antenna design is to find a suitable solution for the antenna system. Using the results from the parametric study a set of critical parameters is extracted to perform a sequential tuning of the antenna parameters to determine a suitable solution for the antenna. The new set of critical parameters are summarized in Table 3.7.

Table 3.7 Critical parameter set

Parameter	Value
Rot	30°
A_h	30 mm
D_h	10 mm
P	54 mm
H	24 mm
R_y	9 mm

3.4.3 Initial antenna design

With a starting parameter set extracted from the results of the parametric study, the antenna can be improved further. The first step in the design procedure will focus on the axial ratio of the antenna system. As the structure of the antenna is electrically large (≈3λ) with multiple parameters, rather than using an optimization algorithm a sequential parameter study was performed to reduce the simulation time and computational cost. The parameters are also interrelated to each other, thus changing one parameter might mean another parameter has to be slightly adjusted to compensate. The parameters are adjusted in a specific sequence related to the previous study in section 3.4.3. The sequence of the parameters are as follows: *Rot*, A_h, D_h, *P*, *H*, and R_y. The sequence is repeated multiple times and tested to ensure the suitable results are obtained.

After an adequate axial ratio is achieved the matching of the antenna is then adjusted to achieve an optimal impedance bandwidth at the design frequency of 2.4 GHz. Adjusting the matching of antenna separately has little effect on the axial ratio performance of the antenna in closed and open states. This is due to that the main mechanism of polarization reconfigurability is through the reflective metasurface. The values of the parameters are given in Table 3.8. The results of the parameter set are discussed below.

Table 3.8 Parameter set for axial ratio and antenna matching for first design iteration

Parameter	Description	Value
Rot	Incident polarization angle of dipole	35°
A_h	Air gap between unit cell and reflector	26 mm
P	Unit cell width	48 mm
H	Unit cell height	24 mm
R_y	Unit cell ellipse *y* radius	6 mm
D_h	Air gap between surface and radiator	9 mm
D_w	Dipole width	3 mm
D_l	Dipole length	50.75 mm
Sub_h	Substrate height	0.813 mm
Sub_w	Substrate width	308 mm
Sub_l	Substrate length	174 mm
G_x	Extra substrate	10 mm

The first result that is discussed is the reflection coefficient of the antenna. To meet the design goal the impedance bandwidth should be below -10 dB from 2.35 GHz to 2.45 GHz for both closed and open states which equates to a bandwidth of 4.1%. Figure 3.18 shows the reflection coefficient of the antenna system. The closed state produces an impedance bandwidth from 2.345 GHz to 2.490 GHz which equates to an impedance bandwidth of 6%. The open state produces an impedance bandwidth from 2.330 GHz to 2.478 GHz, which equates to a bandwidth of 6.1%.

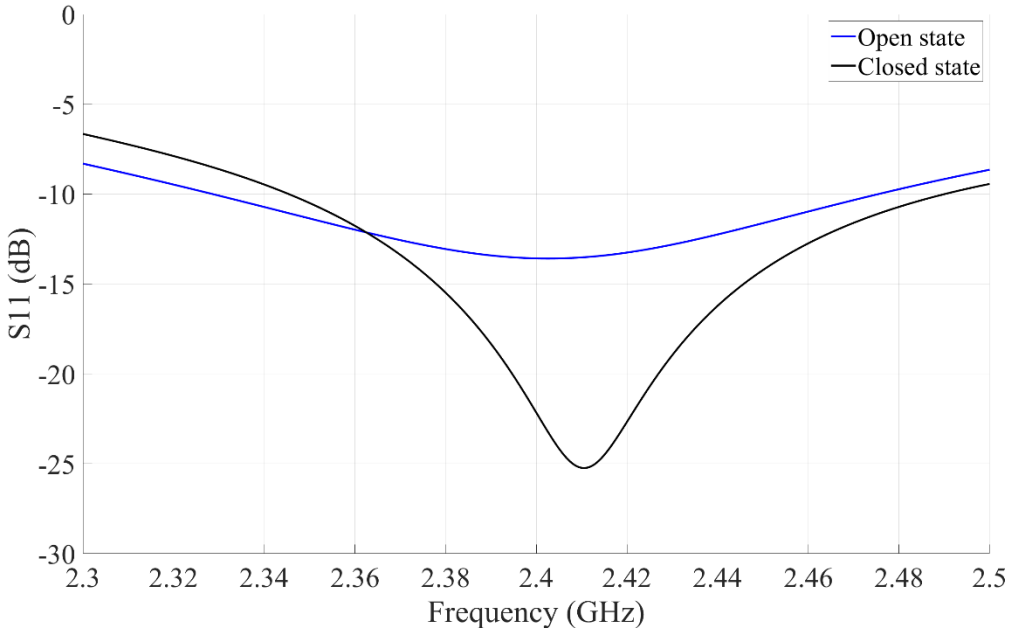

Figure 3.18 Reflection coefficient for initial parameter

As previously discussed for the antenna to be circularly polarized the axial ratio needs to be lower than 3 dB and higher than 10 dB for linear polarization. The design goal is to have an antenna that is linearly and circularly polarized over the operating band from 2.35 GHz to 2.45 GHz. The axial ratio of both closed and open states are shown in Figure 3.19. In the closed state the antenna produces a high axial ratio over the operating bandwidth and a maximum at the centre frequency. This indicates that the antenna should be linearly polarized. The open state produces an axial ratio smaller than 2 dB over the operating bandwidth.

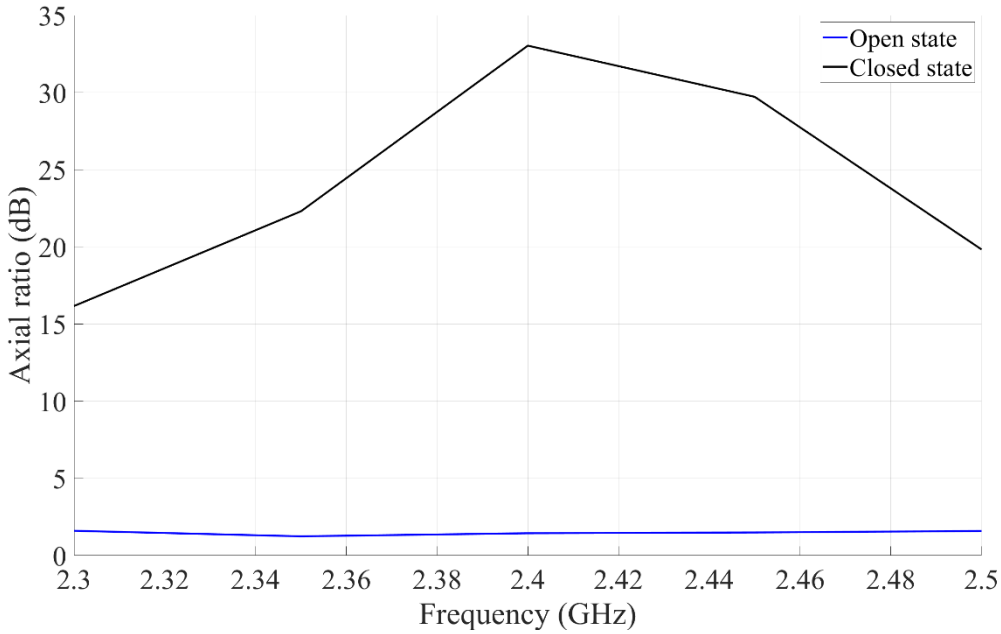

Figure 3.19 Axial ratio performance for initial parameters

Another important antenna metric is the cross-polar discrimination between the co-polarized and cross-polarized patterns in the closed state with linear polarization. The cross-polarization discrimination (XPD) is calculated by taking the difference between the patterns in the broadside direction of the antenna. Only the closed state is calculated as it is one of the design goals for the linear polarization state of the antenna. The goal is to achieve XPD of 15 dB at the centre frequency of 2.4 GHz. Figure 3.20 shows the cross-polar performance of the antenna in the closed state. The XPD is high over the operating band, with a XPD of 14 dB at 2.35 GHz, 23 dB at 2.4 GHz and 25 dB at 2.45 GHz.

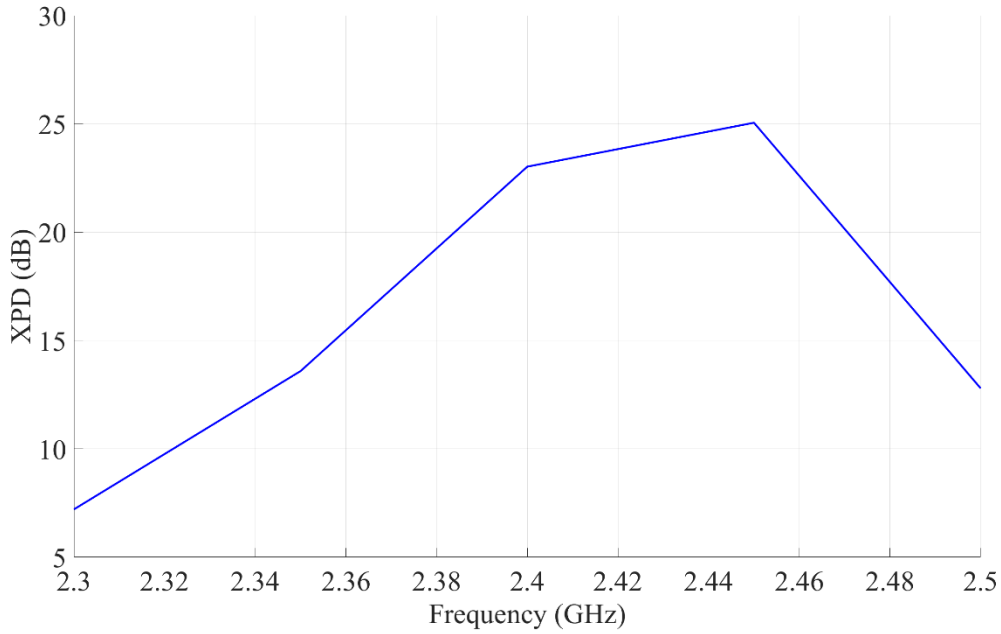

Figure 3.20 Linear cross-polar performance for closed state for initial parameters

The radiation patterns of the antenna are the next part of the design which is critical. While searching for a suitable axial ratio, the radiation patterns were not a priority. In the closed state the antenna should be linear-horizontally polarized. The co-polarized patterns should be unidirectional in the broadside direction whereas the cross-polarized patterns should be at least -10 dB lower than the co-polarized patterns within the half power beamwidth (HPBW) of the co-polarized pattern. In the open state the antenna should be right-hand circularly polarized. The right-hand patterns should be unidirectional in the broadside direction. The left-hand patterns should at least be -10 dB lower than the right-hand patterns within the HPBW of the right-hand pattern.

Shown in Figure 3.21 and Figure 3.22 are the circular patterns for the open state of the antenna. The patterns are taken in the xz-plane (ϕ = 0°) and the yz-plane (ϕ = 90°). The antenna is right-hand circularly polarized with a cross-polarization discrimination of 23 dB in the broadside direction for both cut planes. The circular radiation patterns in the xz-plane have a narrow HPBW with a unidirectional pattern. The radiation patterns in yz-plane improves with a much wider HPBW with a unidirectional pattern. The narrow HPBW

presented in the radiation patterns of the xz-plane can be mitigated at the cost of the circular performance of the antenna. Thus, the narrow beamwidth is accepted for this design as the primary goal is to have a reconfigurable antenna with two polarization states. Overall, the initial patterns produced good results in the circular state of the antenna.

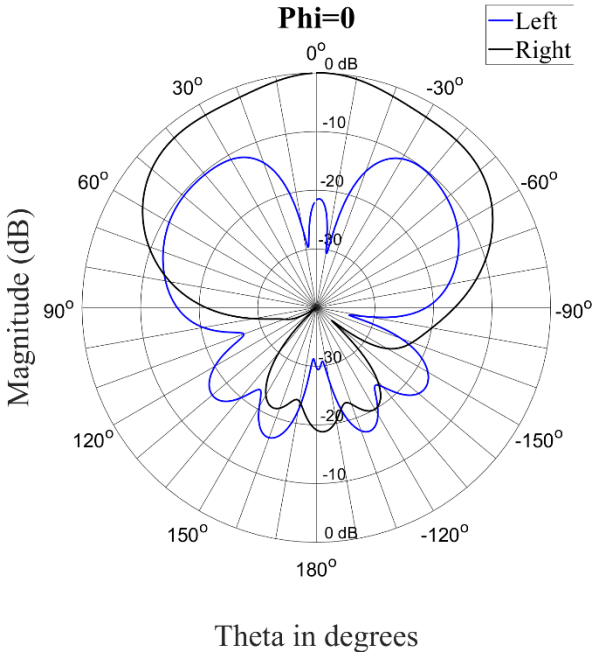

Figure 3.21 Circular radiation patterns at 2.4 GHz with Phi = 0°

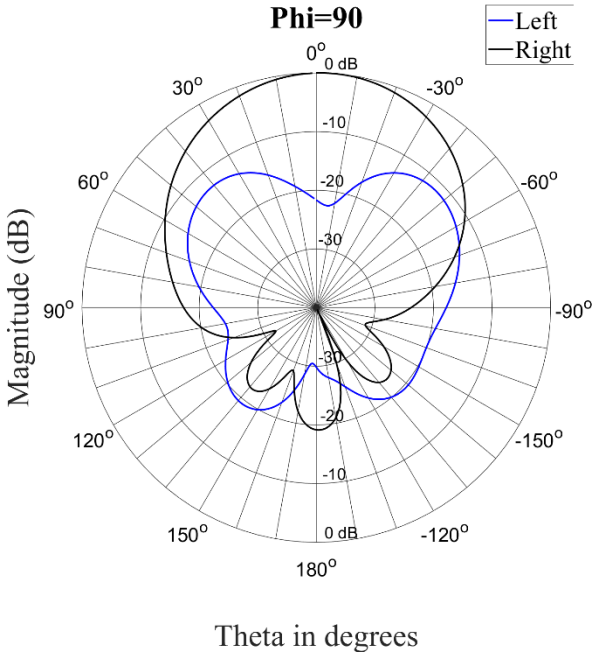

Figure 3.22 Circular radiation patterns at 2.4 GHz with Phi = 90°

The linear radiation patterns of the antenna in the closed state are shown in Figure 3.24 and Figure 3.25, at Phi = 0^{o} and 90^{o}, respectively. The antenna is linear-horizontal polarized. The linear radiation patterns produced a similar trend as the circular patterns. The patterns in the yz-plane remain unidirectional with a wider HPBW with a good cross-polar performance over the 3 dB beamwidth of the pattern. However, the patterns also degrade in the xz-plane as seen in the circular state of the antenna. With the linear state, two side lobes are also produced. Since these lobes are outside the beamwidth of the antenna, they will not affect the cross-polar performance and the functionality of the antenna as required. However, the lobes will create a bad dual polarized antenna in the direction of the main lobes rather than a good linear-horizontal polarized antenna. Thus, the antenna needs to be further improved.

The design process shows that a functional antenna can be obtained following the design steps that are discussed in the previous sections. The main lobes in cross-polarized patterns are not acceptable and it does not meet the design goals of the antenna. Thus, a final design iteration is required to improve the cross-polarized patterns.

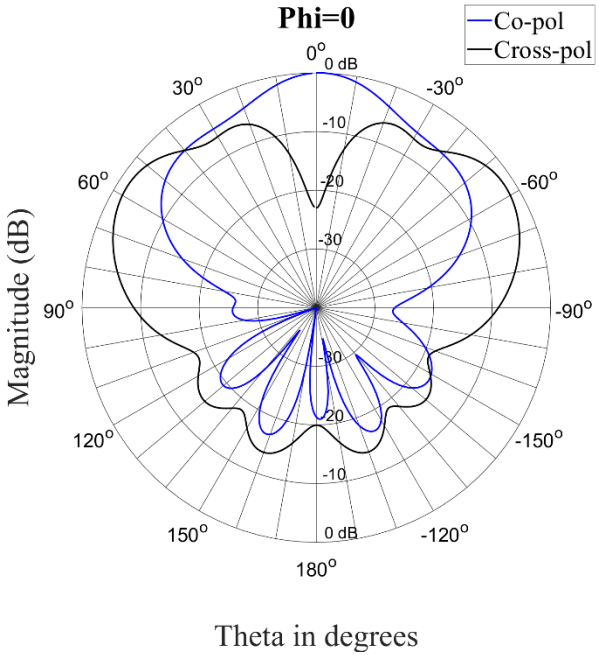

Figure 3.23 Linear radiation patterns at 2.4 GHz for Phi = 0°

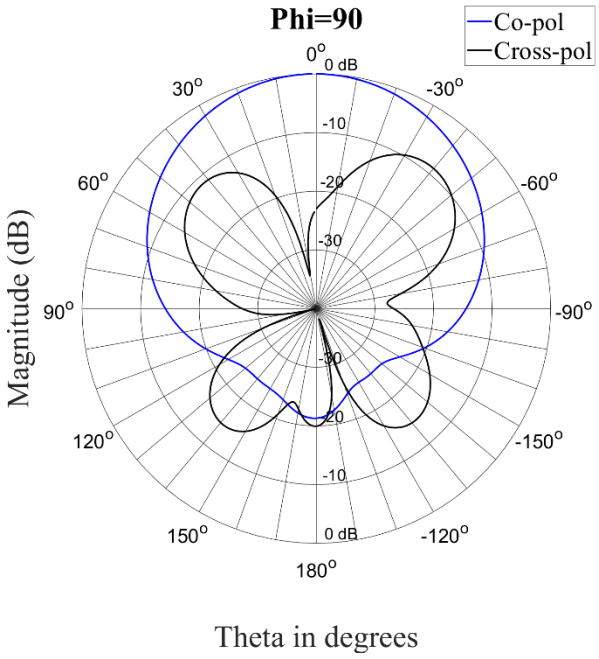

Figure 3.24 Linear radiation patterns at 2.4 GHz for Phi = 90°

3.4.4 Final antenna design

In this section the details of the final design iteration of the antenna is discussed. The focus of this iteration was on achieving suitable radiation patterns, whereas the previous iteration focused only on the axial ratio of the antenna. Again, an iterative process is followed where the parameters are adjusted the same sequence as before. The sequence of the parameters are as follows: *Rot*, A_h, D_h, *P*, *H*, and R_y. The final design iteration is also done manually instead of using an algorithm to limit simulation time. For this iteration the radiation patterns and axial ratio was both considered. During the design iteration there were a few parameter sets that could potentially produce an antenna which met the design goals if they were investigated further. Thus, the presented solution is not the only solution, but the one that was selected to be analysed further. The final parameter set is tabulated in Table 3.9. The final design iteration focused on improving the radiation patterns to meet the design goals with a more balanced performance between the circular and linear states.

Table 3.9 Final antenna parameter set

Parameter	Description	Final design iteration	Initial design iteration
Rot	Incident polarization angle of dipole	25°	35°
A_h	Air gap between unit cell and reflector	27 mm	26 mm
P	Unit cell width	48 mm	48 mm
H	Unit cell height	22 mm	24 mm
R_y	Unit cell ellipse *y* radius	7.8 mm	6 mm
D_h	Air gap between surface and dipole	6 mm	9 mm
D_w	Dipole width	4 mm	3 mm
D_l	Dipole length	50.85 mm	50.75 mm
Sub_h	Substrate height	0.813 mm	0.813 mm
Sub_w	Substrate width	308 mm	308 mm
Sub_l	Substrate length	162 mm	174 mm
G_x	Extra substrate length	10 mm	10 mm

Shown in Figure 3.25 is the reflection coefficient of the final design. The circular state was designed with a mid-point at 2.4 GHz and achieved a bandwidth of 6%. With the design either the circular or linear state's reflection coefficient could be designed at the design frequency, not both. The linear state had a slight offset with a reduced bandwidth of 3.7%. With the antenna design the linear state always operates with a smaller bandwidth.

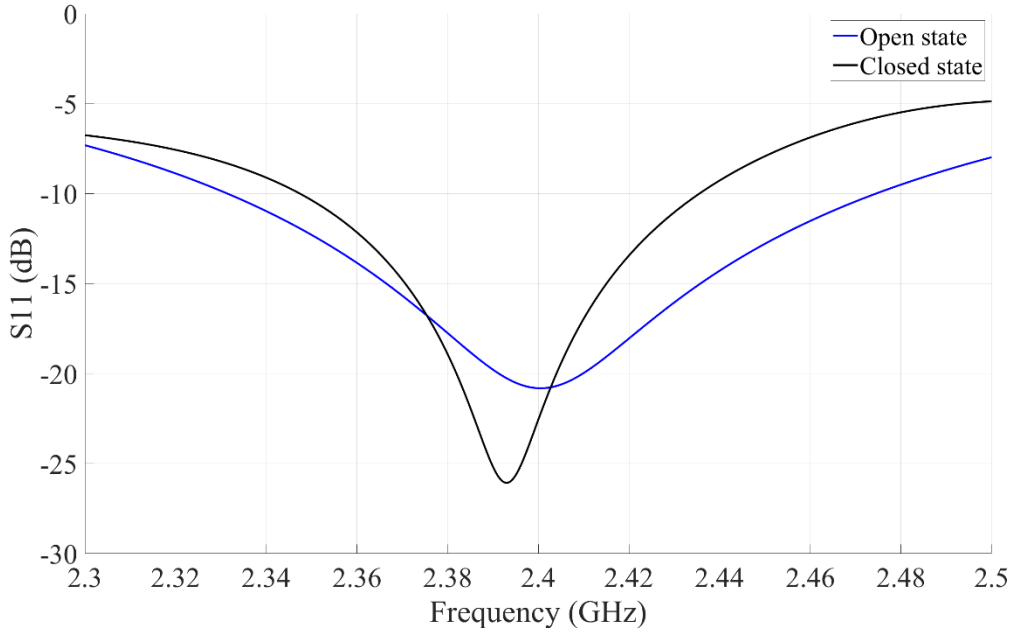

Figure 3.25 Reflection coefficient for final parameters

The simulated axial ratio performance of the final antenna is shown in Figure 3.26. The axial ratio was designed and achieves the lowest point at the design frequency of 2.4 GHz. It produces an adequate bandwidth over the whole operating band, which is limited by the reflection coefficient of the antenna.

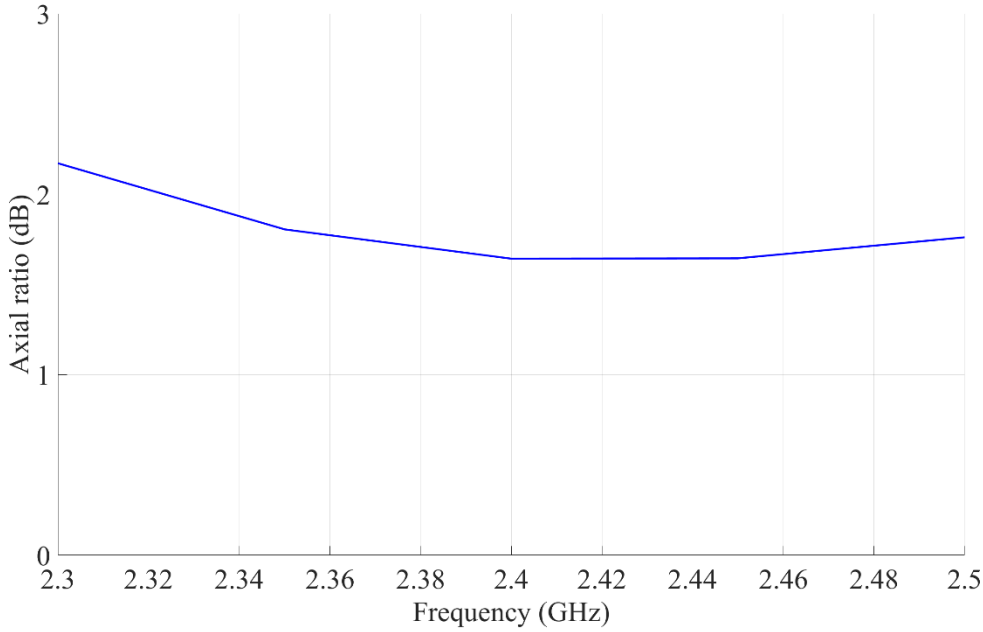

Figure 3.26 Axial ratio performance for final parameters

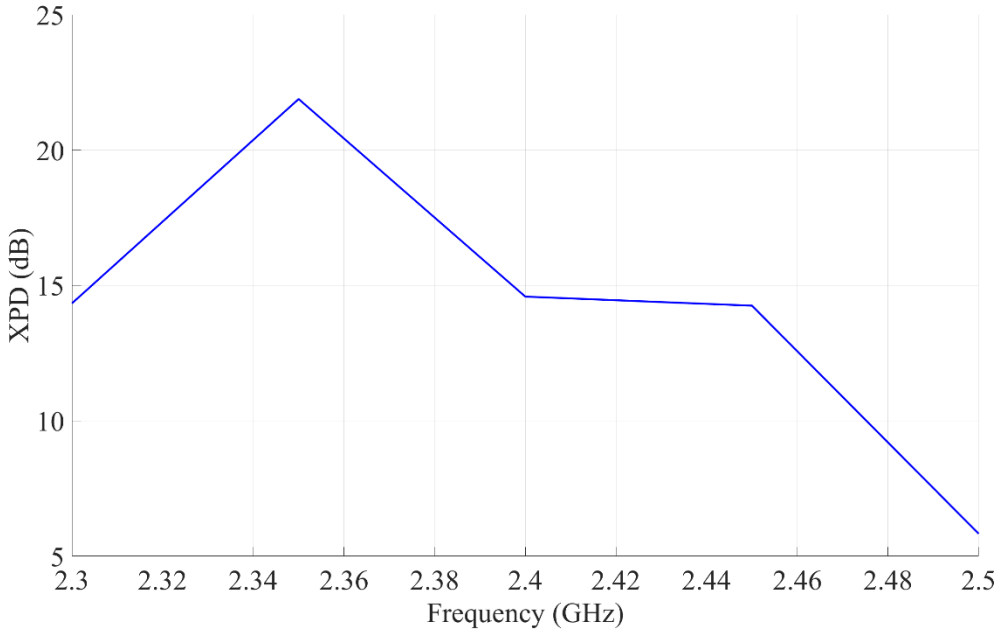

Figure 3.27 Linear cross-polar discrimination for final parameters

The cross-polar discrimination in the linear state of the antenna is reduced from the initial design, as a more balanced approach was taken for this iteration of the antenna design. If this design iteration only focused on one polarization mode of the antenna, the performance of the other mode could be degraded. With the design it is possible to obtain a better circular state with an axial ratio closer to 0 dB at the design frequency, but this creates a linear state with a much lower axial ratio and cross-polar discrimination at the design frequency. The cross-polar performance in the linear state of the antenna is shown in Figure 3.27, here it can be seen that the performance is still satisfactory with a XPD of approximately 15 dB.

In this design iteration a small improvement in the radiation patterns of the antenna is observed. The radiation patterns are shown in Figure 3.28 and Figure 3.29. The circular cross-polar discrimination in the broadside direction between the left and right patterns remained very similar. The side lobe levels of the left polarized patterns were reduced. The optimization process also created a radiation pattern in the xz-plane with a narrower HPBW. Shown in Figure 3.30 and Figure 3.31 is the final 3D radiation patterns where the performance seen in 2D patterns is also mirrored.

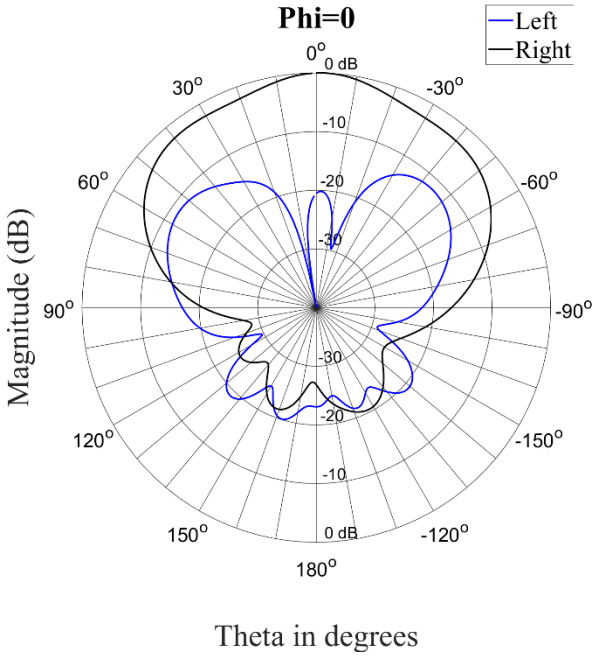

Figure 3.28 Final circular radiation patterns at 2.4 GHz for Phi = 0°

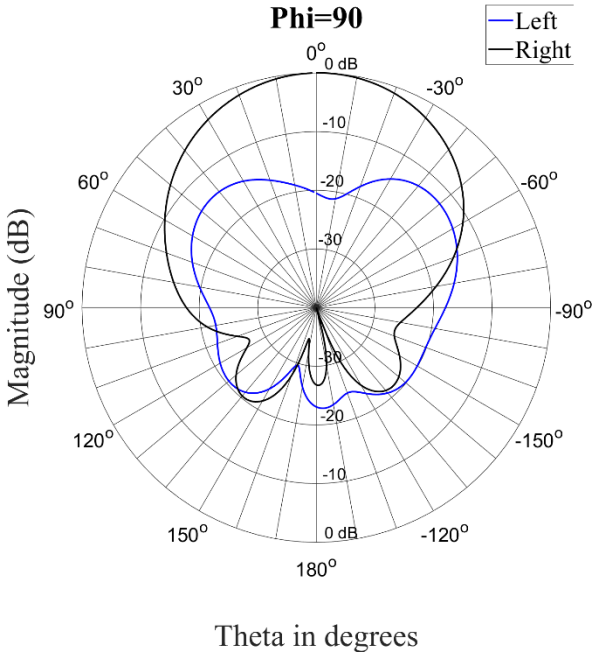

Figure 3.29 Final circular radiation patterns at 2.4 GHz for Phi = 90°

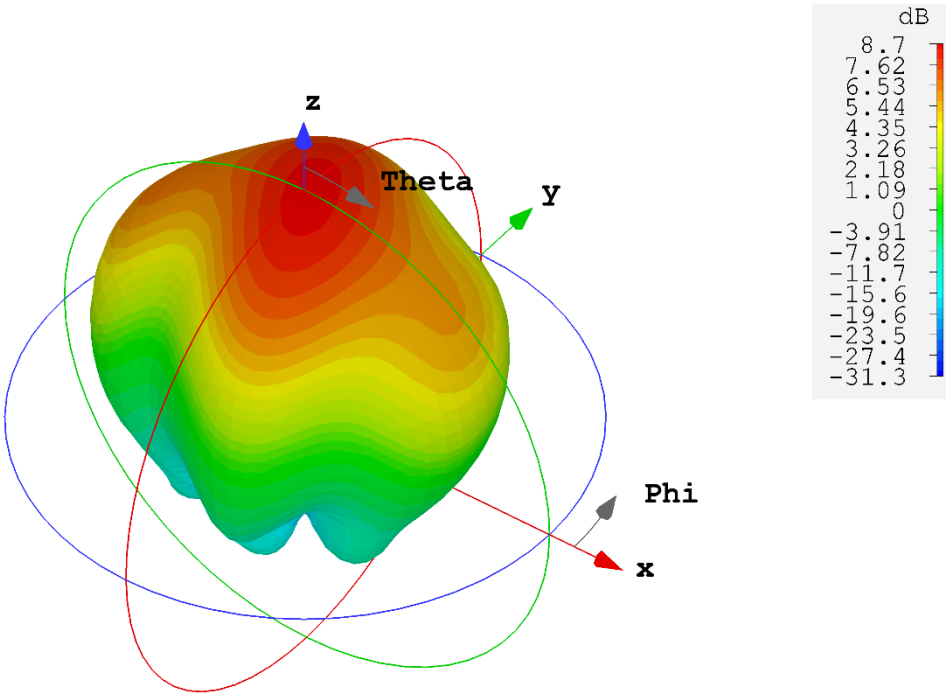

Figure 3.30 Final right hand circularly polarized 3D radiation patterns at 2.4 GHz

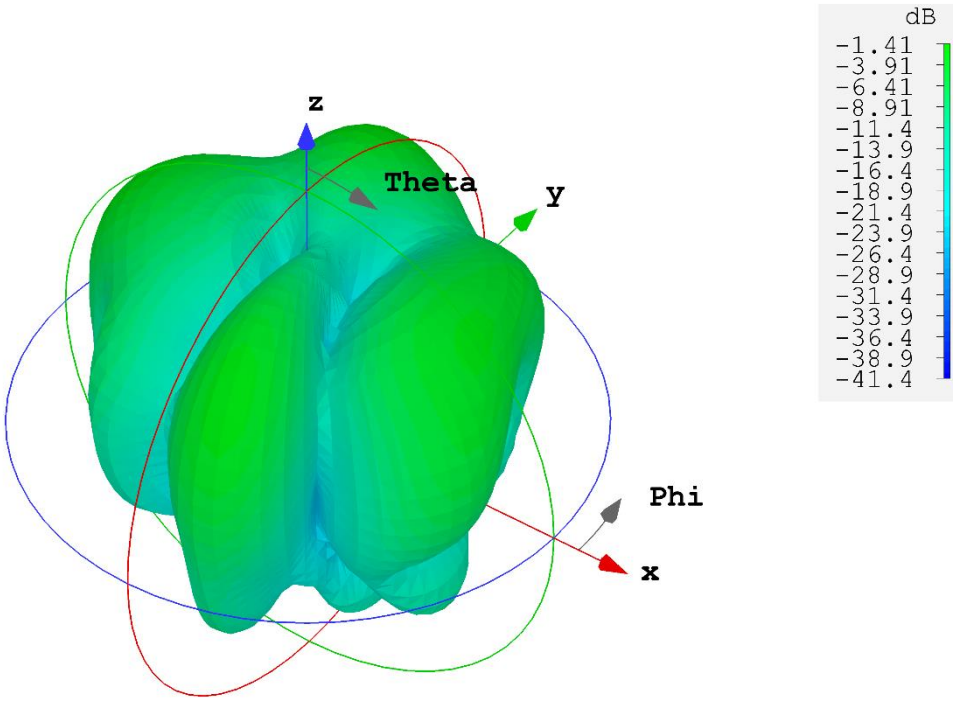

Figure 3.31 Final left hand circularly polarized 3D radiation patterns at 2.4 GHz

Shown in Figure 3.32 and Figure 3.33 are the final radiation patterns for the linear state of the antenna. The larger side lobes that were present with the initial design in the xz-plane are reduced by a significant margin. The radiation patterns within the yz cut plane are also improved to create stable radiation patterns in the broadside direction of the antenna. Shown in Figure 3.34 and Figure 3.35 are the 3D radiation patterns, it can be seen that the cross polarized patterns don't interfere with the co polarized patterns.

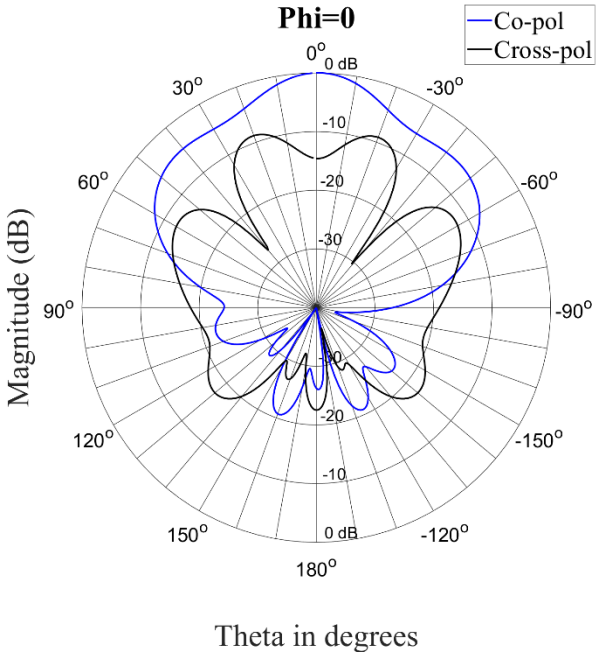

Figure 3.32 Final linear radiation patterns at 2.4 GHz for Phi = 0°

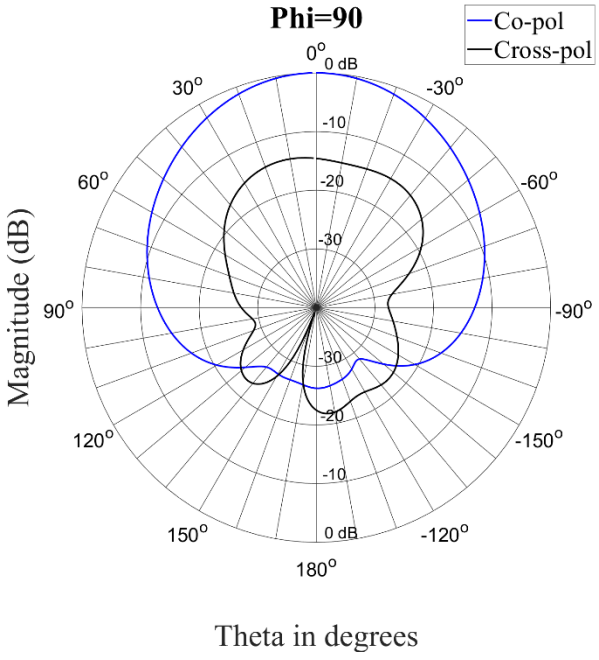

Figure 3.33 Final linear radiation patterns at 2.4 GHz for Phi = 90°

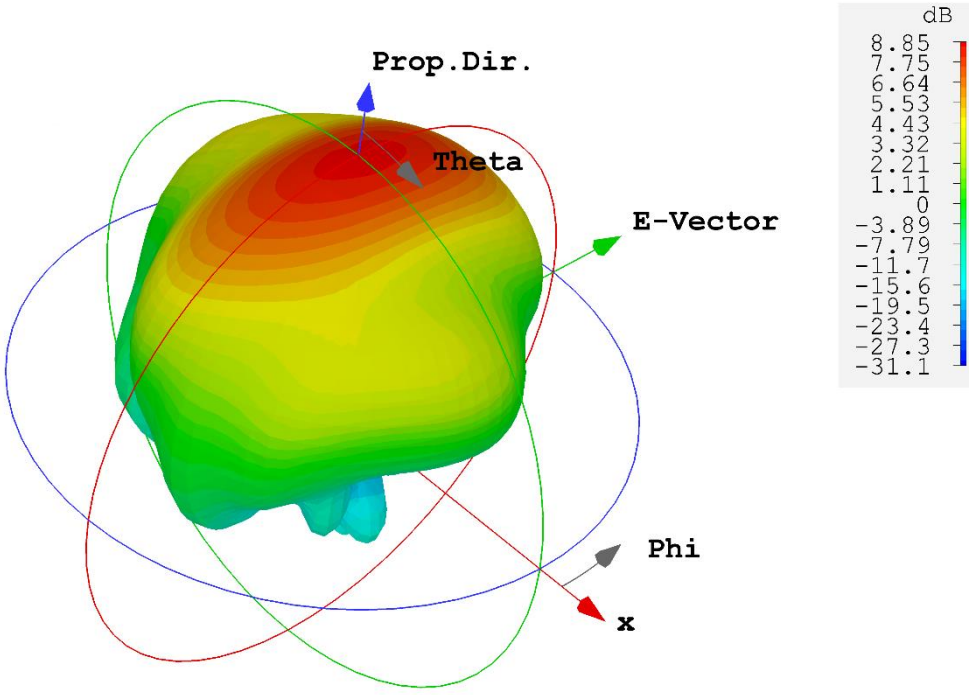

Figure 3.34 Final co-pol linearly polarized 3D radiation patterns at 2.4 GHz

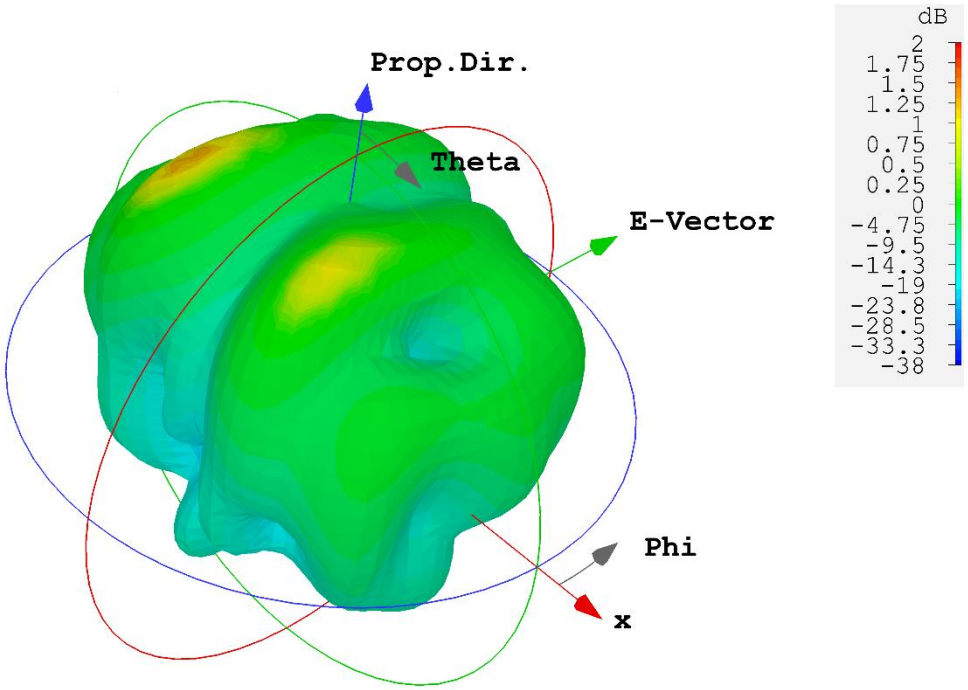

Figure 3.35 Final cross-pol linearly polarized 3D radiation patterns at 2.4 GHz

The final antenna design has to be implemented. The design provided adequate performance in both polarization states of the antenna and demonstrated the concept of the antenna. The design has been designed with ideal switching characteristics where no biasing circuit was required to activate the switched elements. The next section will discuss the technique that is used to implement the switching to achieve antenna reconfigurability

3.5 CHAPTER SUMMARY

The detailed design processed was discussed in this chapter. First, the reflective metasurface derivation was discussed whereby a parametric study was conducted on all the critical parameters of the unit cell. A new antenna structure was then proposed, which combined the reflective metasurface with a dipole. A parametric study was then conducted on the new antenna to better understand the interaction between the dipole and the metasurface. A new parameter set was obtained which was then adjusted to obtain an suitable axial ratio within the operational bandwidth. Although the initial design iteration produced an antenna with

good impedance bandwidth, axial ratio bandwidth, high cross-polar discrimination for the linear state, and acceptable circular patterns, the linear patterns did not meet the design goals. Thus, the antenna was adjusted in a final design iteration to improve the linear patterns and to obtain a final design without any biasing lines for the switching elements.

CHAPTER 4 DETAILS OF SWITCHING ELEMENTS AND BIASING TO ACHIEVE A RECONFIGURABLE ANTENNA

4.1 INTRODUCTION

In order to realize the reconfigurable antenna, switching elements have to be implemented and biased. In this chapter two different types of biasing lines are implemented and modelled and discussed in detail. In Section 4.2 a biasing line in the form of straight wire is used to bias the diodes. Using this method introduced unwanted side lobes into the linear radiation patterns. In Section 4.3 helical coils are used for biasing lines. These biasing lines recreate the radiation patterns that are observed in section 3.4.4 where no biasing line were implemented. These biasing line were critical to feed the PIN diodes on the unit cell elements.

4.2 VERTICAL VIA BIASING LINES

The first feeding method implemented used straight wires/vias. The six rows of diodes were connected in parallel through the use of vertical vias, which are routed through the surface and the ground plane of the antenna. The structure is shown in Figure 4.1.

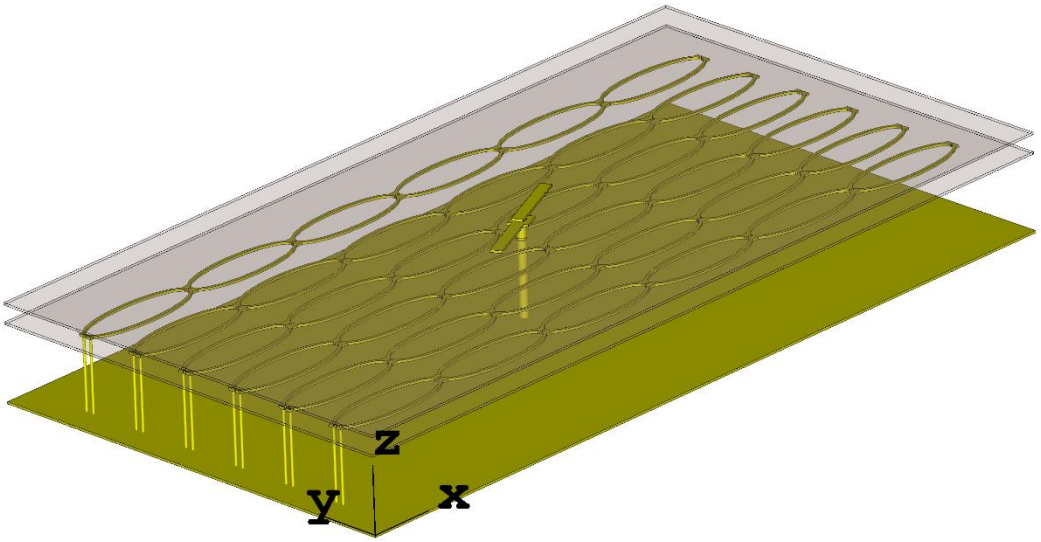

Figure 4.1 Antenna with vertical biasing lines

Shown in Figure 4.2 and Figure 4.3 are the radiation patterns for the antenna with the switches biased with vertical vias in the circular state. The presence of the vias alters the radiation patterns of the antenna in both states of the antenna. The initial design produced patterns with a narrow HPBW in the xz-plane, while the design with the vertical vias produces circular patterns with a wider HPBW. The patterns in both the xz and yz-plane are more uniform than the antenna without vias. The overall performance of the antenna in the circular state is mostly unaffected by the addition of the vertical via biasing lines.

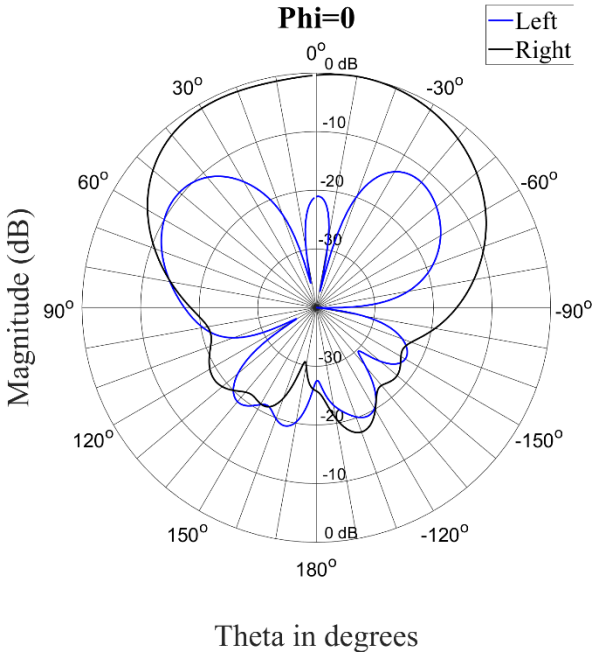

Figure 4.2 Circular radiation patterns at 2.4 GHz with via fed switches for Phi = 0°

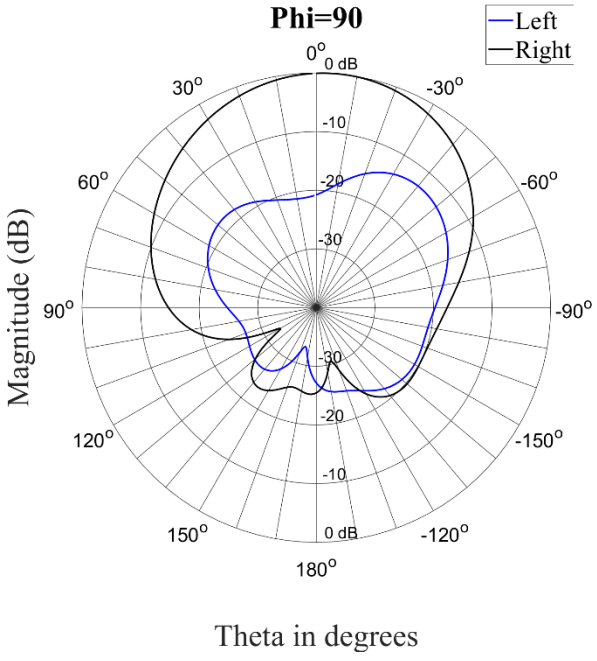

Figure 4.3 Circular radiation patterns at 2.4 GHz with via fed switches for Phi = 90°

The performance of the antenna in the linear state is affected more by the addition of the vertical vias to the antenna. The biggest change in performance is seen in the radiation

patterns as shown in Figure 4.4 and Figure 4.5. The HPBW is slightly wider in the antenna with the vias. The patterns remain unidirectional.

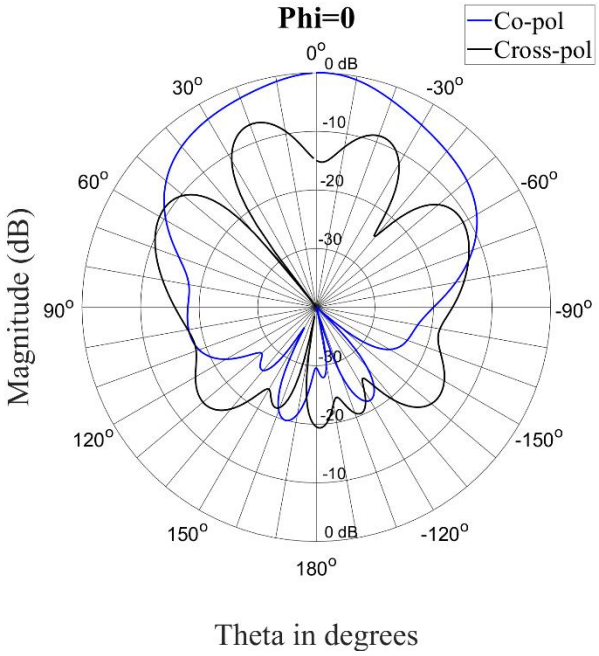

Figure 4.4 Linear radiation patterns at 2.4 GHz with via fed switches for Phi = 0°

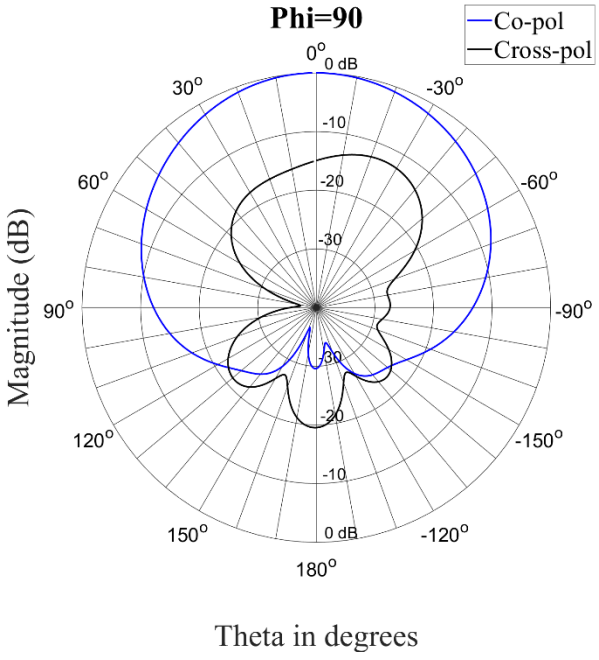

Figure 4.5 Linear radiation patterns at 2.4 GHz with via fed switches for Phi = 90°

The 2D azimuth and elevation cuts through the patterns show that the patterns are altered slightly with the addition of the vias. The axial ratio performance and the cross-polar performance of the antenna remains similar to the design without vias. However, the performance parameters are only measured in the broadside direction of the antenna where the performance remained unchanged.

Only by looking at the 3D cross-polarized patterns in the linear state, an extra side lobe with a higher level can be seen within the operating beamwidth of the antenna as the HPBW is wider. The pattern is shown in Figure 4.6. Compared to the initial design, these side lobes are outside the operational beamwidth of the antenna because of the narrow HPBW of the initial design.

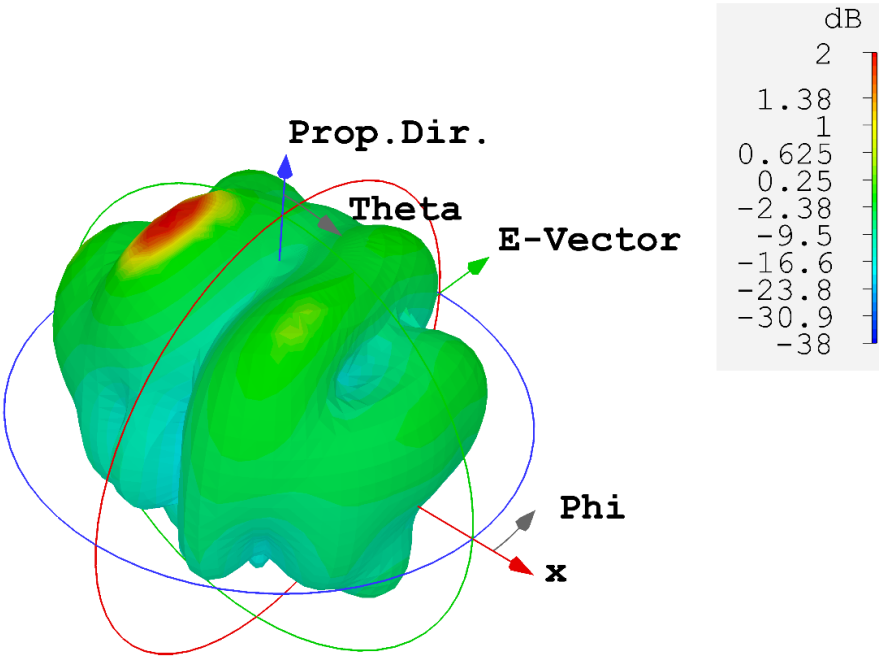

Figure 4.6 3D Cross-polar radiation pattern with via fed switches at 2.4 GHz

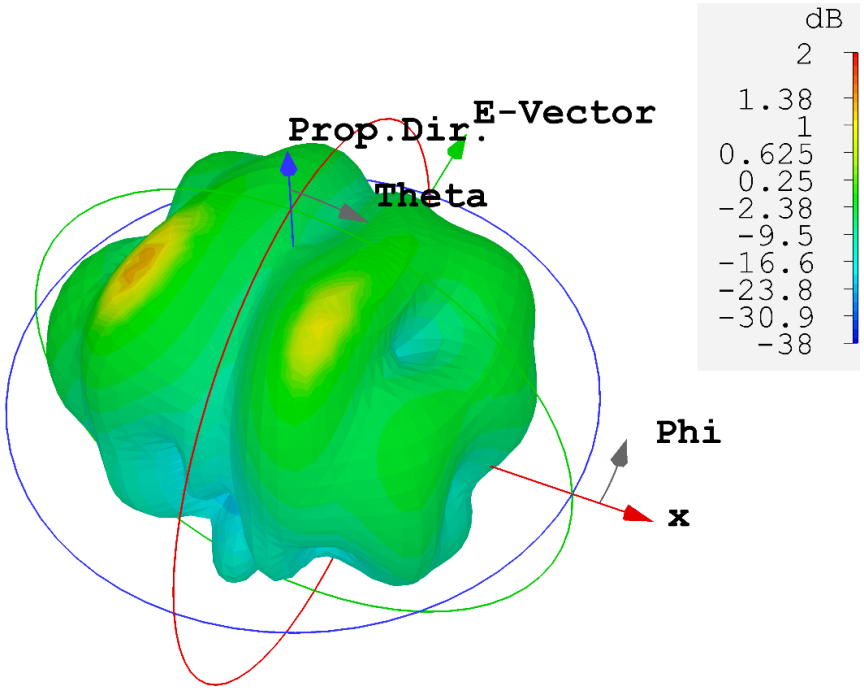

Figure 4.7 3D Cross-polar radiation pattern initial design at 2.4 GHz

4.3 HELICAL COIL BIASING LINES

From the first feeding method it is clear that the PIN diodes and biasing circuity has a negative impact on the performance of the antenna as it produced unwanted sidelobes within the operational beamwidth of the antenna. With the implementation and simulation of the antenna with the via biasing lines, a new challenge was revealed. The linear vias between the surface and ground plane caused RF interference and reflections, which negatively impacts the performance of the antenna. In [10] PIN diodes were used to switch between dipole elements to create an antenna with reconfigurable polarization. RF interference caused by the PIN diodes on the surface of the antenna was also experienced. Ferrite chokes were used successfully to minimize the interference. In [33] a study was conducted on the basic effect of switches on the performance of reconfigurable antennas. To block any RF interference created from the switching elements an inductor in a form of a choke was implemented in series with the biasing circuitry.

Thus, to eliminate and normalize the antenna performance a type of choke in the form of a helical coil feed line is proposed to eliminate the negative effects of the biasing lines. The implemented structure is shown in Figure 4.8 and Figure 4.9. The coils had a diameter of 10 mm and 18 windings. It was found as the windings increased the results improved thus, the maximum number of windings possible was used.

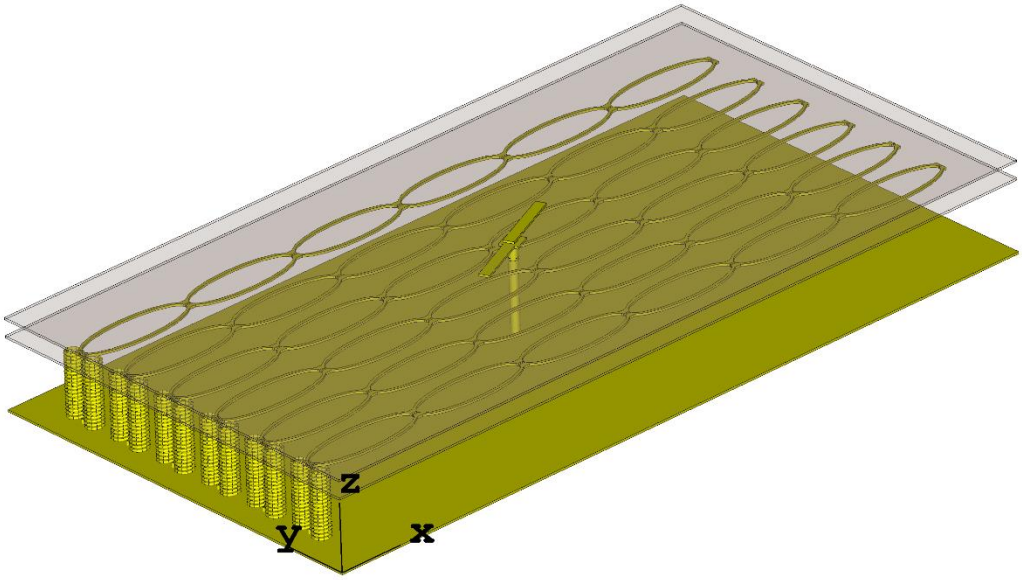

Figure 4.8 Antenna with helical coils for biasing lines

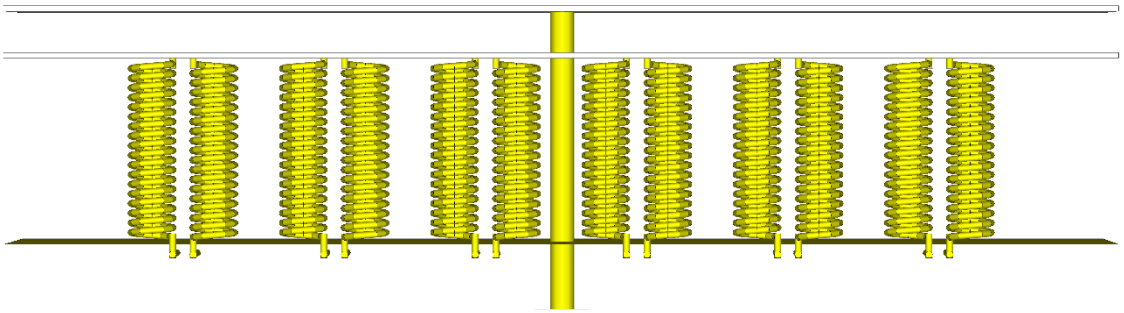

Figure 4.9 Side view of antenna with helical coils for biasing lines

The simulated antenna patterns with the coil solution in the circular state are provided in Figure 4.10 and Figure 4.11. The coils eliminated the effects of the biasing lines on the radiation patterns of the antenna. The results correlate well with the final design without any biasing lines.

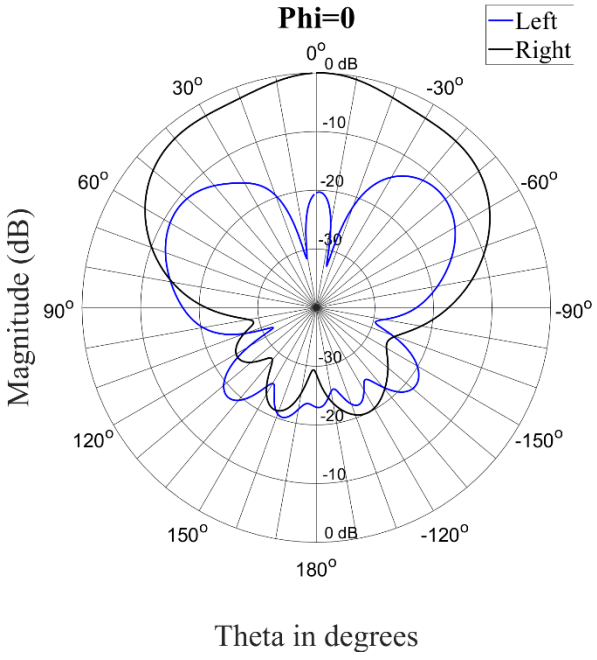

Figure 4.10 Circular radiation patterns at 2.4 GHz with coil fed switches for Phi = 0°

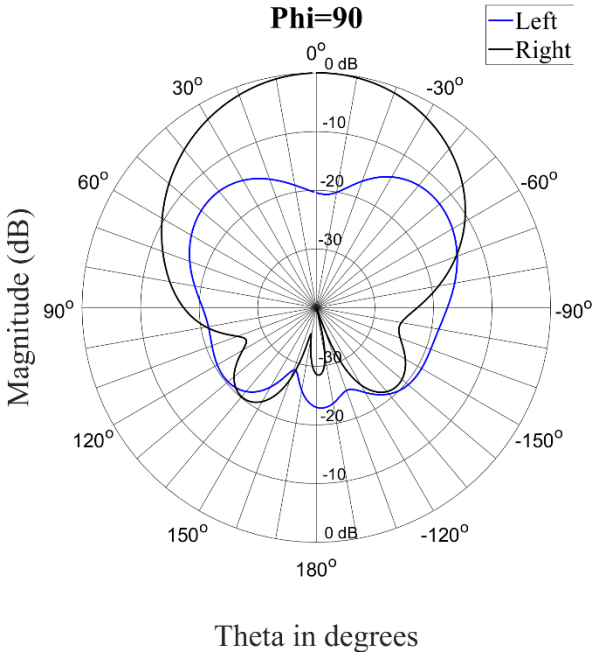

Figure 4.11 Circular radiation patterns at 2.4 GHz with coil fed switches for Phi = 90°

The results for the linear state are shown in Figure 4.12 and Figure 4.13. Again, the results correlate very well with the final design without biasing lines.

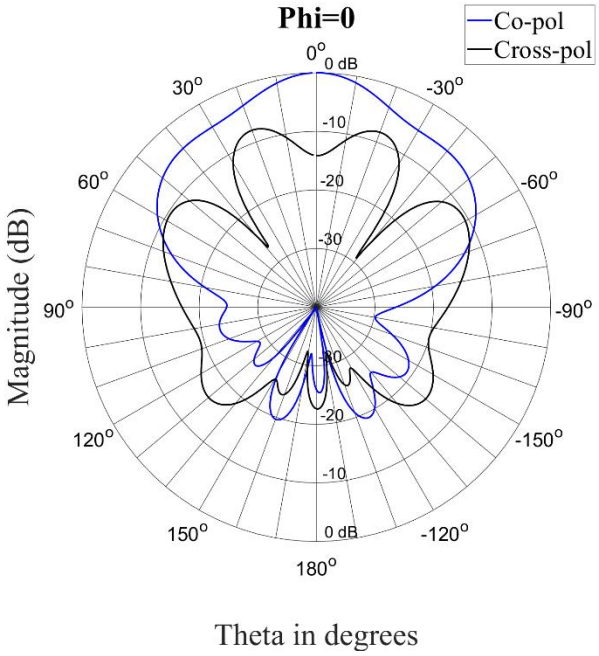

Figure 4.12 Linear radiation patterns at 2.4 GHz with coil fed switches for Phi = 0°

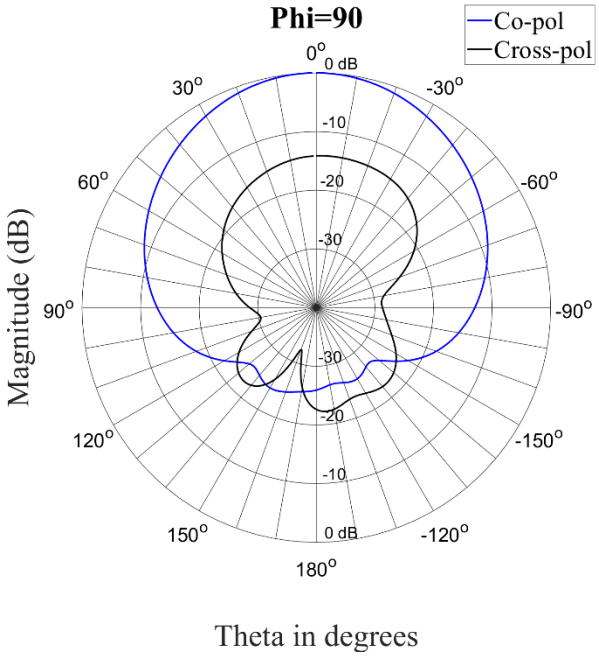

Figure 4.13 Linear radiation patterns at 2.4 GHz with coil fed switches for Phi = 90°

The overall performance of the antenna with the coils is almost identical to the antenna design without any biasing lines. The cross-polar discrimination and axial ratio correlated well with the initial design. To design an effective antenna, it is critical to implement the helical coils to mitigate the effect of any biasing lines on performance of the antenna.

4.4 CHAPTER SUMMARY

In this chapter the implementation of the PIN diodes are discussed. It was found that some biasing methods introduced negative effects on the linear radiation patterns. Two biasing methods were investigated, the first was straight wire/vias and the second helical coils. The vias had a detrimental effect on the radiation patterns, mostly in the linear state of the antenna. A mitigating solution in form of helical coils was then implemented to eliminate the negative effects of the linear vias. The coils produced favourable results and were therefore selected to be implemented as the biasing method for the PIN diodes. The design could then be manufactured.

CHAPTER 5 MEASURED RESULTS

5.1 INTRODUCTION

With the theoretical design completed the antenna was manufactured and measured. Three versions of the antenna were manufactured and measured. The same metasurface and radiating element was used with only the switching elements changed between the three versions. The first version was the antenna with no biasing circuitry, which used copper strips to emulate the switches. The second version was the antenna where straight wires was used as the feeding method for the switches, and the third version used the helical coils as a method of feeding the switches. Both biasing methods were implemented in manufacturing to better understand the operation of the biasing circuitry which was studied in Chapter 4. The implementation challenges as well as measured results are discussed in detail in this Chapter. The measurement setup is shown in Figure 5.1. All measurements were conducted at the Compact Range at the University of Pretoria.

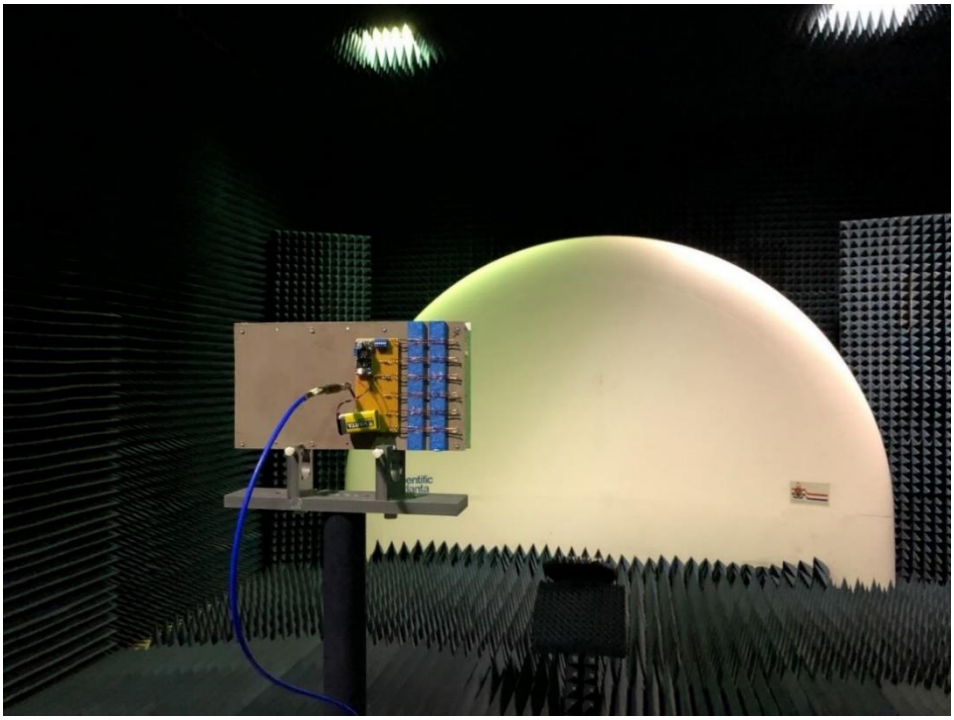

Figure 5.1 Antenna measurement setup

5.2 MANUFACTURED ANTENNA

The antenna was manufactured on ROGERS 4003C substrate with a height of 0.813 mm and copper thickness of 35µm. It is critical to implement the switching elements with the structure of the antenna. A PIN diode was selected as the switching element as it is easily controlled with biasing using a low junction voltage. The PIN diode selected for the antenna system is a BAR65 with a junction voltage and current draw of 0.93V and 100mA, respectively. This diode has a compact SC79 packaging, which will have a very small footprint on the structure. When the diode is biased it acts as a closed switch, thus to control the antenna polarization, a DC voltage has to be applied to all the switchable elements. Each row of unit cells requires roughly 0.65 W to turn on the PIN diodes. To do this a buck converter capable of a 5A output was used with the voltage adjusted to 1.25V. This then requires a series resistance of 0.45 Ω to limit the forward current to roughly 100mA. The current path through the coils has a measured resistance of 0.5 Ω thus no current limiting resistor is required. To power the buck converter a 9V battery with a rating of 600mAh is

used which will be sufficient for the short periods the antenna is in the linear state. The antenna was also powered through a bench power supply to verify functionality.

The first version of the antenna was manufactured exactly as the theoretical design without PIN diodes. The diodes are emulated with the addition of copper strips at the switch locations. The second version was manufactured with the addition of the PIN diodes on the unit cell structure. The PIN diodes are biased through straight wires that connect everything in a parallel configuration. With the third version, the straight wires were replaced with helical coils. The manufactured antenna with helical coils is shown in Figure 5.2 and Figure 5.3. A section of the metasurface, which is positioned underneath the dipole surface is shown with a soldered PIN diode in Figure 5.4.

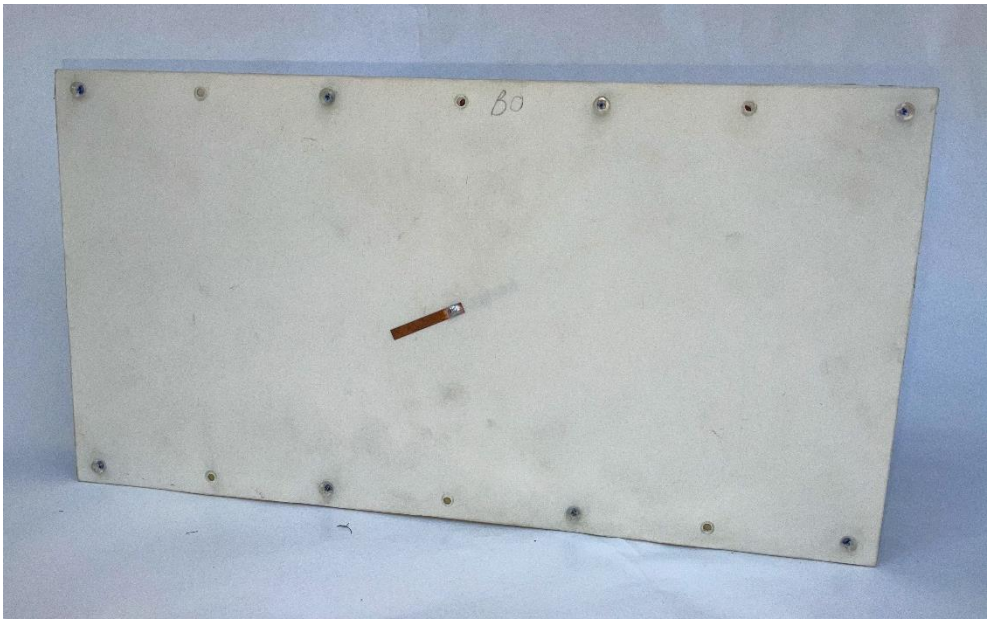

Figure 5.2 Manufactured antenna front view

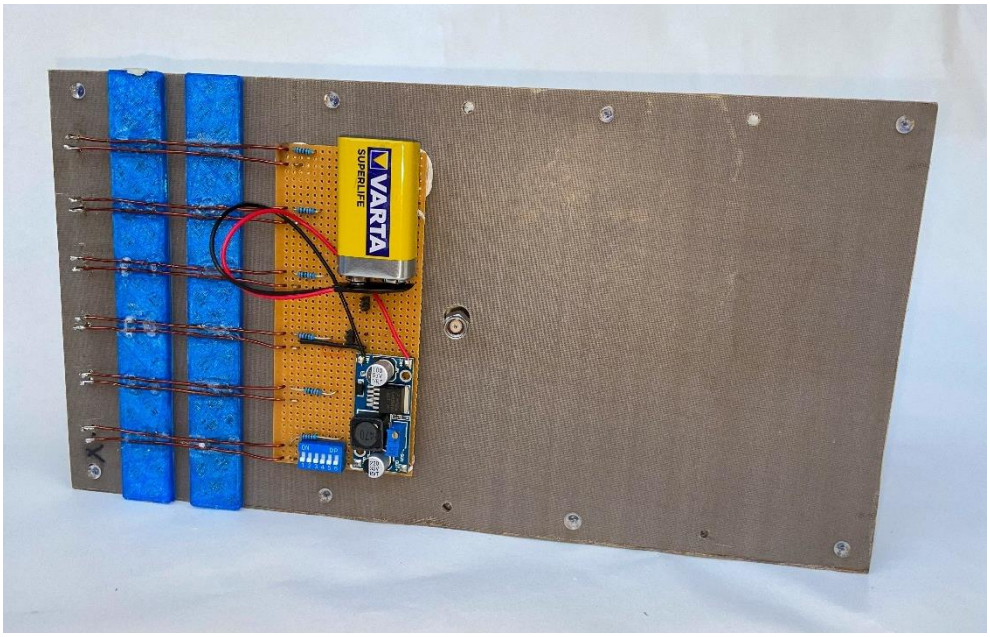

Figure 5.3 Manufactured antenna rear view

Figure 5.4 PIN diode implementation

5.3 MEASURED RESULTS

5.3.1 Reconfigurable antenna with no biasing lines

To verify the initial design and concept that was established in Chapter 3, the antenna was measured with no biasing lines. The switches were implemented using copper tape to short the unit cell connections to obtain the linear state of the antenna, and removed to obtain and measure the circular state.

5.3.1.1 Reflection coefficient

The first measurement that is discussed is the reflection coefficient and the impedance bandwidth of the antenna. The measured and simulated reflection coefficient of the antenna in the linear state is shown in Figure 5.5. An impedance bandwidth, with S11 better than -10 dB, is measured from 2.353 GHz to 2.45 GHz, which equates to a bandwidth of 4%. This is close to the simulated bandwidth of 3.7%. The measured reflection coefficient had a slight offset compared to the simulated one, bringing it closer to designed operation range of 2.35 GHz to 2.45 GHz.

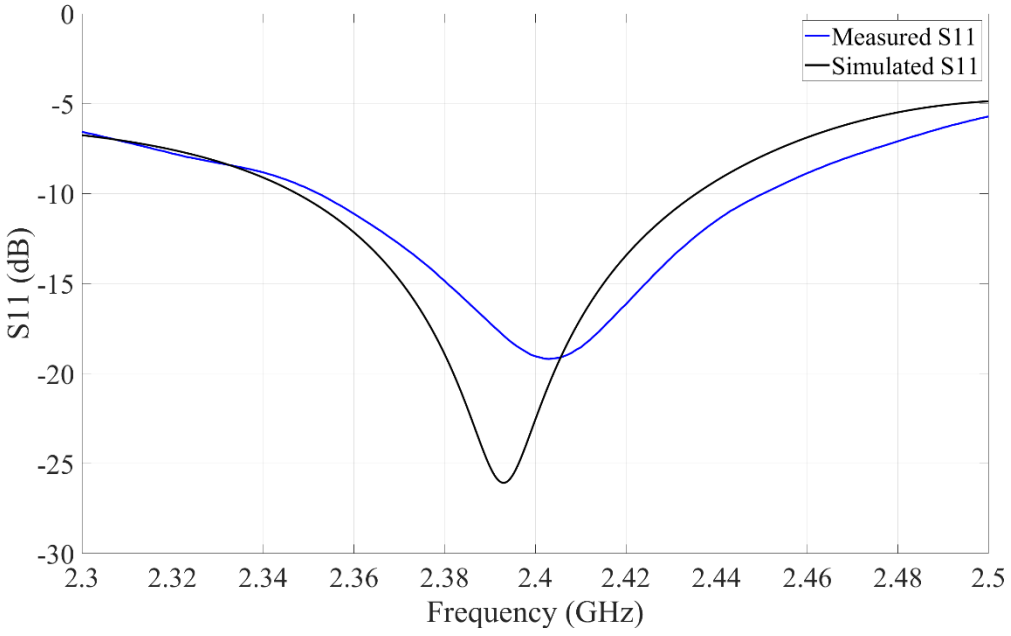

Figure 5.5 Measured and simulated S11 for the antenna with no biasing line in linear state

The measured and simulated reflection coefficient of the antenna in circular state is shown in Figure 5.6. A good correlation is obtained between the measured and simulated results. An impedance bandwidth is measured from 2.317 GHz to 2.466 GHz, resulting in a 6.2% bandwidth, which is very similar to the simulated 6%.

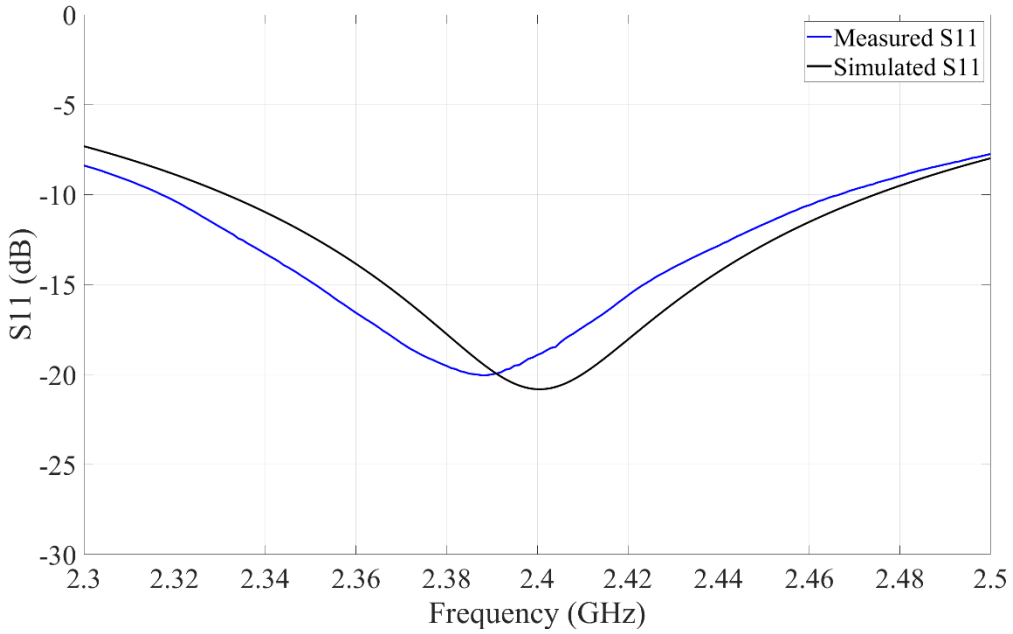

Figure 5.6 Measured and simulated S11 of the antenna with no biasing line in circular state

5.3.1.2 Cross-polar discrimination

To evaluate the linear performance, the cross-polar discrimination is measured in the broadside direction of the antenna. The results are shown in Figure 5.7. The antenna performed well with a XPD of 20 dB at the design frequency. The overall cross-polar performance over the operating band is < 14.5 dB. The performance is on par with the simulations except for frequencies above 2.4 GHz.

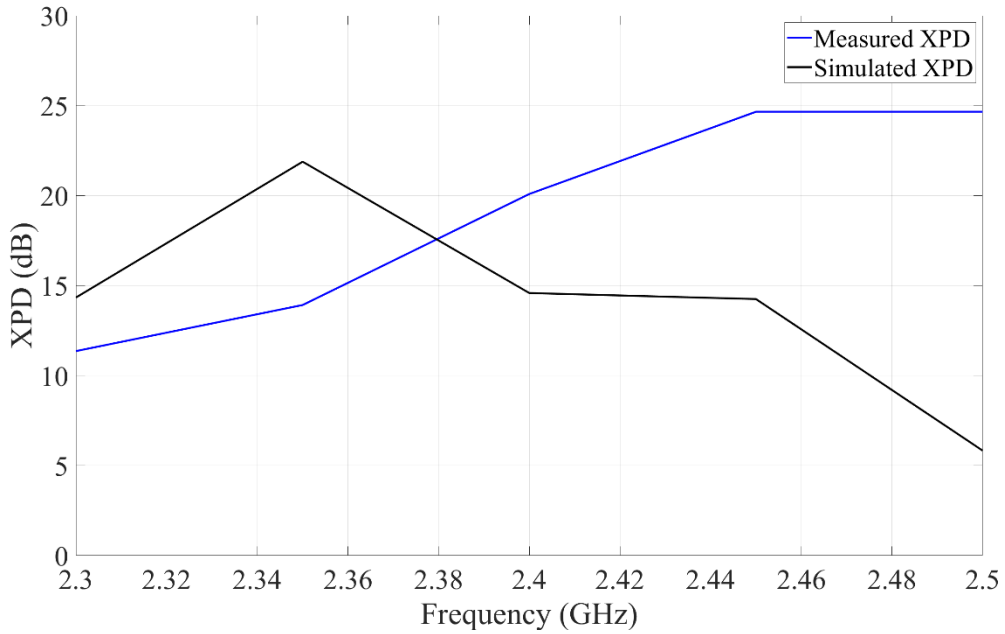

Figure 5.7 Linear cross-polar discrimination of the antenna with no biasing lines in linear state

5.3.1.3 Axial ratio

To evaluate the circular performance, the axial ratio of the antenna is calculated using the measured results. A comparison between the measured and simulated results are shown in Figure 5.8. As seen from the graph, the measured axial ratio has a bandwidth over the entire operating band (2.35-2.45 GHz). From the measured results, a bandwidth of 8.3% is achieved, this could be wider but the measurements were only carried out over a frequency range of 2.3 GHz to 2.5 GHz. The measured results performed slightly better than the simulated design.

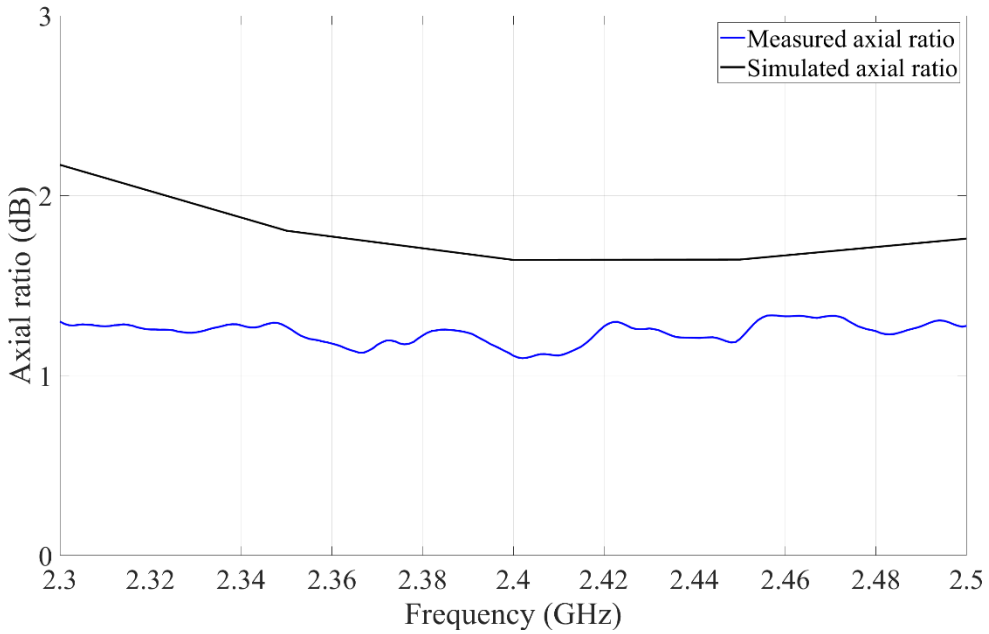

Figure 5.8 Simulated and measured axial ratio of the antenna with no biasing line in circular state

5.3.1.4 Radiation patterns

The performance of the antenna was also analysed by measuring the radiation patterns. The main characteristics that are observed include the mode of operation, the overall shape of the radiation patterns, the linear and circular cross-polar discrimination, and the front-to-back ratio. As the main goal of the antenna is reconfigurability, the gain of the antenna was not a design parameter that was optimized. This also reflects the design choices that were made in Chapter 3. The patterns were measured at the three critical design frequencies of the antenna, namely2.35, 2.4, and 2.45 GHz. The patterns were measured in two cut planes (ϕ = 0° and ϕ = 90°). A comparison between the measured and simulated patterns of the antenna in the linear state are provided in Figure 5.9 to Figure 5.14.

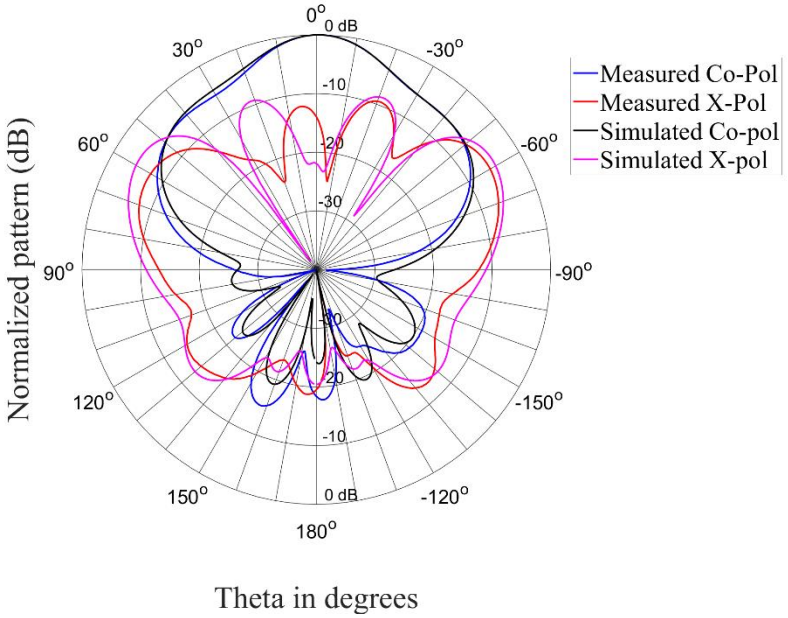

Figure 5.9 Simulated and measured radiation patterns of the antenna in linear state with no biasing lines at 2.35 GHz with Phi = 0º

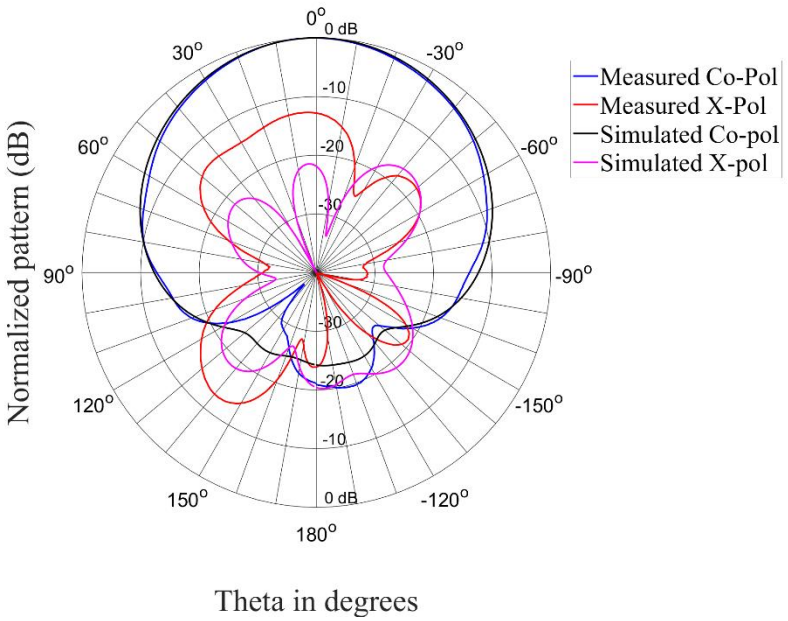

Figure 5.10 Radiation patterns of the antenna in linear state with no biasing lines at 2.35 GHz with Phi = 90º

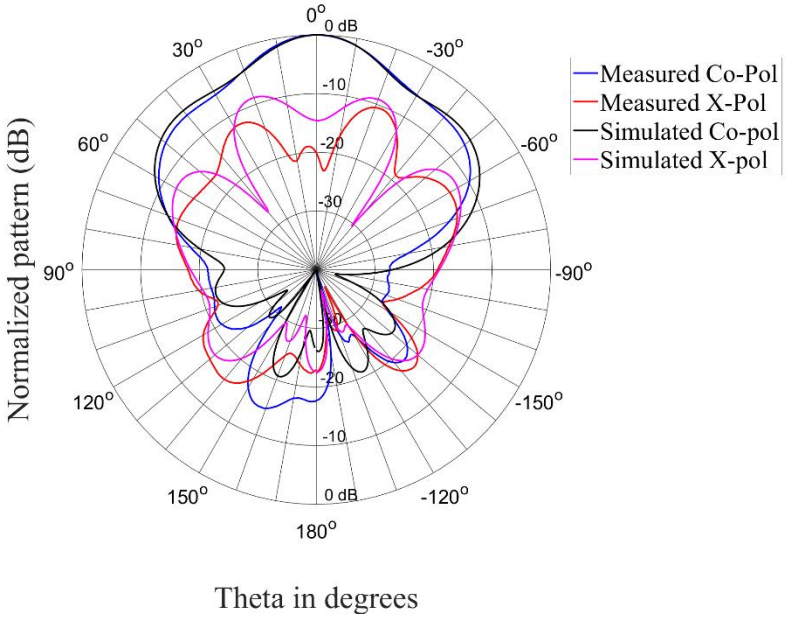

Figure 5.11 Radiation patterns of the antenna in linear state with no biasing lines at 2.4 GHz with Phi = 0º

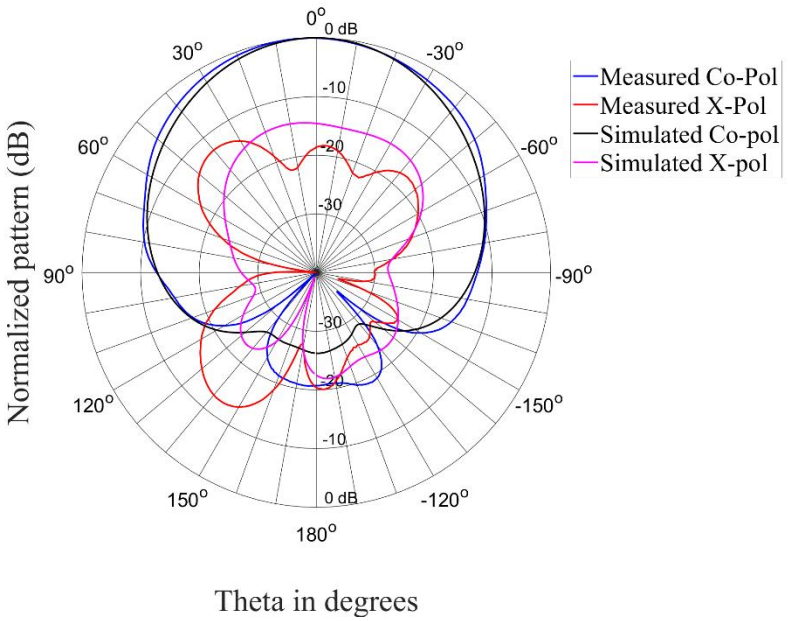

Figure 5.12 Radiation patterns of the antenna in linear state with no biasing lines at 2.4 GHz with Phi = 90º

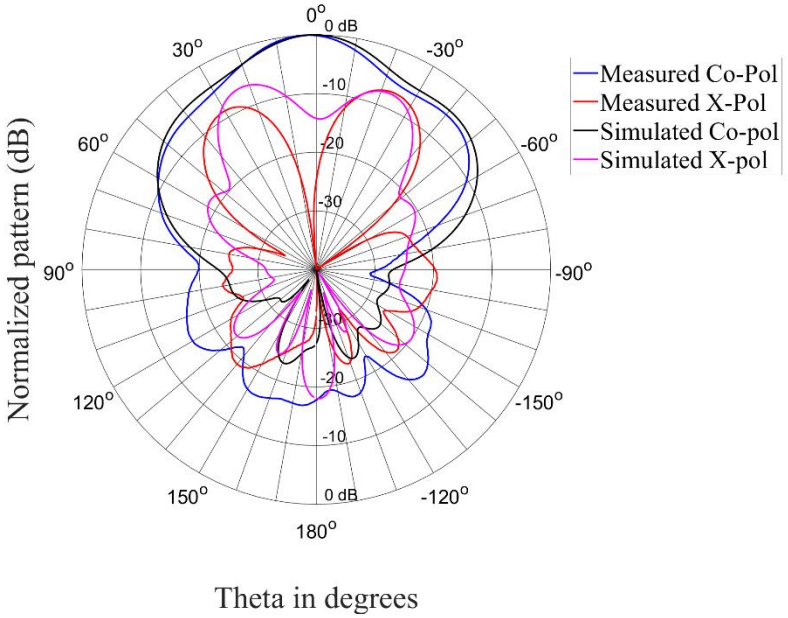

Figure 5.13 Radiation patterns of the antenna in linear state with no biasing lines at 2.45 GHz with Phi = 0º

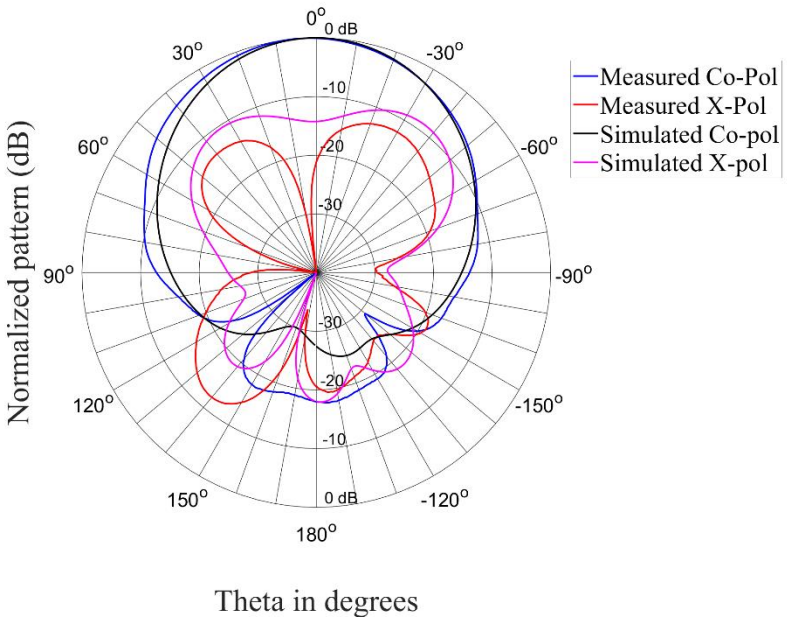

Figure 5.14 Radiation patterns of the antenna in linear state with no biasing lines at 2.45 GHz with Phi = 90º

As seen from the figures, the co-polarized patterns at a 0° cut angle presents unidirectional patterns over the operational band (2.35 GHz - 2.45 GHz), with a narrow main beam. This correlates well to the simulated results at this cut angle. Low cross-polarized patterns are achieved within the beamwidth of the antenna as seen at a 0° cut angle. The pattern also produces a low front-to-back ratio for the operating bandwidth as seen at the 0° cut angle plots.

Table 5.1 Summarized front-to-back ratio of the antenna in linear state

	2.35 GHz	2.4 GHz	2.45 GHz
Front to back ratio (dB)	18	17	16

Unidirectional co-polarized radiation patterns are achieved in the 90^{o} cut plane with a wider beamwidth compared to the 0^{o} cut plane. Low level cross-polarized patterns are measured within the beamwidth of the antenna leading to good cross-polar performance within the cut angle plane. The results also correlate well with simulation results.

The measured and simulated results for the circular state of the antenna are shown in Figure 5.15 to Figure 5.20.

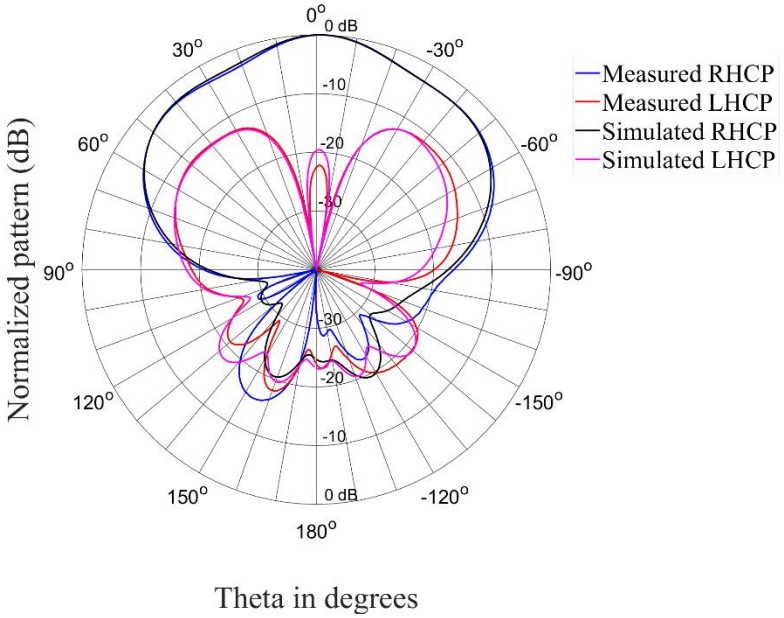

Figure 5.15 Radiation patterns of the antenna in circular state with no biasing lines at 2.35 GHz with Phi = 0º

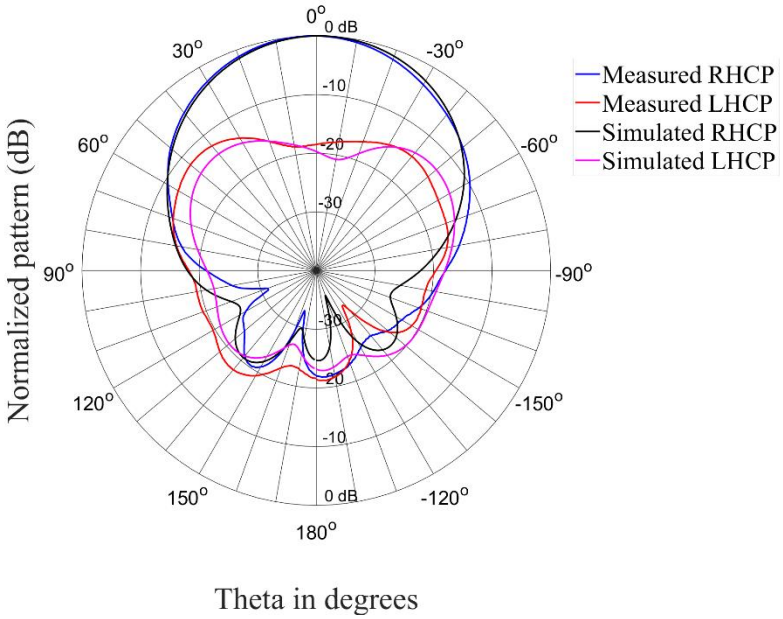

Figure 5.16 Radiation patterns of the antenna in circular state with no biasing lines at 2.35 GHz with Phi = 90º

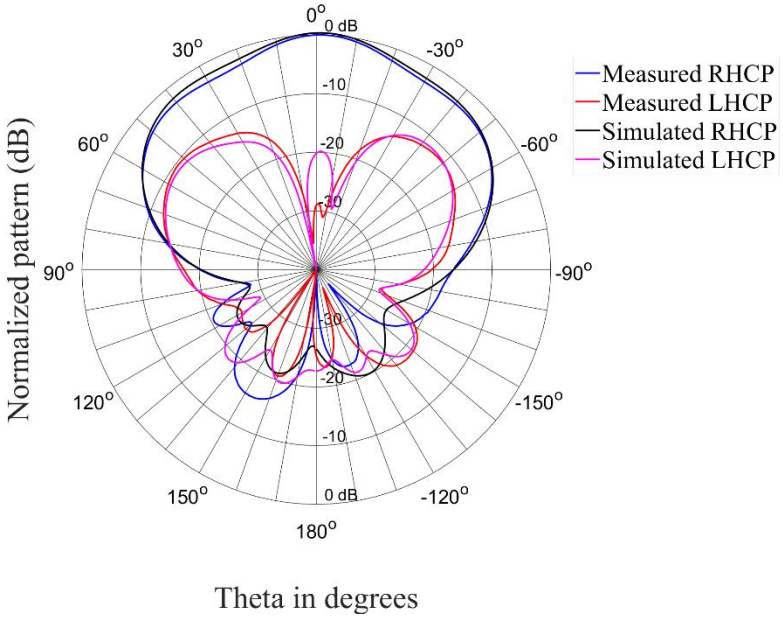

Figure 5.17 Radiation patterns of the antenna in circular state with no biasing lines at 2.4 GHz with Phi = 0º

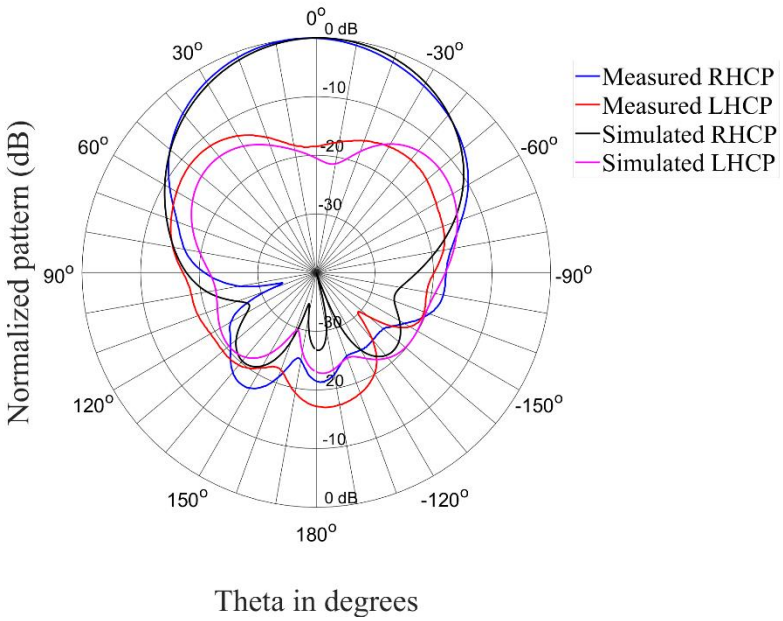

Figure 5.18 Radiation patterns of the antenna in circular state with no biasing lines at 2.4 GHz with Phi = 90º

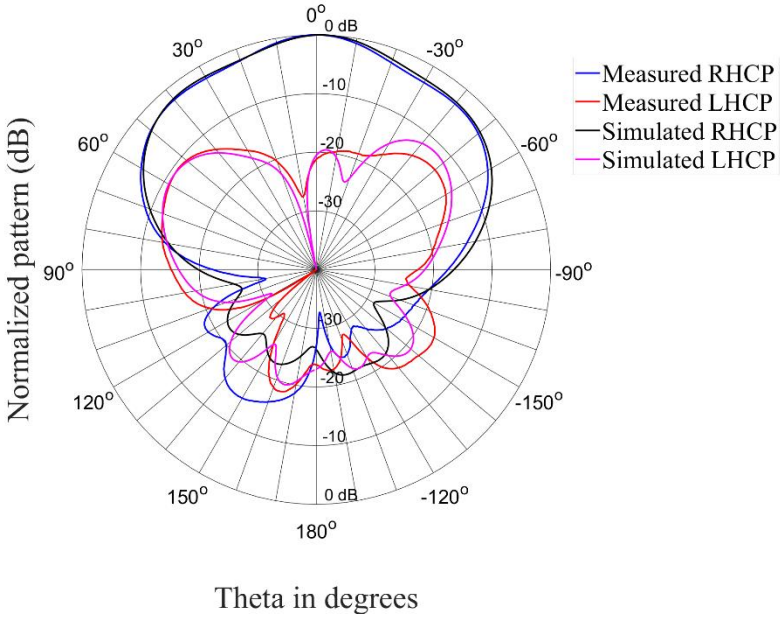

Figure 5.19 Radiation patterns of the antenna in circular state with no biasing lines at 2.45 GHz with Phi = 0º

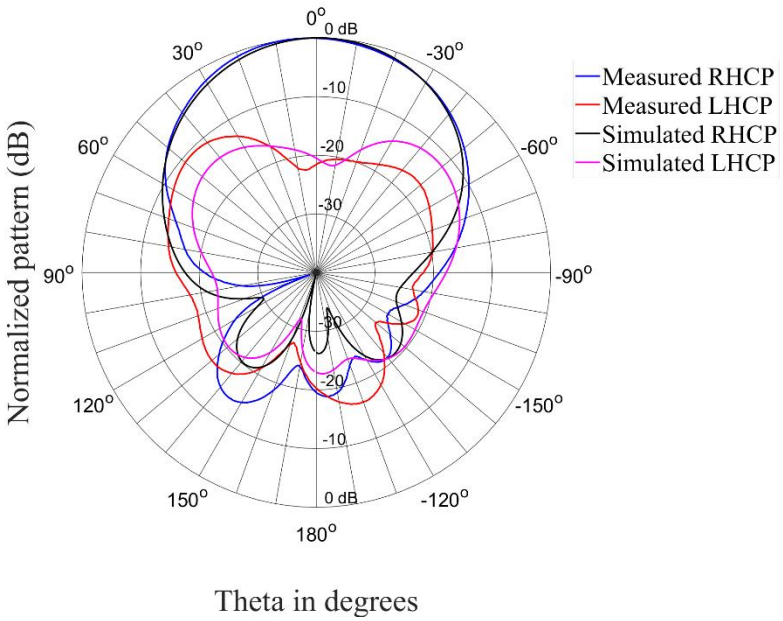

Figure 5.20 Radiation patterns of the antenna in circular state with no biasing lines at 2.45 GHz with Phi = 90º

As designed, the antenna is right-hand circularly polarized. Both cut angles show that the antenna achieves good circular cross-polar discrimination between the left and right patterns of the antenna. The front-to-back ratio of the RHCP patterns is also high. Table 5.2 provides a summary of these values at the three critical frequencies.

Table 5.2 Circular state characteristics summary

	2.35 GHz	2.4 GHz	2.45 GHz
Front to back ratio (dB)	18	19	19
Cross-polar discrimination (dB)	18	18	21

The radiation patterns in the 0° cut angle plane are also unidirectional with a main lobe in the broadside direction with a narrow beamwidth like those seen in the linear state. The patterns in 90° cut angle plane are also unidirectional with a wider beamwidth. The measured results correlate well with simulated results in both cut angle planes.

5.3.2 Vertical vias for biasing lines

The antenna was configured with vertical vias and measured. This was done to confirm simulations, as the simulations had shown a negative impact on the radiation patterns of the antenna from the addition of the vertical vias.

5.3.2.1 Reflection coefficient

The measured and simulated reflection coefficient of the antenna in linear state is shown in Figure 5.21. The impedance bandwidth is measured from 2.33 GHz to 2.437 GHz, which equates to a bandwidth of 4.4%, compared to the 3.7% of bandwidth from the simulated design. The measured reflection coefficient is shifted slightly to the left which decreases the operation range compared to the design range of 2.35 GHz to 2.45 GHz.

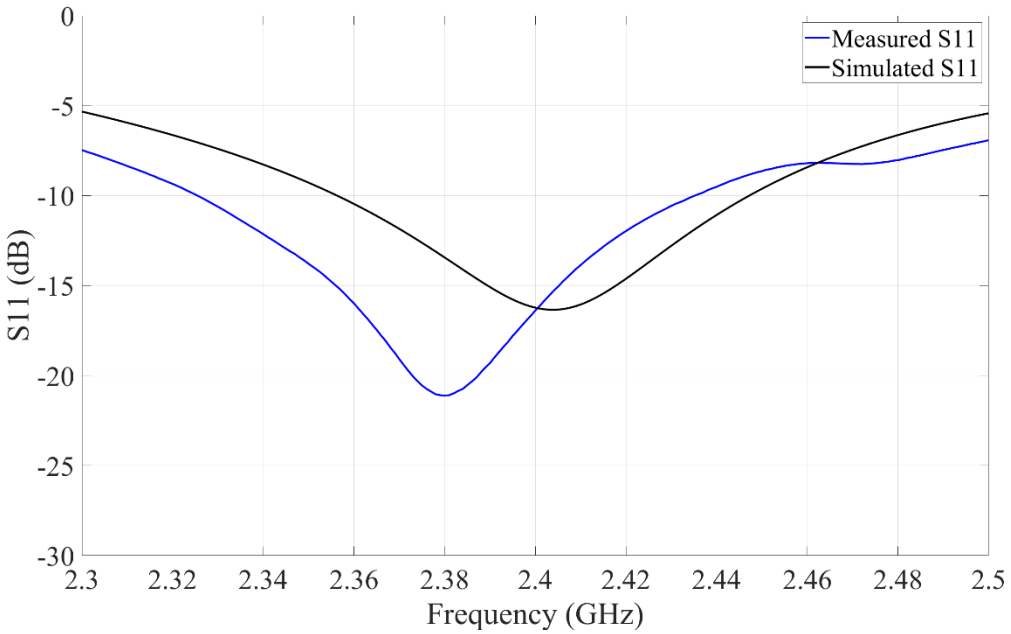

Figure 5.21 S11-Parameter of the antenna with vertical vias in linear state

The reflection coefficient of the antenna in circular state is shown in Figure 5.22. The bandwidth is measured from 2.338 GHz to 2.5 GHz, which equates to bandwidth of 6.75% compared to a simulated bandwidth of 5.8%. The bandwidth is slightly higher as measurements were only done between 2.3 GHz and 2.5 GHz. The measured reflection coefficient correlate well with the simulated data with a slight right shift.

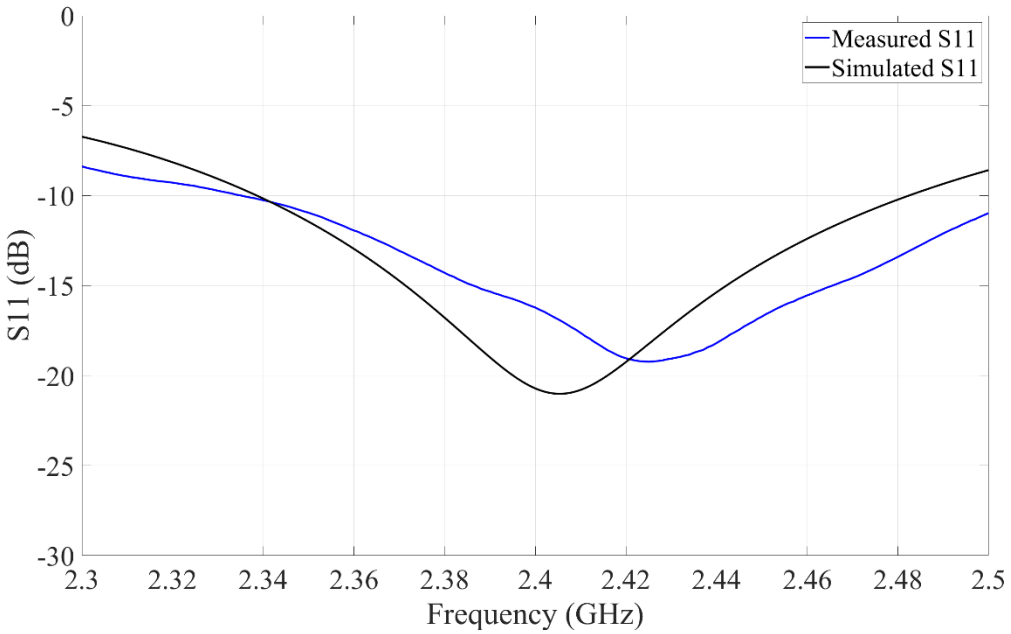

Figure 5.22 Measured and simulated S11-parameter of the antenna with vertical vias in circular state

5.3.2.2 Cross-polar discrimination

Shown in Figure 5.23 is the cross-polar performance of the antenna with vertical vias. At the design frequency of 2.4 GHz, the antenna produces a XPD of 16 dB compared to the simulated value of 15 dB. The simulated results show a high XPD throughout the entire operating bandwidth of the antenna.

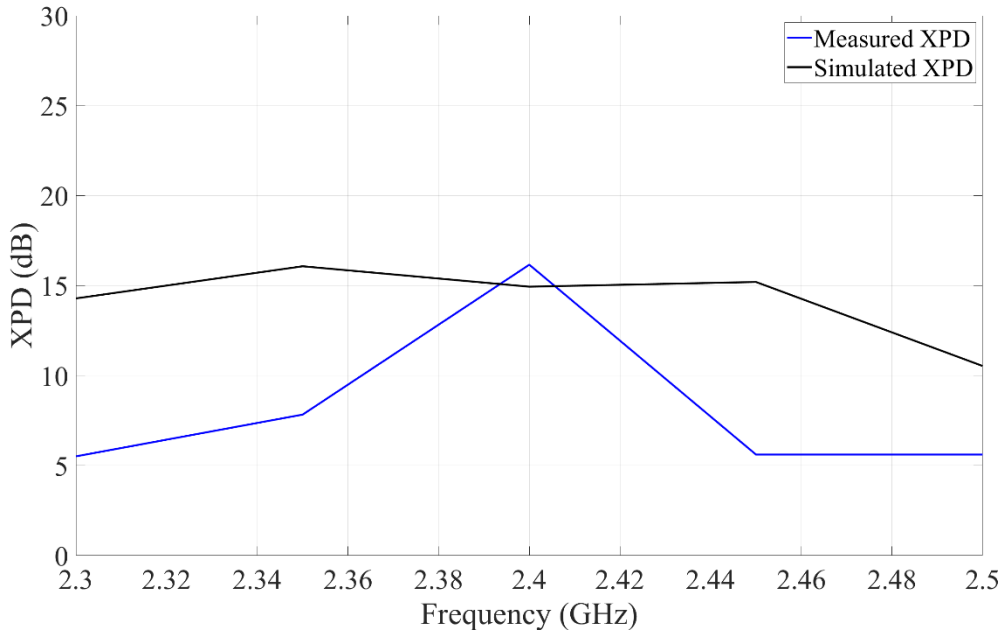

Figure 5.23 Cross-polar discrimination of antenna with vertical vias in linear state

5.3.2.3 Axial ratio

The measured axial ratio of the antenna is shown Figure 5.24. The axial ratio bandwidth remains under 3 dB over the operation band of the antenna equating to a bandwidth of 8.3%. The measured results correlate well with the simulations.

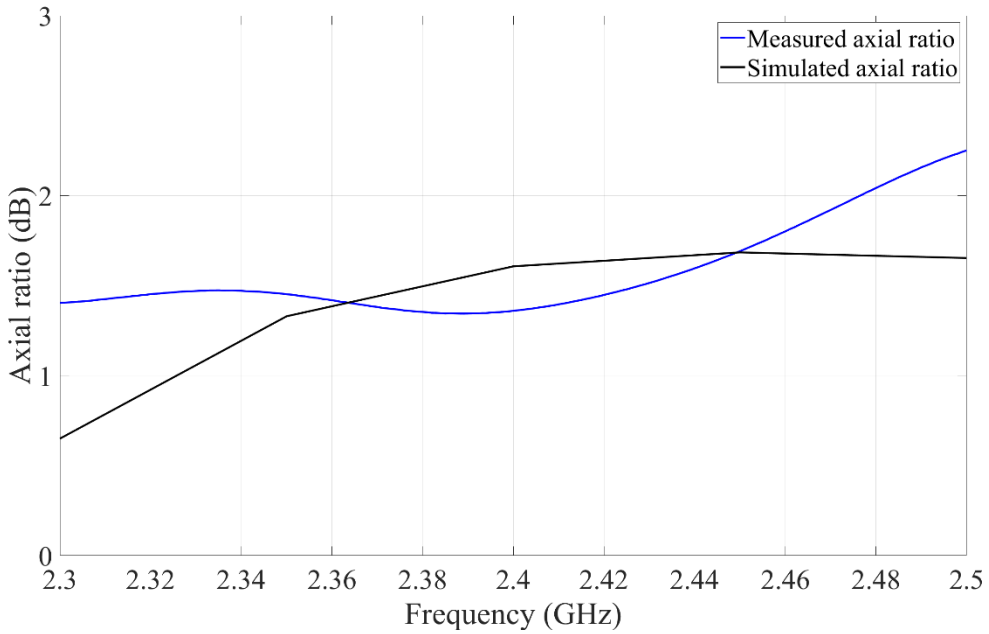

Figure 5.24 Axial ratio of the antenna with vertical vias in circular state

5.3.2.4 Radiation patterns

The radiation patterns of the antenna in the linear state are shown from Figure 5.25 to Figure 5.30. As seen in the figures, the co-polarized patterns have a unidirectional pattern and a less pointy pattern as seen with the antenna with no vias. The measured patterns in both the cut angle planes correlate well with simulated results. The measured cross-polarized patterns are however much worse than the simulated results in both cut angles. This corresponds to the problem experienced with the vertical vias in simulation, namely that the cross-polar performance was reduced because of the interference and reflections of the vias. The average front-to-back ratio for the operating range is 18 dB, which is still satisfactory.

Shown in Figure 5.31 to Figure 5.36 is the radiation patterns for the circular state of the antenna. With the circular state, the addition of the vertical vias had little effect on the circular performance of the antenna. The results correlated well with simulation. A detailed discussion will be done in the end of the chapter.

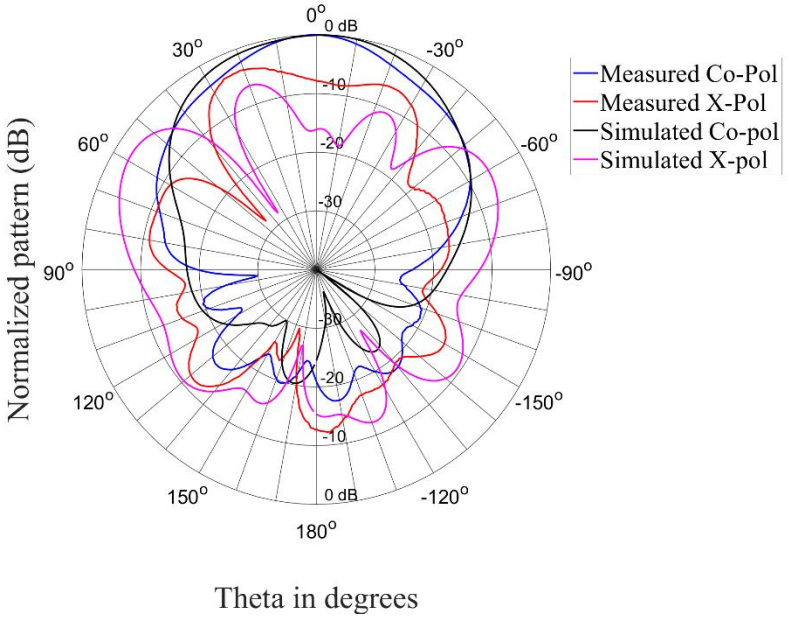

Figure 5.25 Radiation patterns of the antenna in linear state with vertical vias at 2.35 GHz with Phi = 0º

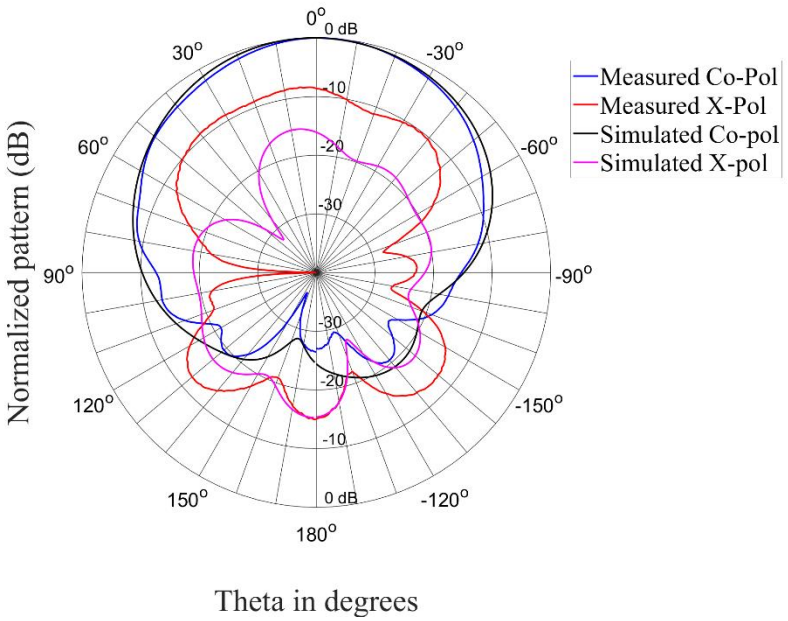

Figure 5.26 Radiation patterns of the antenna in linear state with vertical vias at 2.35 GHz with Phi = 90º

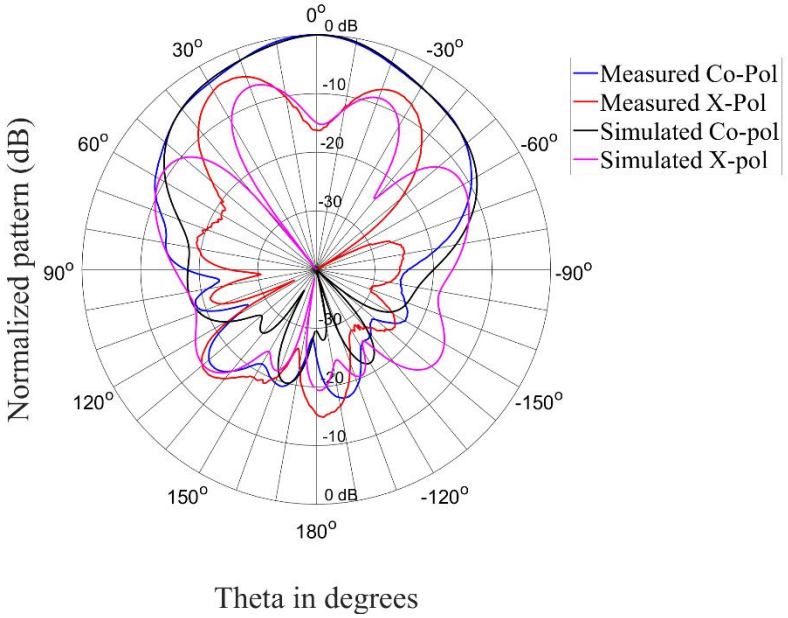

Figure 5.27 Radiation patterns of the antenna in linear state with vertical vias at 2.4 GHz with Phi = 0º

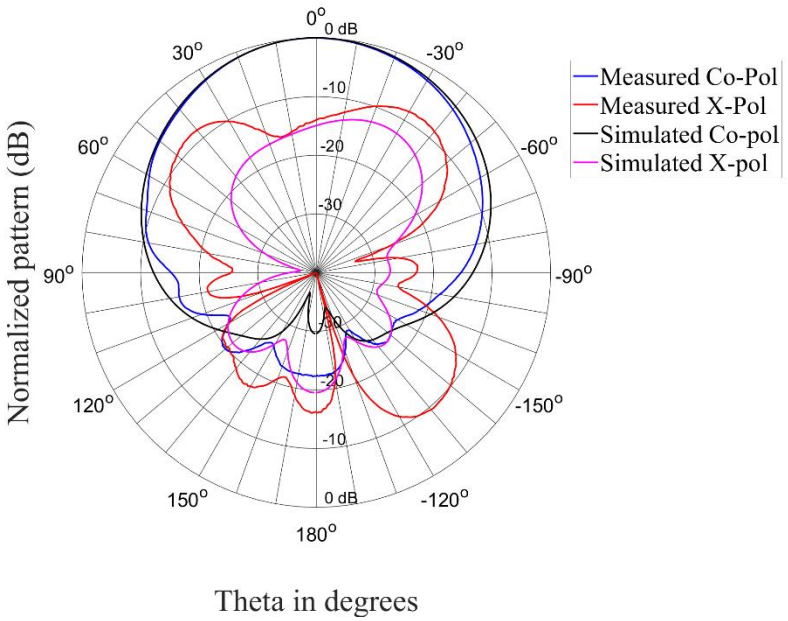

Figure 5.28 Radiation patterns of the antenna in linear state with vertical vias at 2.4 GHz with Phi = 90º

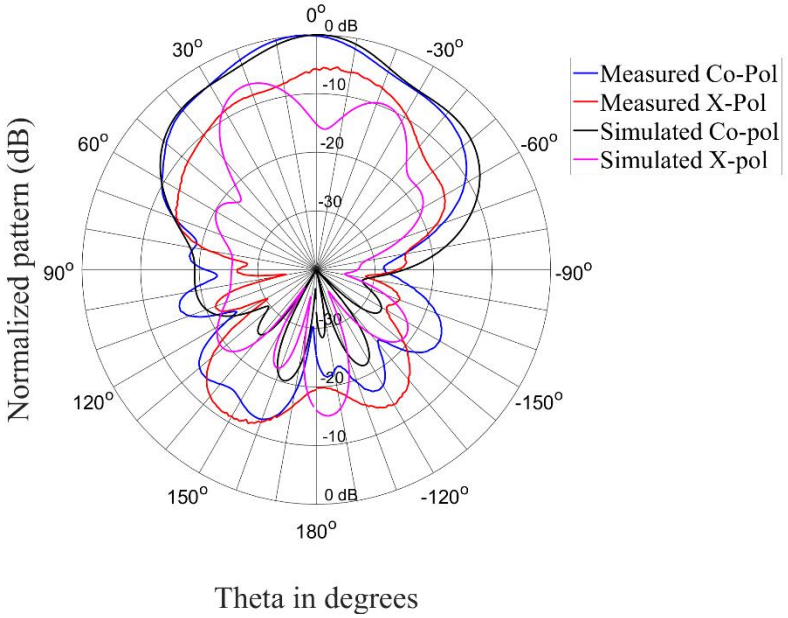

Figure 5.29 Radiation patterns of the antenna in linear state with vertical vias at 2.45 GHz with Phi = 0º

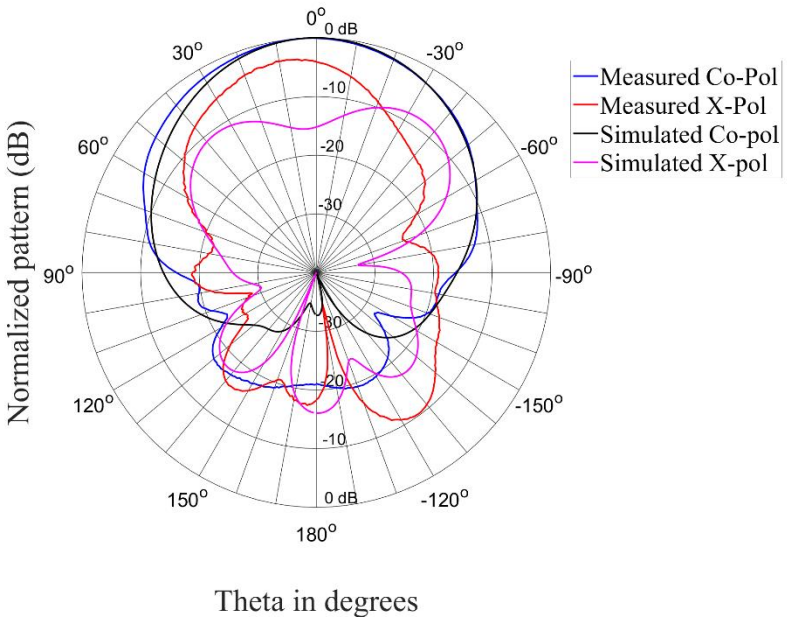

Figure 5.30 Radiation patterns of the antenna in linear state with vertical vias at 2.45 GHz with Phi = 90º

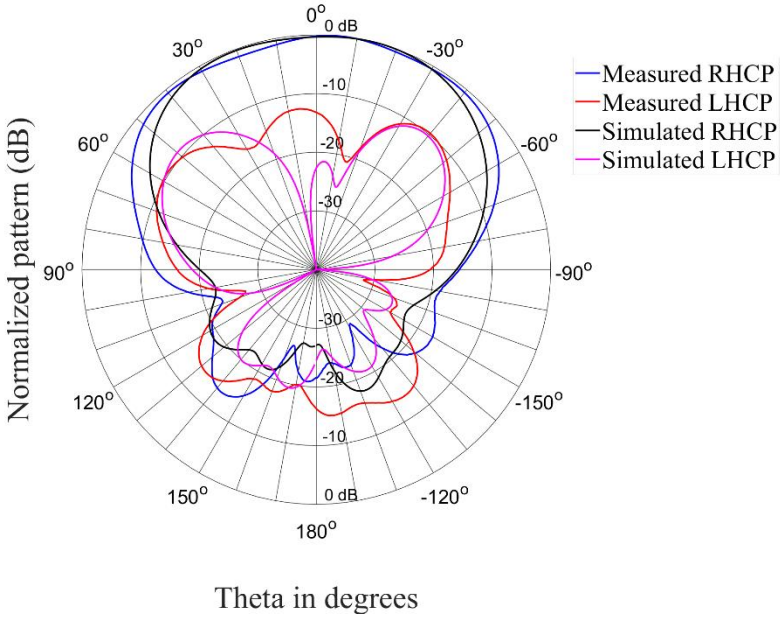

Figure 5.31 Radiation patterns of the antenna in circular state with vertical vias at 2.35 GHz with Phi = 0º

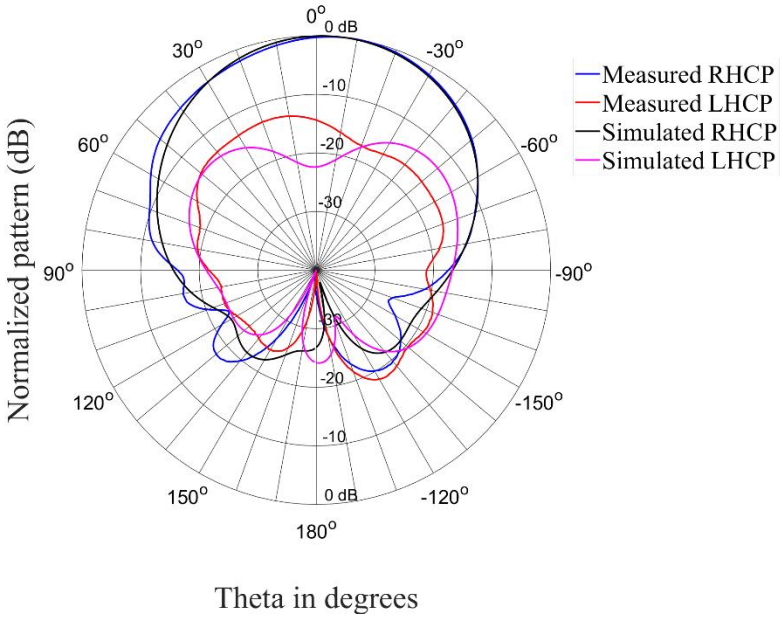

Figure 5.32 Radiation patterns of the antenna in circular state with vertical vias at 2.35 GHz with Phi = 90º

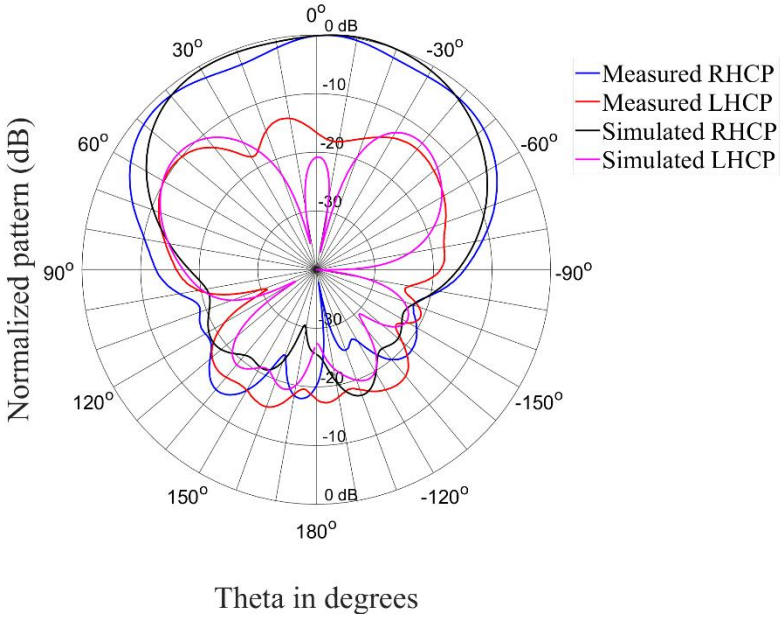

Figure 5.33 Radiation patterns of the antenna in circular state with vertical vias at 2.4 GHz with Phi = 0º

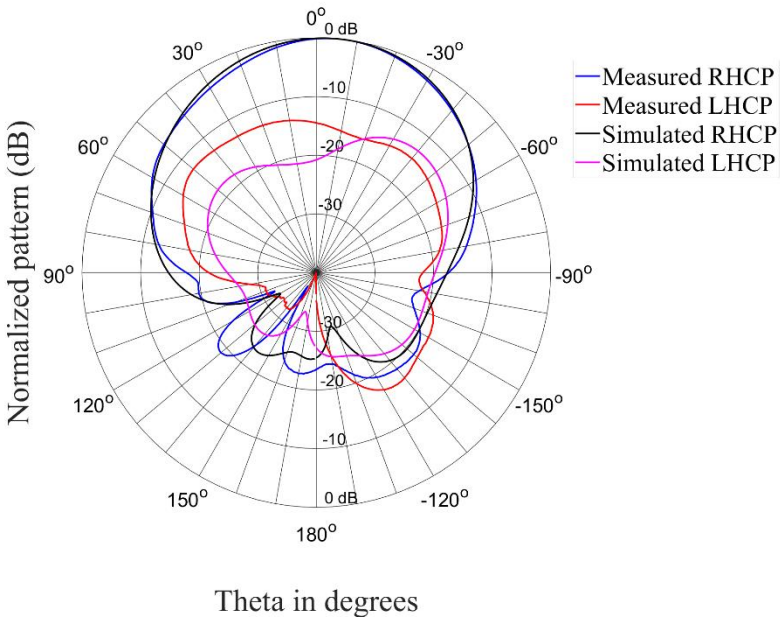

Figure 5.34 Radiation patterns of the antenna in circular state with vertical vias at 2.4 GHz with Phi = 90º

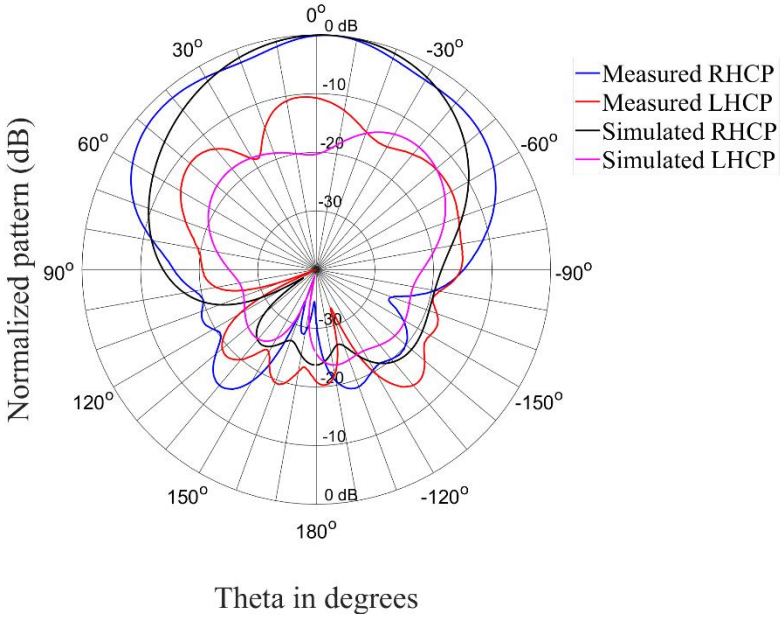

Figure 5.35 Radiation patterns of the antenna in circular state with vertical vias at 2.45 GHz with Phi = 0º

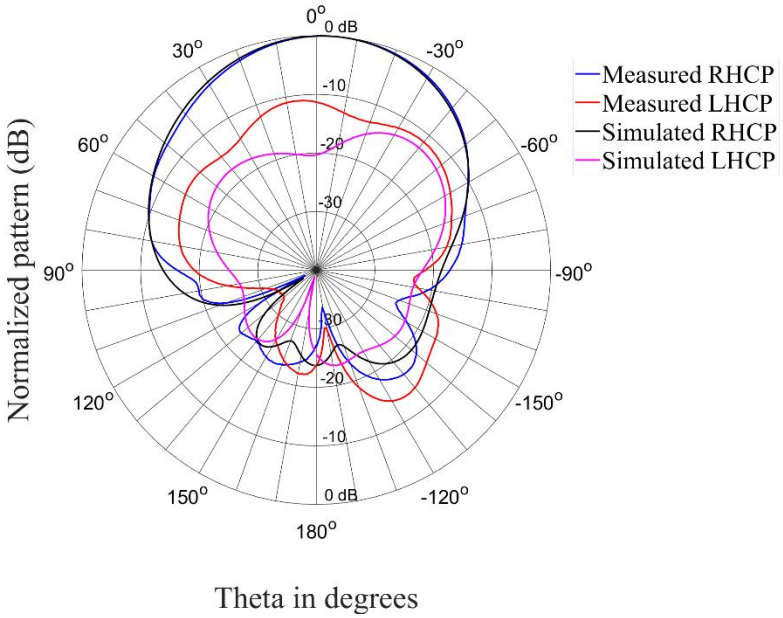

Figure 5.36 Radiation patterns of the antenna in circular state with vertical vias at 2.45 GHz with Phi = 90º

5.3.3 Helical coils for biasing lines

The last set of measurements that will be presented is the final version of the antenna where helical coils were added to mitigate the negative effects of the vertical vias as discussed in Chapter 3. In the manufacturing process some challenges were faced with the implementation of the coils.

5.3.3.1 Reflection coefficient

The reflection coefficient of the antenna in the linear state is shown in Figure 5.37. The bandwidth is measured from 2.33 GHz to 2.44 GHz, which equates to a bandwidth of 4.5%. The measured reflection coefficient is slightly shifted to the left of the design frequency, putting it out of bounds for the highest operating frequency of the antenna.

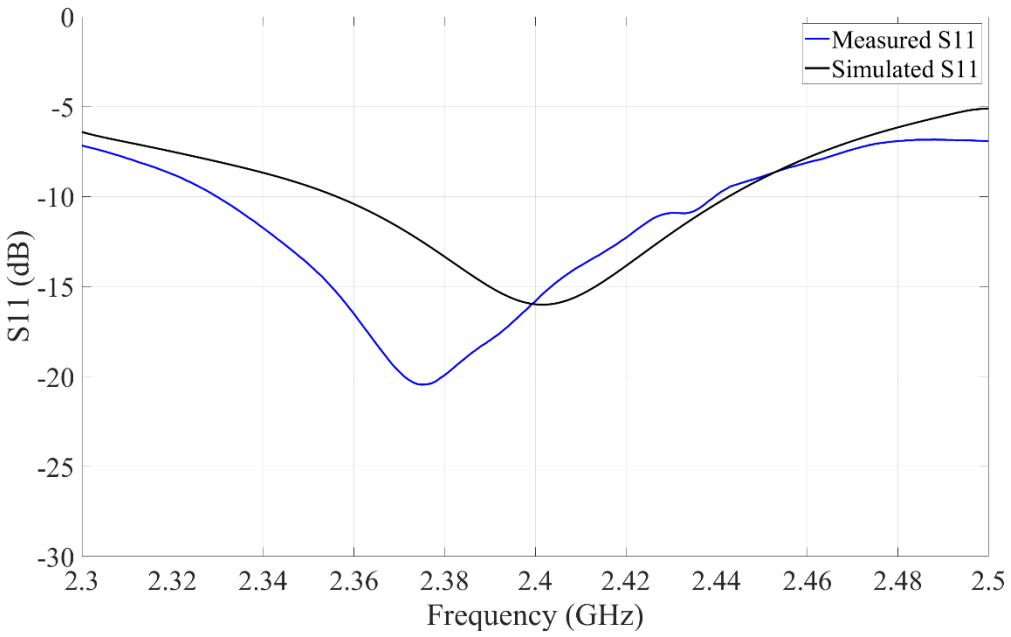

Figure 5.37 Measured and simulated S11-Parameter for antenna with helical coils in linear state

Shown in Figure 5.38 is the reflection coefficient for the antenna in the circular state. The impedance bandwidth is measured from 2.328 GHz to 2.498 GHz, which equates to a bandwidth of 7%. As seen in this graph, the measured results have an extra resonant frequency forming around 2.45 GHz. Overall, the matching is better compared to the simulation results.

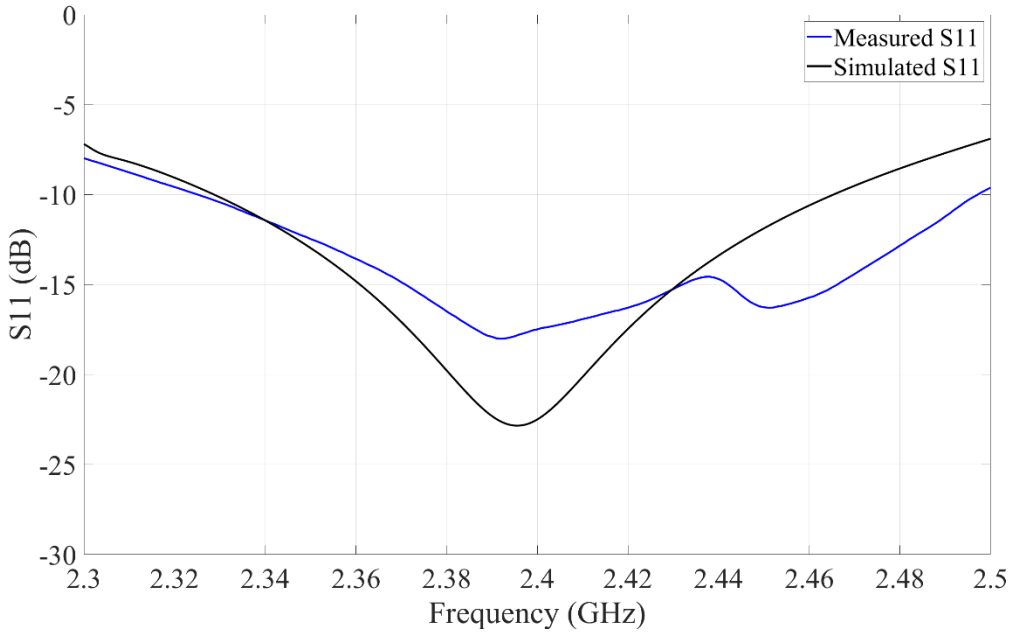

Figure 5.38 Measured and simulated S11-Parameter of the antenna with helical coils in circular state

5.3.3.2 Cross-polar discrimination

The cross-polar discrimination of the antenna with helical coils is shown in Figure 5.39. The cross-polar performance of the antenna is less than expected compared to the simulated results. At the design frequency the XPD is measured as 7 dB, with an XPD of 15.5 dB measured at 2.35 GHz. The correlation between the trend of the measured and simulated results is very good over the band. However, there is an offset between the level of the measured and simulated XPD. This indicates that a manufacturing problem could possibly be present. The details are discussed in the discussion section that follows the results.

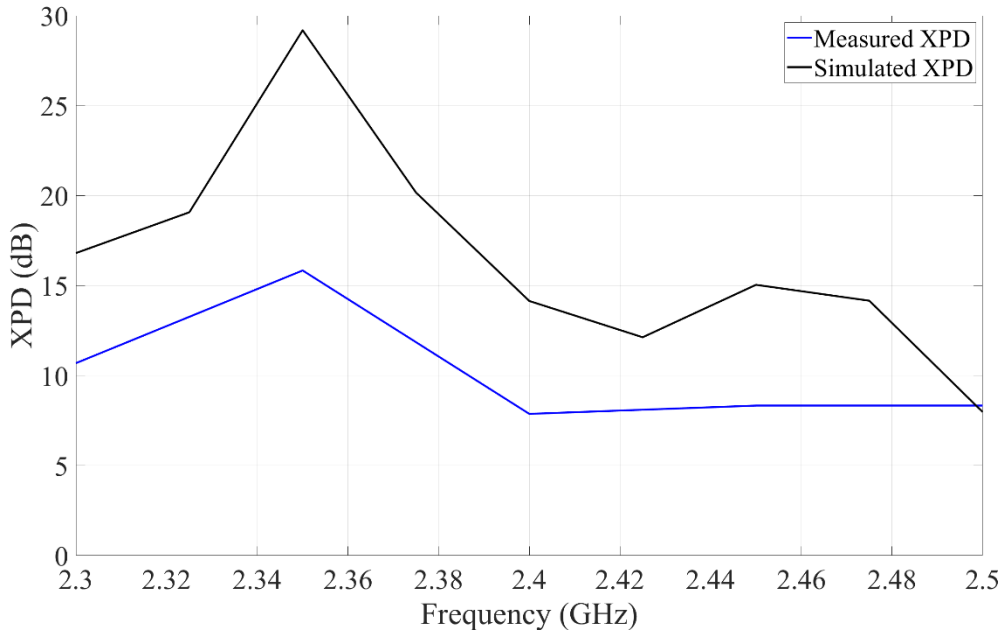

Figure 5.39 Linear cross-polar discrimination of antenna with helical coils in linear state

5.3.3.3 Axial ratio

The measured axial ratio of the antenna is shown in Figure 5.40. As with the vertical vias the circular performance of the antenna is mostly unaffected by the addition of the biasing lines. The axial ratio bandwidth is lower than 3 dB throughout the measurement range, and is in the order of 8.3%. This also correlates well with the simulated results.

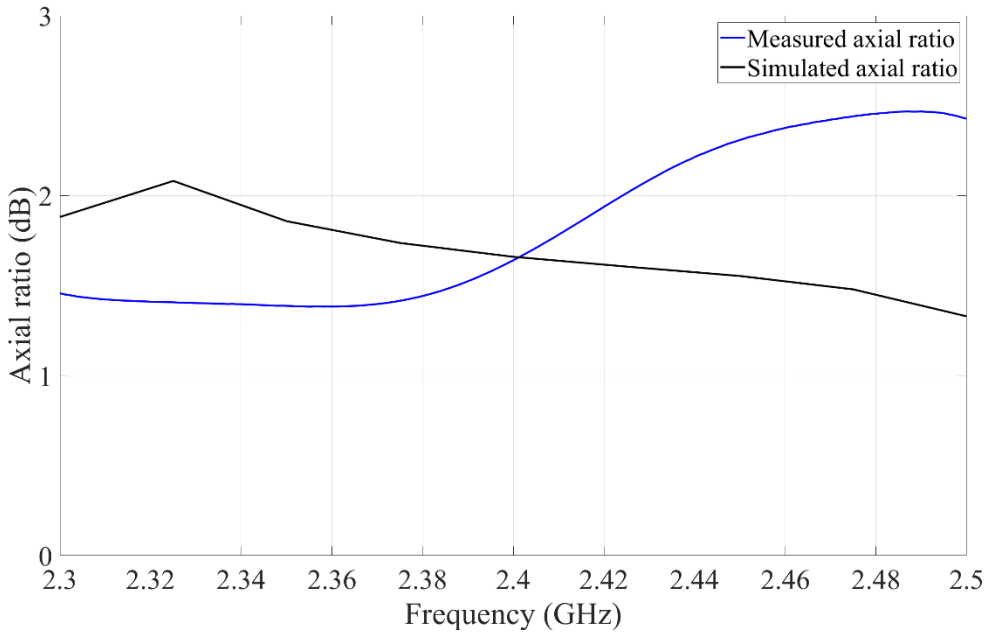

Figure 5.40 Axial ratio of the antenna with helical coils in circular state

5.3.3.4 Radiation patterns

The radiation patterns of the antenna with helical coils were measured at the critical frequencies in both linear and circular polarization states. The radiation patterns for the linear state are shown in Figure 5.42 to Figure 5.46.

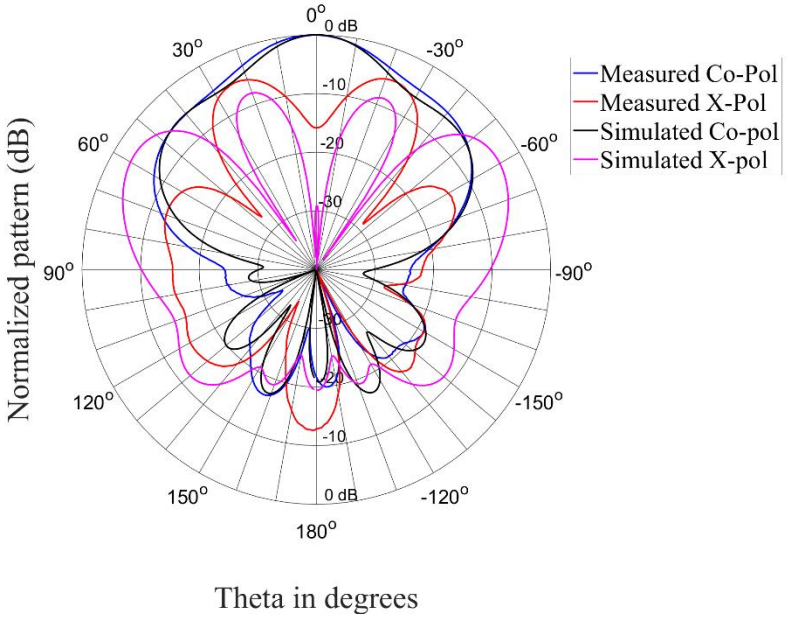

Figure 5.41 Radiation patterns of the antenna in linear state with helical coils at 2.35 GHz with Phi = 0º

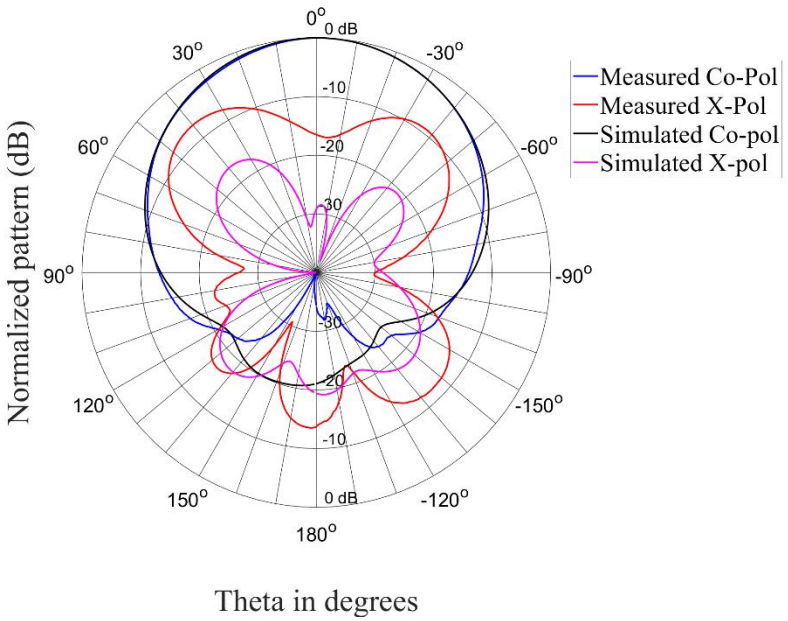

Figure 5.42 Radiation patterns of the antenna in linear state with helical coils at 2.35 GHz with Phi = 90º

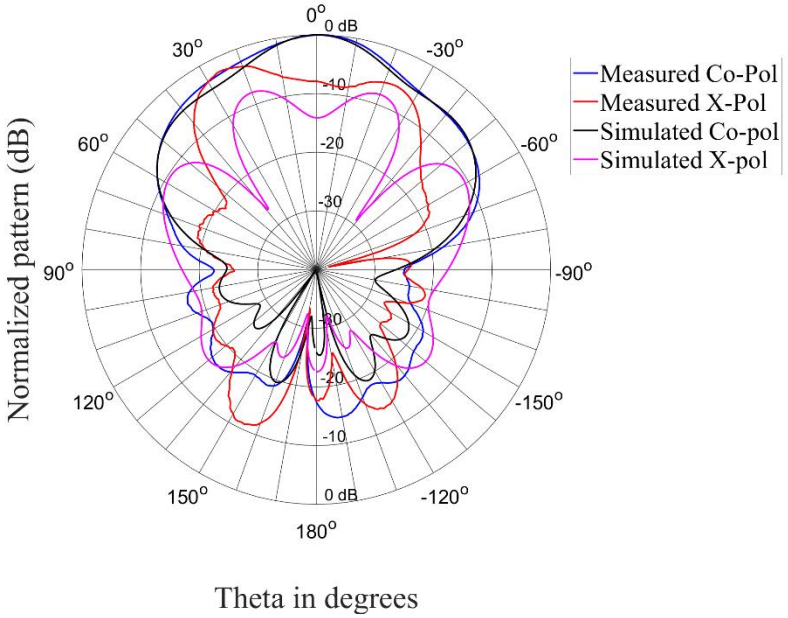

Figure 5.43 Radiation patterns of the antenna in linear state with helical coils at 2.4 GHz with Phi = 0º

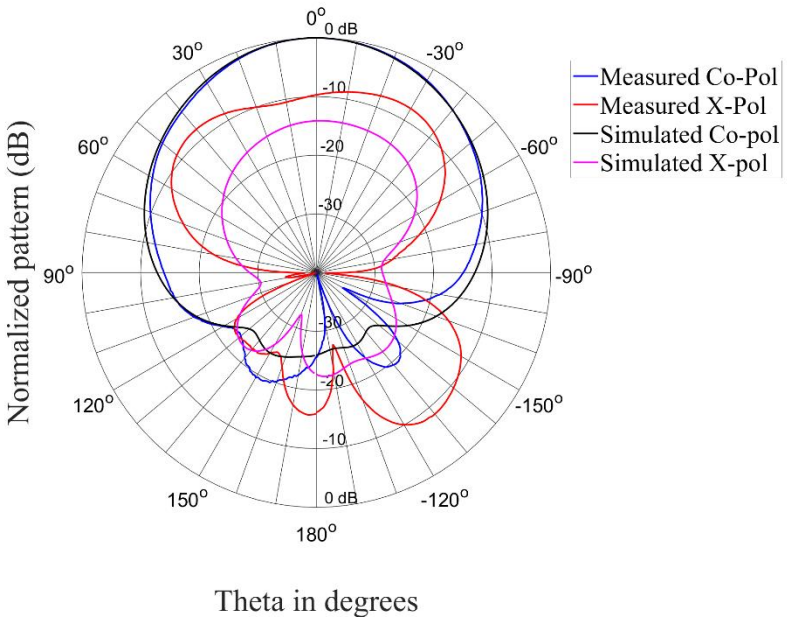

Figure 5.44 Radiation patterns of the antenna in linear state with helical coils at 2.4 GHz with Phi = 90º

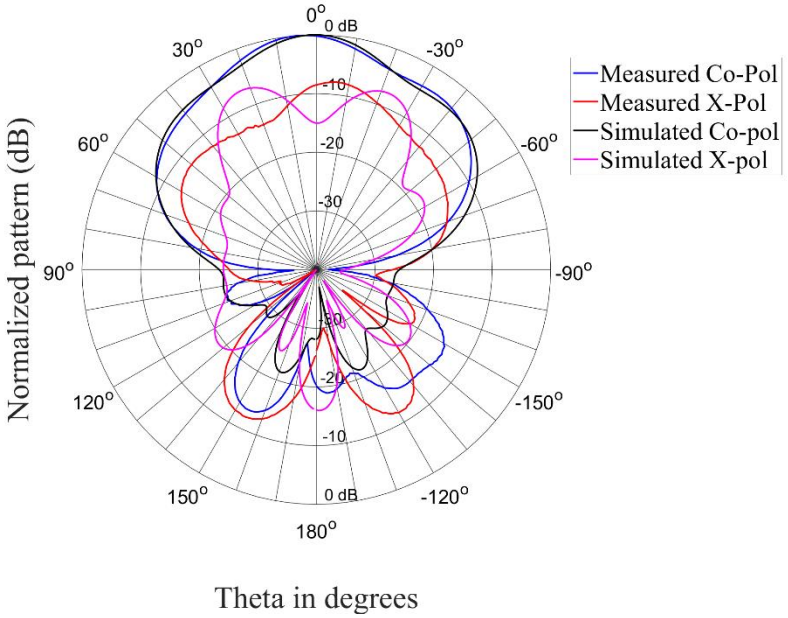

Figure 5.45 Radiation patterns of the antenna in linear state with helical coils at 2.45 GHz with Phi = 90º

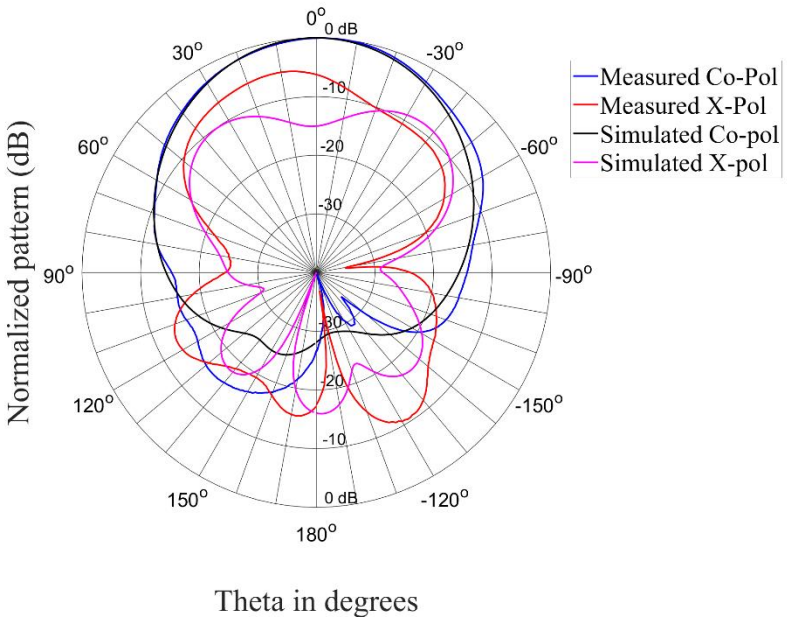

Figure 5.46 Radiation patterns of the antenna in linear state with helical coils at 2.45 GHz with Phi = 90º

Excellent co-polarized patterns within the operation bandwidth are achieved with very good correlation between the measured and simulated results. This indicates that the coils function as intended since the patterns revert to those of the initial design where no biasing lines were implemented. The patterns are unidirectional with a narrow main lobe. The front-to-back ratio of the antenna is summarized in Table 5.3.

Table 5.3 Summarized front-to-back ratio for antenna in linear state

	2.35 GHz	2.4 GHz	2.45 GHz
Front to back ratio (dB)	20.2	17	20

The correlation between the measured and simulated cross-polarized patterns are adequate in terms of the general shape, however the measured levels are very high and do not meet the design goals. Consequently, the antenna in the current state will only function as a bad dual linear antenna.

Shown in Figure 5.47 to Figure 5.52 are the radiation patterns for the antenna in the circular state.

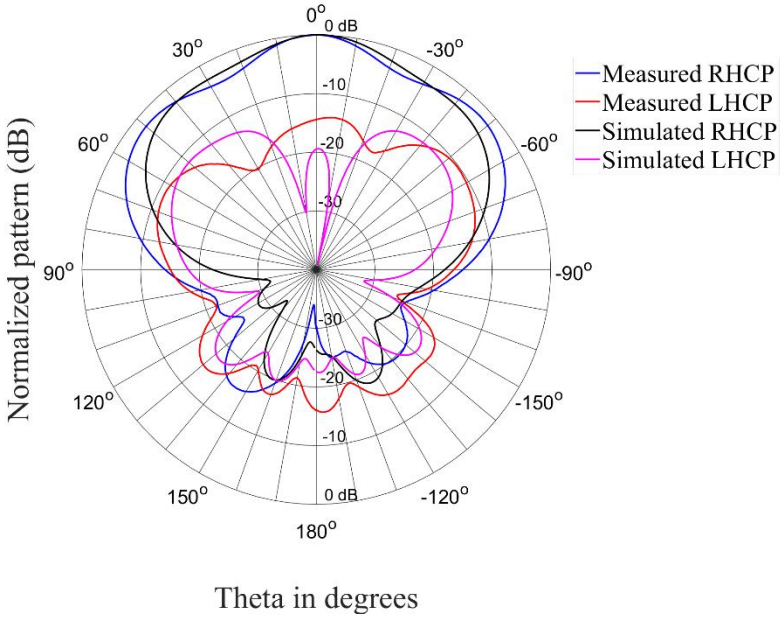

Figure 5.47 Radiation patterns of the antenna in circular state with helical coils at 2.35 GHz with Phi = 0º

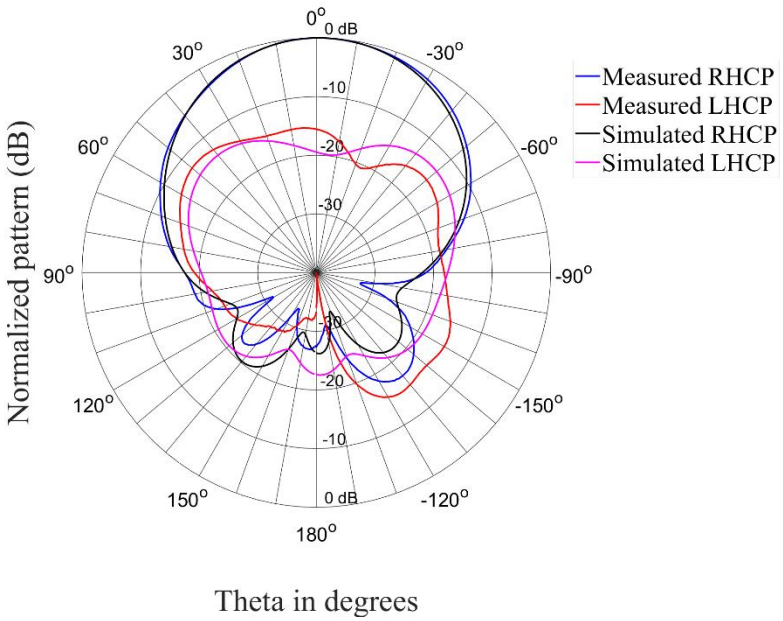

Figure 5.48 Radiation patterns of the antenna in circular state with helical coils at 2.35 GHz with Phi = 90º

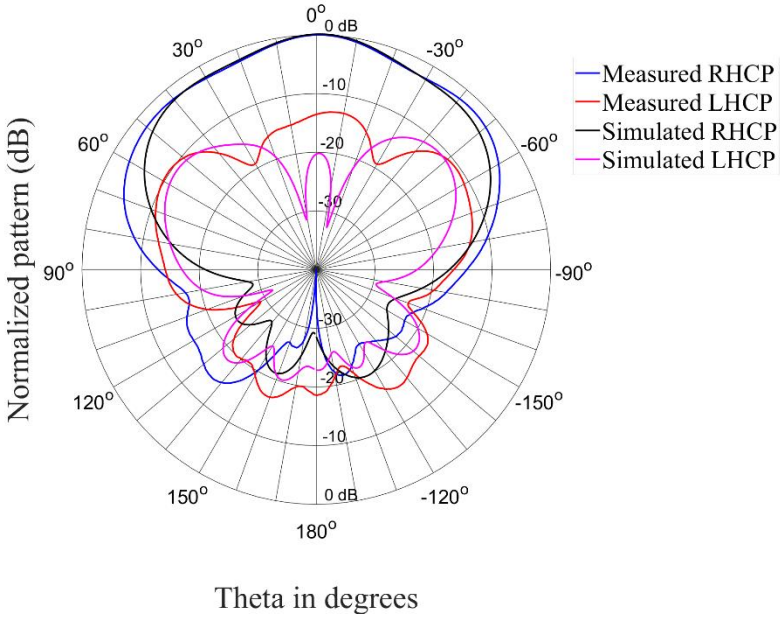

Figure 5.49 Radiation patterns of the antenna in circular state with helical coils at 2.4 GHz with Phi = 0º

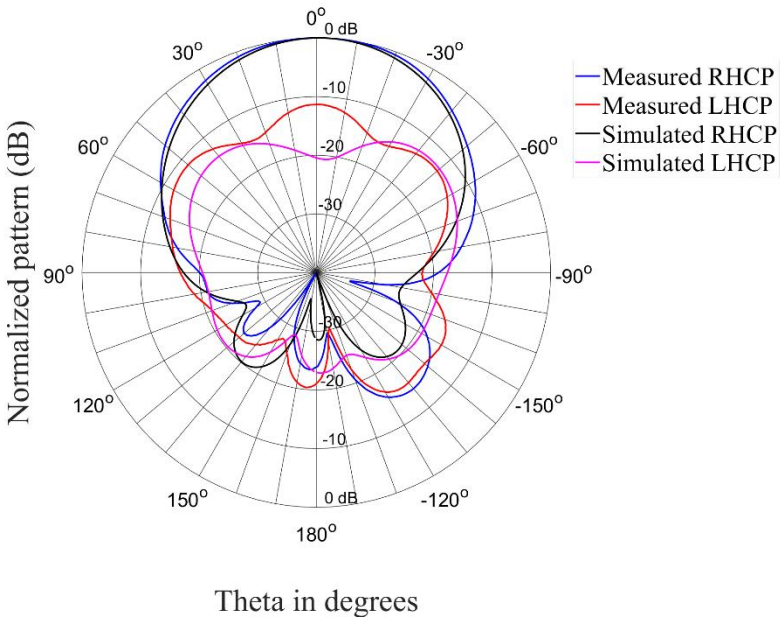

Figure 5.50 Radiation patterns of the antenna in circular state with helical coils at 2.4 GHz with Phi = 90º

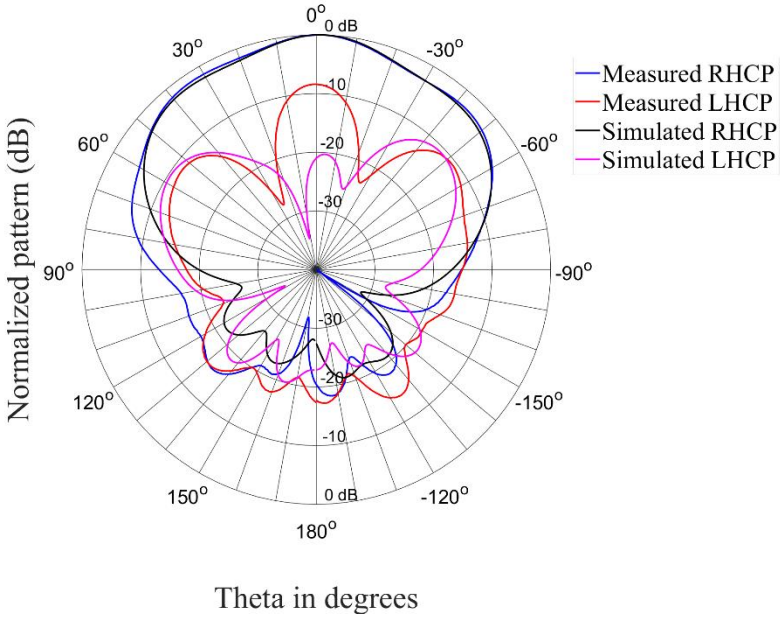

Figure 5.51 Radiation patterns of the antenna in circular state with helical coils at 2.45 GHz with Phi = 0º

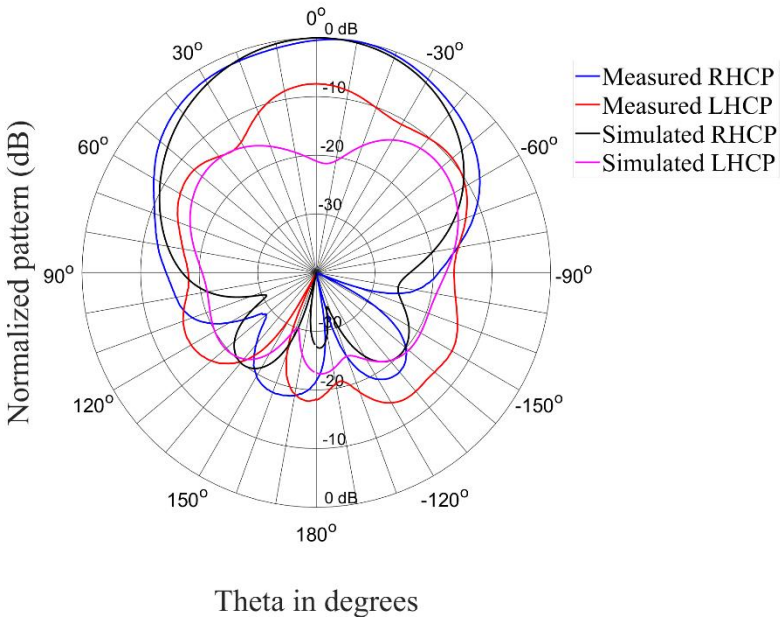

Figure 5.52 Radiation patterns of the antenna in circular state with helical coils at 2.45 GHz with Phi = 90º

The left-hand circularly polarized patterns correlate well with the simulated results. The coils are effective at normalizing the patterns to that of the initial design without the additional biasing lines. The circular characteristics is summarized in Table 5.4. The antenna achieves a very good front-to-back ratio over the operational band. The performance of the left-hand circular polarized patterns are degraded with much higher levels than that with of the simulations. The cross-polar discrimination is summarized in Table 5.4.

Table 5.4 Summarized circular characteristics for antenna in circular state

	2.35 GHz	2.4 GHz	2.45 GHz
Front-to-back-ratio (dB)	27	23	20
Cross-polar discrimination (dB)	15	11	8

5.3.3.5 Gain

The gain of the antenna with helical coils was measured and the results are presented here. The gain of the antenna in linear and circular state is shown in Figure 5.53 and Figure 5.54, respectively. It can be seen that the gain of the antenna in the linear state is slightly lower than the simulated results over the band. The measured and simulated gain at the center frequency is measured as 6.8 dBi and 8.3 dBi, respectively. In the circular state the measured gain is also lower than the simulated gain. The measured gain is also 6.8 dBi and the simulated gain 8.2 dBi. The decrease in performance can also be attributed to the implementation of the helical coils.

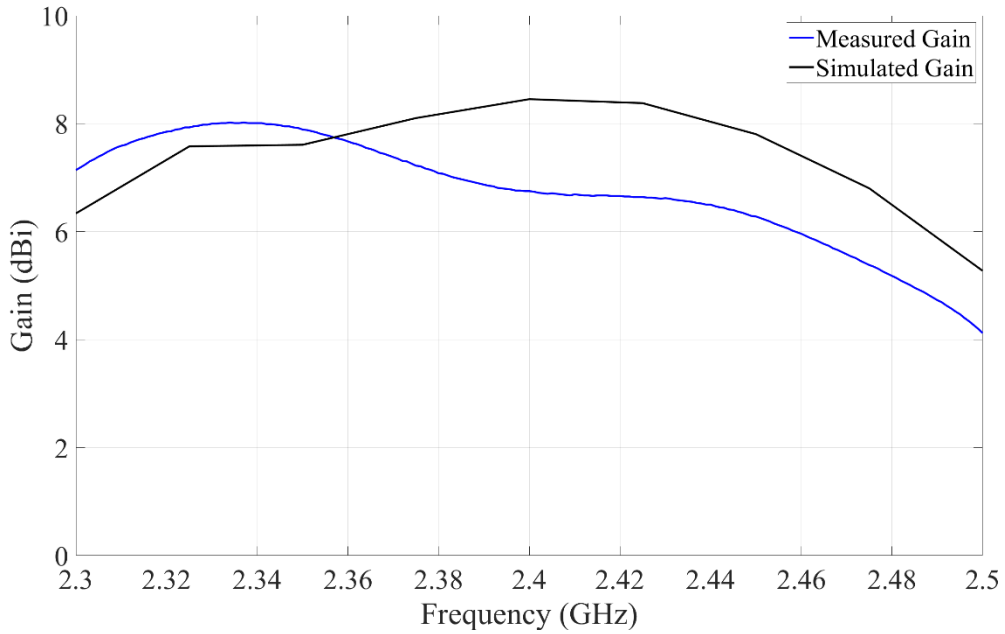

Figure 5.53 Measured gain of the antenna in linear state

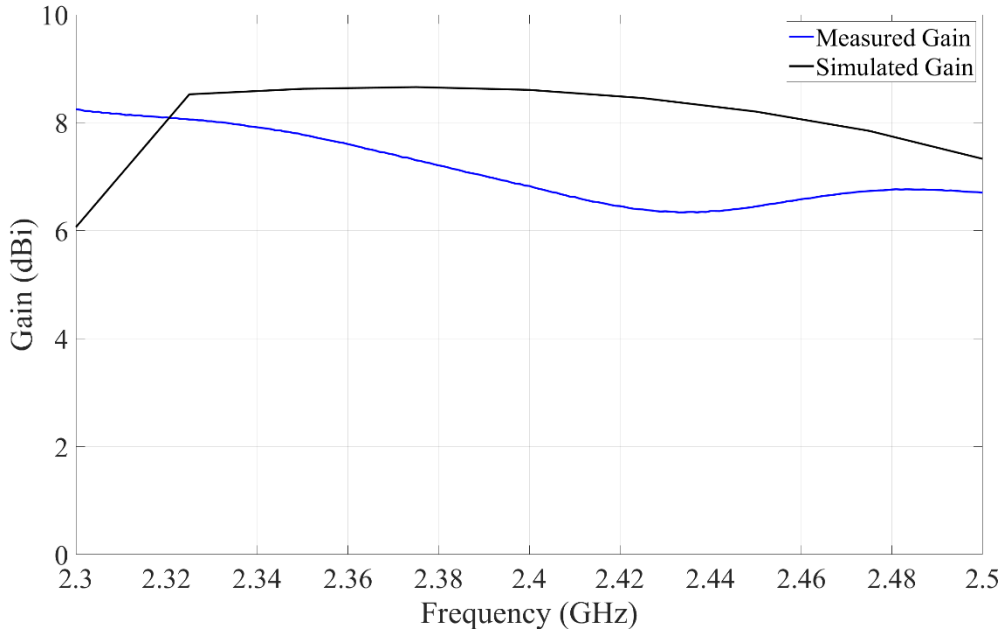

Figure 5.54 Measured gain of the antenna in circular state

5.4 DISCUSSION

From the measured results it can be confirmed that the antenna design functioned as expected. It therefore proves the overall concept of the design of electrically reconfiguring antenna through an active metasurface to achieve polarization reconfigurability.

The overall performance of the manufactured antenna was good, but the implementation of the active elements on the antenna proved difficult and the results had degraded performance where active elements were used.

The manual implementation of the switches using copper foil tape produced excellent results, which correlated very well with the simulated results of the design. There were some frequency shifts in the reflection coefficients of the measured data, but this could be attributed to the flexibility of the substrate that is used. The stability of the substrate is critical to maintain the exact air spacing between the various surfaces. With only eight screws supporting the various surfaces, flex could be observed in the structure when adjusting the antenna for measurement. A potential solution for future work that could mitigate this would be the addition of an extra substrate to emulate the air spacing, such as polystyrene. Some differences were also noted in the cross -polarized patterns of the measured data. The flexibility of the antenna would also attribute to minor changes in the patterns, as the antenna was very sensitive to parameter changes. Overall, the measurements proved that design concept worked and the addition of active switches could be made to easily switch between the linear and circular state of the antenna.

Measurements were taken of the antenna with vertical vias feeding the PIN diodes on the metasurface. Implementing any form of vias proved very difficult as the vias had to be soldered and aligned with precision on a very thin layer of copper that proved unstable. With the vias implemented, the spacing between surfaces was also imperfect. This again attributed to frequency shifts that are observed in the reflection coefficients of the antenna modes. Any future work will require more advanced techniques to implement accurate biasing lines as

hand soldering vias produced manufacturing errors that could be mitigated. However, the antenna produced results that correlated with the design simulations except that linear performance was limited due to lower cross-polar performance. The change that was observed in the simulated co-polarized patterns with the addition of vias was also observed in the measurement data. This confirmed that a different method of implementing the biasing lines had to be used.

The implementation of the helical coils presented the biggest challenge of the antenna manufacturing. All the coils were hand winded with a specific number of coil windings required as designed. All coils were winded with magnetic wire. This method produced coils with varying properties between each coil. Some coils were springier while other coils had more flex. To get consistent coils a supporting core needs to be used otherwise implementation will be a very difficult practice. As the coils were stiff, it was a challenge to implement them on a thin copper layer and this produced varying results with some more skew than others. The coils also introduced a more uneven substrate as some of them had more spring tension in them lifting the substrate. To improve the results, machine made coils will be required. All of these manufacturing challenges added to some mixed results that were obtained during measurements. With the coils implemented, the co-polarized patterns of the linear state correlated well with the simulated results. Looking at the patterns, the effect of the coils is as expected in normalizing the patterns to that of a design without biasing lines. The major problem is with the cross-polarized patterns of the antenna where the performance is degraded. Throughout the operating bandwidth the XPD is quite low and cross-polar patterns have much higher side lobes compared to the simulation. This is attributed to addition of the coils and the manner in which they are implemented. There might also be more complex interactions with resonant modes that are created from the reflections of the coils within the cavity between the ground plane and the metasurface. This can be observed in the reflection coefficient of both linear and circular states of the antenna where new resonant frequencies are identified around 2.44 GHz. Even with these defects the circular performance of the antenna is still adequate. The radiation patterns are also normalized to correlate with the design without biasing lines and produced an excellent axial

ratio bandwidth. The circular cross-polar discrimination is also affected by the coils as the left-hand polarized levels are slightly higher. The general shape of radiation pattern correlate well with the simulated design.

The measured data of the antenna conclusively proved the concept of creating an active metasurface to create an antenna with polarization reconfigurability with electrical switches. More work is required in the area of integrating electrical switches within the reactive region of a radiating element.

5.5 CHAPTER SUMARRY

Within this chapter the measured results are shown for three antenna solutions that are required to validate the design process of Chapter 3. The first measurements shown were captured using the antenna with no biasing lines, where the switches were emulated with copper foil, in the compact range. The second measurement is done where PIN diodes are implemented in conjunction with vertical vias and lastly measurements of the antenna with helical coils with PIN diodes are shown.

After this a detailed discussion of the results are provided to confirm the challenges of the design and how some challenges could be mitigated in future work.

CHAPTER 6 CONCLUSION

6.1 SUMMARY OF WORK

The objective of the dissertation was to design a reconfigurable antenna based on an active reflective metasurface. The antenna had to be able to switch between polarization states using electrical switches in the form of PIN diodes. It was critical that the design demonstrates the concept of electrical reconfiguration of the antenna through an active reflective metasurface.

In Chapter 2 a literature study on reconfigurable antennas is conducted, with the focus on reconfigurable polarization. The study revealed that there are multiple methods of reconfiguration through the modification of radiating elements and feed networks to achieve polarization diversity. Another method identified was the use of metasurfaces to reconfigure the polarization of incident waves. This method was also extended by the addition of radiating elements. In most of the literature the performance of the antennas was only enhanced with the addition of metasurfaces and lacked reconfigurability. Some active metasurfaces in transmittive configurations were successfully combined with radiating elements. What was lacking in literature was the use of active reflective metasurface configurations to achieve polarization configurability as this could provide potential benefits. A reflective surface can operate as both a polarizer and a reflector to enhance the performance of a radiating element. Thus, an antenna with an active metasurface in a reflective configuration was pursued.

In Chapter 3 a design procedure is established for the design of an antenna with an active reflective metasurface. First a reconfigurable reflective metasurface is designed based on an

infinite series of unit cells in simulation. With a metasurface designed the addition of a radiating element could be made. Unfortunately, the addition of a radiating element is more complex as the metasurface characteristics are changed with the addition of a dipole. To better understand the interaction between the reflective metasurface and the radiating element a parametric study is performed after which a starting set of parameters are extracted for the antenna system. The parameters are then optimized for the optimal axial ratio in both linear and circular states. As the focus is only on the axial ratio in the initial design iteration, a final design iteration is performed to find suitable radiation patterns. The final design iteration is then ready to be implemented.

In Chapter 4 the implementation of the antenna design and the switchable elements are discussed. To activate the PIN diodes on the metasurface a forward voltage needs to be applied to bias them. To achieve this vertical vias were implemented. However, the vias degraded the pattern performance of the antenna in the linear state by introducing additional side lobes in the cross-polarized patterns within the HPBW of the co-polarized patterns. To mitigate the effect of the vias, helical coils which acted as chokes were introduced. The addition of these coils normalized the linear patterns and the design could be manufactured.

In Chapter 5 the measured results for three manufactured versions of the antenna are provided and discussed. The antenna was first manufactured with no switches and then switches were emulated with copper foil tape. The antenna was then implemented with vertical vias after which helical coils were implemented for biasing the PIN diodes. The results with no switches correlated very well with simulated results and demonstrated that the basic concept could be implemented. Unfortunately, with the addition of the biasing lines the antenna performance was degraded, as expected. The trend between measured and simulated results correlated well with the former having lower levels. The measurement with the helical coils showed that the patterns were normalized to that of the original design, but cross-polar performance in both linear and circular states was lower. The implementation of coils was very difficult as the hand manufacturing of the coils were inconsistent and added additional constraints to the design. These manufacturing inconsistencies attributed to the

decreased performance of the antenna. However even with the lower antenna performance, the concept of a reconfigurable antenna with an active reflective metasurface was developed.

In conclusion a reconfigurable antenna with an active reflective metasurface was designed with success. It correlated well with simulated design with reduced performance. A generalized design procedure was also established to base future work on.

6.2 CONTRIBUTION

The result of this research is a new reconfigurable antenna capable of achieving linear horizontal and right-hand circular polarization states by activating switchable elements on the antenna. The antenna is based on an active reflective metasurface that was devised from a similar transmittive metasurface. Reconfigurability is achieved with PIN diodes on the unit cell elements within the reflective metasurface.

The antenna had a physical size of 308 x 162 x 35 mm^3 and an impedance bandwidth of 4.5% in the linear state, 7% in the circular state, and an axial ratio bandwidth of 8.3%. This gives the antenna an effective bandwidth of 4.5% in the linear state and 7% in the circular state. The first version of the antenna with ideal switching elements produced good cross-polar performance and unidirectional patterns in both linear and circular states which was unfortunately degraded by the implementation of the helical coils used to normalize the radiation patterns.

When compared to literature the antenna performed well overall in terms of the set design goals. A comparison of the various types of antennas with reconfigurable polarization is presented in Table 6.1. Most of the antennas are reconfigurable in multiple polarization states where most of the antennas are implemented with an active transmittive metasurface [16], [17], [21]. Only two antennas are similar to the proposed antenna, as they are also implemented on an active reflective metasurfaces [19], [20]. These two antennas however only achieve two circular polarization states, where the proposed antenna can achieve both

linear and circular polarization states. The proposed antenna also achieves a better effective bandwidth than both these antennas.

Consequently, the proposed antenna is one of a few antennas that is based on an active reflective metasurface and, to the knowledge of the author, the only one capable of both circular and linear polarization states. The antenna achieved performance that is comparable with other antennas with reconfigurable polarization. However, the primary objective was to prove the design concept of an antenna based on an active reflective metasurface. This was proved and the performance of the antenna can be improved in future work.

A summary of the research contribution:

- An antenna design concept based on active reflective metasurface with reconfigurable polarization. Even though the final manufactured antenna had problems that was created by the biasing network the concept of this research was proved and can be expanded upon in future work.

Table 6.1 Comparison of antennas with reconfigurable polarization

Ref.	Reconfiguration method	Control method	Polarization states	F_c (GHz)	I_{BW} (%)		XPD (dB)		AR_{BW} (%)	Eff_B w (%)
					Lin.	Circ.	Lin.	Circ.		
[4]	Alter radiating element structure	PIN diodes	LHCP, RHCP, LP	3.9	2.6, 5.4	28.6	>3	>18	15.4	15.4
[6]	Alter feed network structure	PIN diodes	LHCP, RHCP, LP	6	30	25	>20	>20	21	20
[16]	Alter transmittive metasurface elements	MEMS	CP, LP	5.5	1.8	1.8	Not given	Not given	2.4	1.6
[17]	Rotate metasurface structure	Mechanical rotation	LHCP, RHCP, LP	3.5	25	37	50	15	14	11
[21]	Alter transmittive metasurface elements	PIN diodes	LHCP, LP	13.7	21	23	10	>18	14	13
[19]	Alter **reflective** metasurface elements	Varactor diodes	LHCP, RHCP	1.4	N/A	12.8	N/A	>20	2.85	2.85
[20]	Alter **reflective** metasurface elements	PIN diodes	LHCP, RHCP	2.55	N/A	17	N/A	>15	4.58	1.6
This work	Alter **reflective** metasurface elements	PIN diodes	RHCP, LP	2.4	4.5	7	7	11	8.3	4.5

6.3 FUTURE WORK

During the literature study and the design of the antenna a few areas for future work was identified:

- An improved understanding of the interaction of the biasing circuitry on radiating elements that must be used to control active elements on metasurfaces.
- PCB biasing structures in the form of a zig zag shape etched on a vertical PCB layer.
- Array implementations using active reflective metasurfaces to control and add another degree of freedom to the antenna design with enhanced performance.
- Using a reflective metasurface to achieve more modes of operations such as pattern and frequency diversity with a sensible operating bandwidth.

REFERENCES

[1] J. G. Andrews *et al.*, “What will 5G be?,” *IEEE J. Sel. Areas Commun.*, vol. 32, no. 6, pp. 1065–1082, 2014.

[2] C. Balanis, *Modern Antenna Handbook*. Hoboken, USA: John Wiley & Sons, 2011.

[3] R. L. Haupt and M. Lanagan, “Reconfigurable antennas,” *IEEE Antennas Propag. Mag.*, vol. 55, no. 1, pp. 49–61, 2013.

[4] W. Lin and H. Wong, “Polarization reconfigurable wheel-shaped antenna with conical-beam radiation pattern,” *IEEE Trans. Antennas Propag.*, vol. 63, no. 2, pp. 491–499, 2015.

[5] N. Nguyen-Trong, L. Hall, and C. Fumeaux, “A Frequency-and Polarization-Reconfigurable Stub-Loaded Microstrip Patch Antenna,” *IEEE Trans. Antennas Propag.*, vol. 63, no. 11, pp. 5235–5240, 2015.

[6] W. W. Yang, X. Y. Dong, W. J. Sun, and J. X. Chen, “Polarization reconfigurable broadband dielectric resonator antenna with a lattice structure,” *IEEE Access*, vol. 6, pp. 21212–21219, 2018.

[7] J. Hu, Z. C. Hao, and W. Hong, “Design of a wideband quad-polarization reconfigurable patch antenna array using a stacked structure,” *IEEE Trans. Antennas Propag.*, vol. 65, no. 6, pp. 3014–3023, 2017.

[8] R. Lian, Z. Tang, and Y. Yin, “Design of a broadband polarization-reconfigurable fabry-perot resonator antenna,” *IEEE Antennas Wirel. Propag. Lett.*, vol. 17, no. 1, pp. 122–125, 2018.

[9] Y. Liu, H. Liu, and S. Gong, “Wideband polarization-reconfigurable antenna based on tightly coupled array mechanism,” in *IET Conference Publications*, 2018, vol. 2018, no. CP741, pp. 2–4.

[10] W. Lin and H. Wong, "Wideband Circular Polarization Reconfigurable Antenna," *IEEE Trans. Antennas Propag.*, vol. 63, no. 12, pp. 5938–5944, 2015.

[11] W. Yang, W. Che, H. Jin, W. Feng, and Q. Xue, "A Polarization-Reconfigurable Dipole Antenna Using Polarization Rotation AMC Structure," *IEEE Trans. Antennas Propag.*, vol. 63, no. 12, pp. 5305–5315, 2015.

[12] J. Hu, G. Q. Luo, and Z. C. Hao, "A Wideband Quad-Polarization Reconfigurable Metasurface Antenna," *IEEE Access*, vol. 6, pp. 6130–6137, 2017.

[13] Y. Li *et al.*, "Achieving wide-band linear-to-circular polarization conversion using ultra-thin bi-layered metasurfaces," *J. Appl. Phys.*, vol. 117, no. 4, pp. 1–7, 2015.

[14] L. Li, Y. Li, Z. Wu, F. Huo, Y. Zhang, and C. Zhao, "Novel polarization-reconfigurable converter based on multilayer frequency-selective surfaces," *Proc. IEEE*, vol. 103, no. 7, pp. 1057–1070, 2015.

[15] Y. Li, Y. Wang, and Q. Cao, "Design of a Multifunctional Reconfigurable Metasurface for Polarization and Propagation Manipulation," *IEEE Access*, vol. 7, pp. 129183–129191, 2019.

[16] Z. Li, D. Rodrigo, L. Jofre, and B. A. Cetiner, "A new class of antenna array with a reconfigurable element factor," *IEEE Trans. Antennas Propag.*, vol. 61, no. 4, pp. 1947–1955, 2013.

[17] H. L. Zhu, S. W. Cheung, X. H. Liu, and T. I. Yuk, "Design of polarization reconfigurable antenna using metasurface," *IEEE Trans. Antennas Propag.*, vol. 62, no. 6, pp. 2891–2898, 2014.

[18] K. Kandasamy, B. Majumder, J. Mukherjee, S. Member, K. P. Ray, and S. Member, "Low-RCS and Polarization-Reconfigurable Antenna Using Cross-Slot-Based Metasurface," *IEEE Antennas Propag. Lett.*, vol. 14, pp. 1638–1641, 2015.

[19] B. Liang, B. Sanz-Izquierdo, E. A. Parker, and J. C. Batchelor, "A frequency and polarization reconfigurable circularly polarized antenna using active ebg structure for satellite navigation," *IEEE Trans. Antennas Propag.*, vol. 63, no. 1, pp. 33–40, 2015.

[20] W. Li *et al.*, "Polarization-Reconfigurable Circularly Polarized Planar Antenna Using Switchable Polarizer," *IEEE Trans. Antennas Propag.*, vol. 65, no. 9, pp. 4470–4477, 2017.

[21] W. Li *et al.*, "A Reconfigurable Polarization Converter Using Active Metasurface and Its Application in Horn Antenna," *IEEE Trans. Antennas Propag.*, vol. 64, no. 12, pp. 5281–5290, 2016.

[22] G. I. Kiani and V. Dyadyuk, "Quarter-wave plate polariser based on frequency selective surface," in *European Microwave Week 2010, EuMW2010: Connecting the World, Conference Proceedings - European Microwave Conference, EuMC 2010*, 2010, no. September, pp. 1361–1364.

[23] S. Tian, H. Liu, and L. Li, "Design of 1-bit digital reconfigurable reflective metasurface for beam-scanning," *Appl. Sci.*, vol. 7, no. 9, pp. 1–8, 2017.

[24] Z. Li, Y. Mu, J. Han, X. Gao, and L. Li, "Dual-polarized antenna design integrated with metasurface and partially reflective surface for 5G communication," *EPJ Appl. Metamaterials*, vol. 7, no. 3, pp. 1–7, 2020.

[25] X. Ma, C. Huang, M. Pu, C. Hu, Q. Feng, and X. Luo, "Single-layer circular polarizer using metamaterial and its application in antenna," *Microw. Opt. Technol. Lett.*, vol. 54, no. 7, pp. 1770–1774, 2012.

[26] H. L. Zhu, S. W. Cheung, K. L. Chung, and T. I. Yuk, "Linear-to-circular polarization conversion using metasurface," *IEEE Trans. Antennas Propag.*, vol. 61, no. 9, pp. 4615–4623, 2013.

[27] C. Chen *et al.*, "A circularly-polarized metasurfaced dipole antenna with wide axial-ratio beamwidth and RCS reduction functions," *Prog. Electromagn. Res.*, vol. 154, pp. 79–85, 2015.

[28] Y. Huang, L. Yang, J. Li, Y. Wang, and G. Wen, "Polarization conversion of metasurface for the application of wide band low-profile circular polarization slot antenna," *Appl. Phys. Lett.*, vol. 109, no. 5, pp. 1–6, 2016.

[29] Q. Chen, H. Zhang, Y. J. Shao, and T. Zhong, "Bandwidth and gain improvement of an L-shaped slot antenna with metamaterial loading," *IEEE Antennas Wirel. Propag. Lett.*, vol. 17, no. 8, pp. 1411–1415, 2018.

[30] S. X. Ta, Q. S. Ho, K. K. Nguyen, and C. Dao-Ngoc, "Single-dipole antenna on a metasurface for broadband circularly polarized radiation," *J. Electromagn. Waves Appl.*, vol. 32, no. 4, pp. 413–427, 2018.

[31] S. X. Ta and I. Park, "Low-Profile Broadband Circularly Polarized Patch Antenna

Using Metasurface," *IEEE Trans. Antennas Propag.*, vol. 63, no. 12, pp. 5929–5934, 2015.

[32] C. Zhou, S. W. Cheung, Q. Li, and M. Li, "Bandwidth and gain improvement of a crossed slot antenna with metasurface," *Appl. Phys. Lett.*, vol. 110, no. 21, pp. 1–5, 2017.

[33] I. Yeom, J. Choi, S. S. Kwoun, B. Lee, and C. Jung, "Analysis of RF front-end performance of reconfigurable antennas with RF switches in the far field," *Int. J. Antennas Propag.*, vol. 2014, pp. 1–14, 2014.